X-ray Emission from Single Massive Stars

Constraints on Wind-Shock Physics and Mass-Loss Rates

David Cohen

Swarthmore College

with Stan Owocki & Jon Sundqvist (U. Delaware), Maurice Leutenegger (GSFC),
Marc Gagné & Véronique Petit (West Chester University), Alex Fullerton (STScI),
Emma Wollman (Swarthmore ’09; Caltech), Erin Martell (Swarthmore ’09; U. Chicago),
James MacArthur (Swarthmore ’11; Sandia National Laboratory)

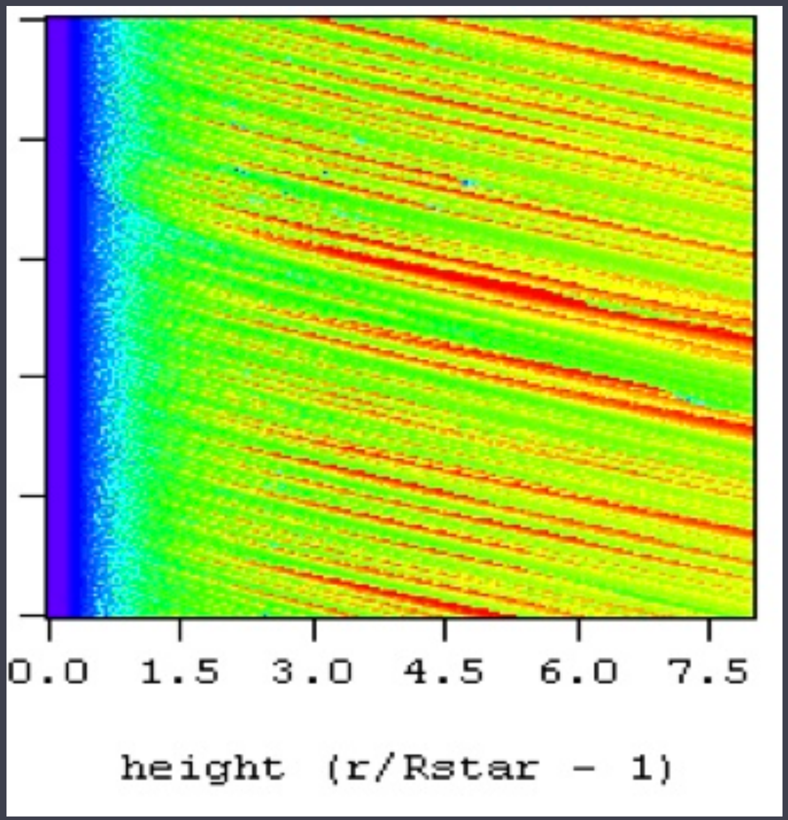

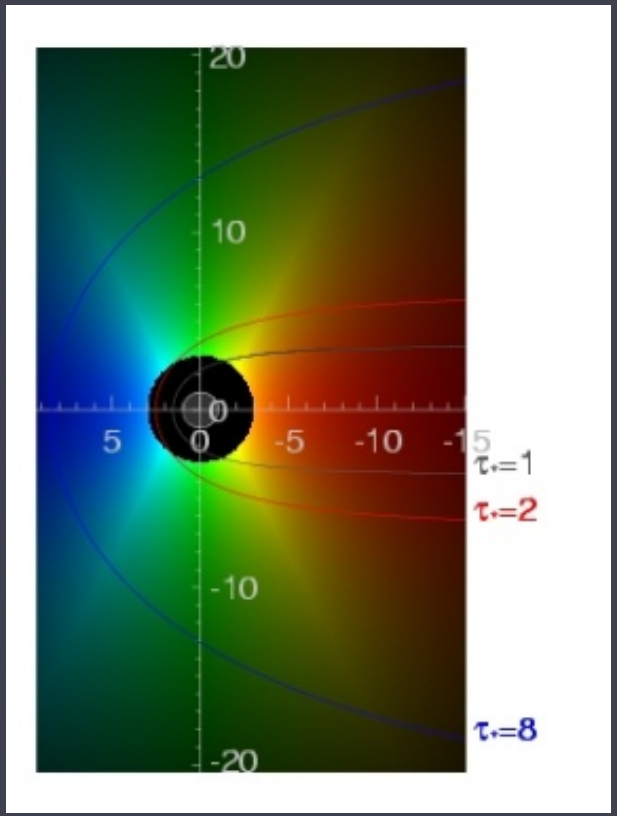

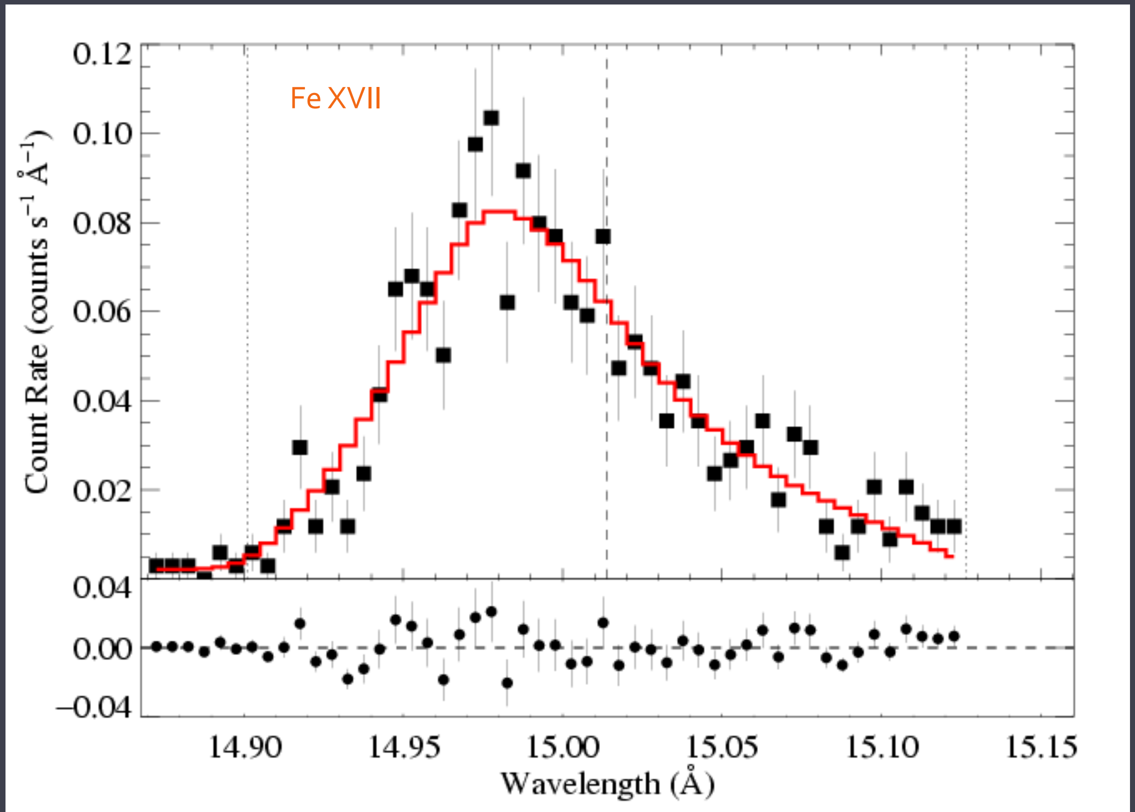

Massive Stars: luminous, with strong winds

ESO: Carina Nebula

very luminous ($L_{bol} \sim 10^5$ - 10^6 L_{sun}), impact on Galactic environment, nucleosynthesis, supernova end-state

ESO: Carina Nebula

strong radiation-driven winds ($\dot{M}$ ~ 10^{-6} to 10^{-5} M_{sun}/yr and v_∞ ~ 2000 to 3000 km/s)

ESO: Carina Nebula

HD 93129A

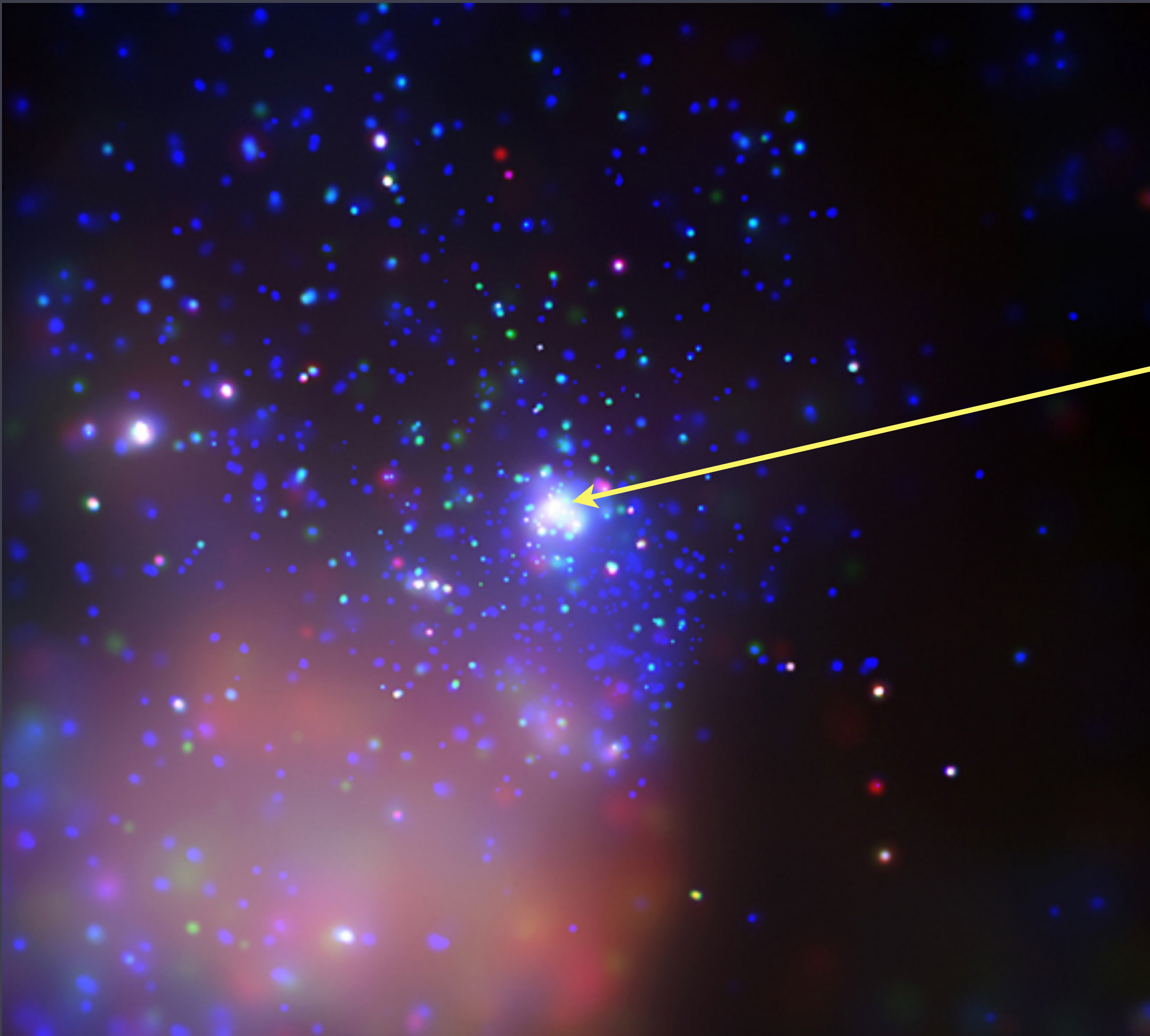

Tr 14: *Chandra*

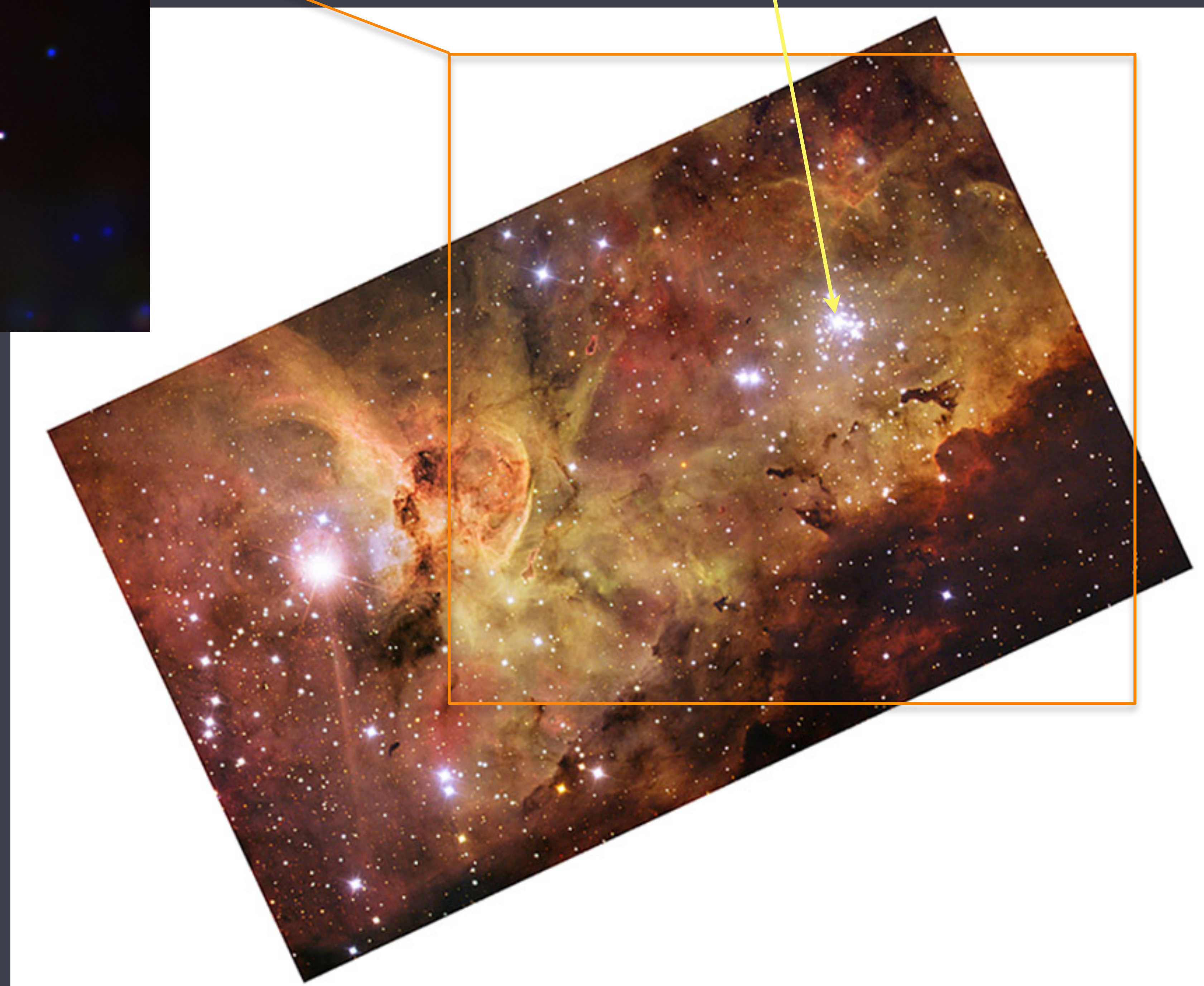

Carina: ESO

O supergiants are quite X-ray luminous (L_x up to 10^{33} erg/s)

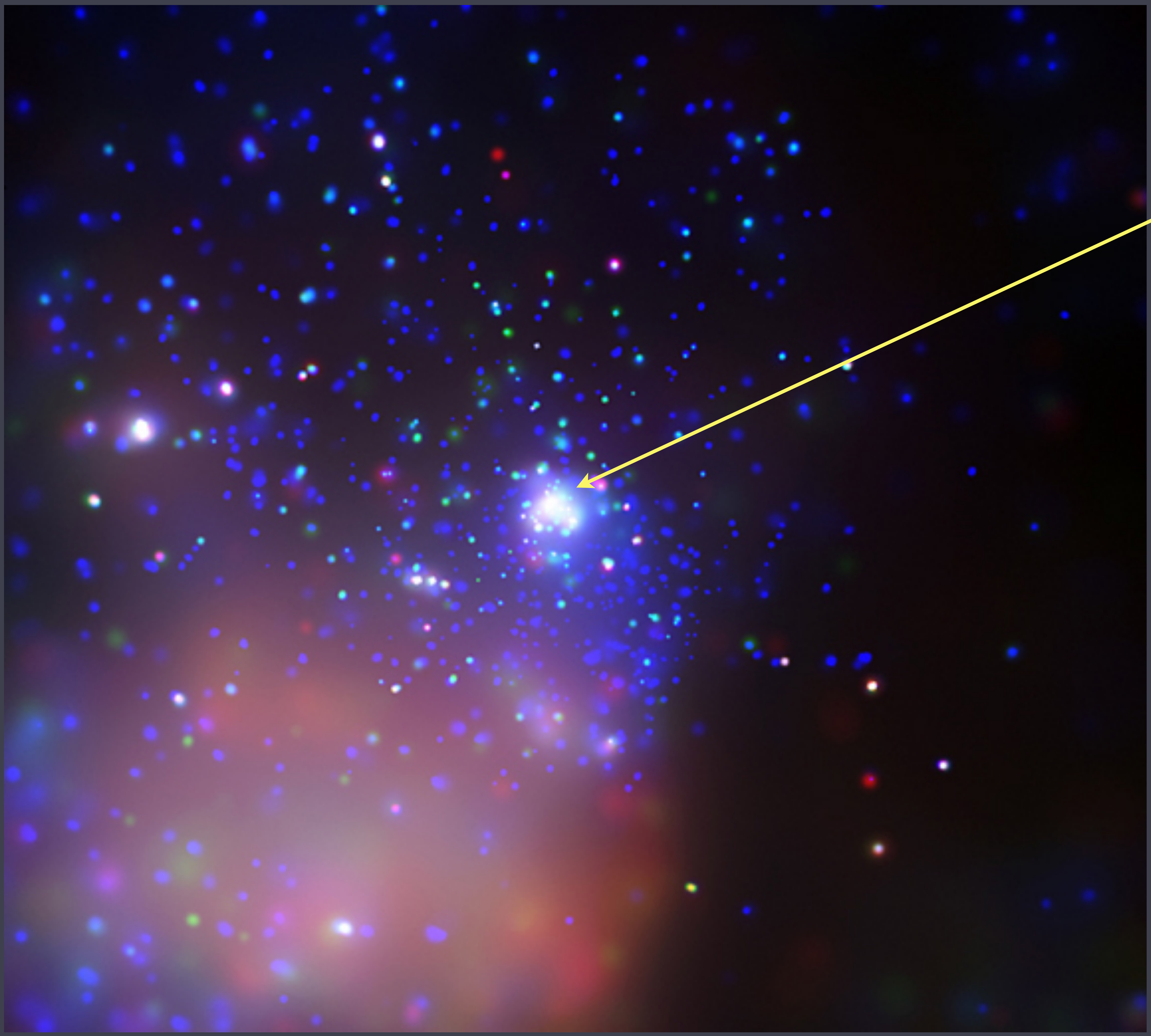

Tr 14: *Chandra*

Outline: Wind Shock Physics and Mass-Loss Rates

- X-rays arise in post-shock cooling zones distributed throughout the stellar wind
- Line profile shapes: mass-loss rates
- Line profile shapes: kinematics and location
- Broadband X-ray spectra: plasma temperature distribution and wind absorption (for an independent mass-loss rate measurement)

Theory

Numerical simulations of the line-driving instability (LDI)

self-excited instability

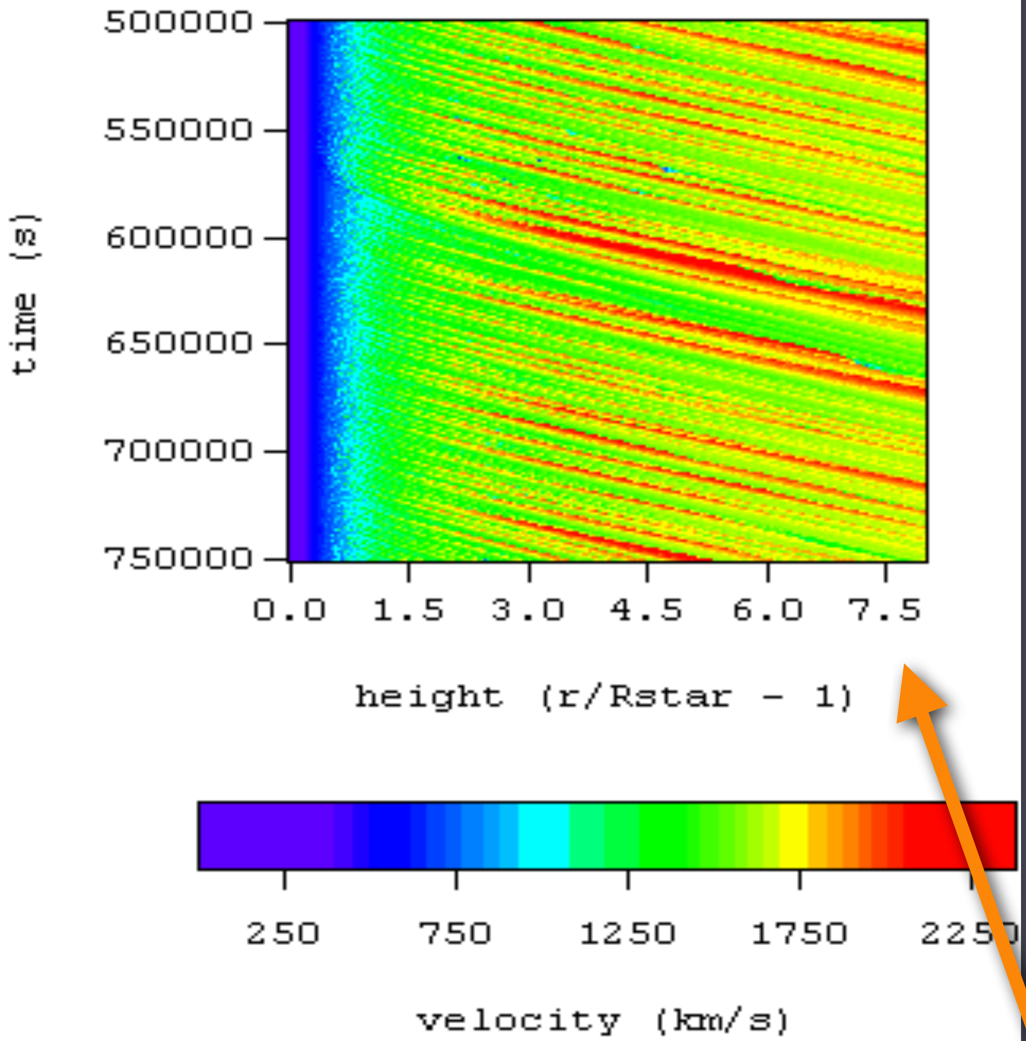

Owocki, Cooper, Cohen 1999

excited by turbulence at the wind base

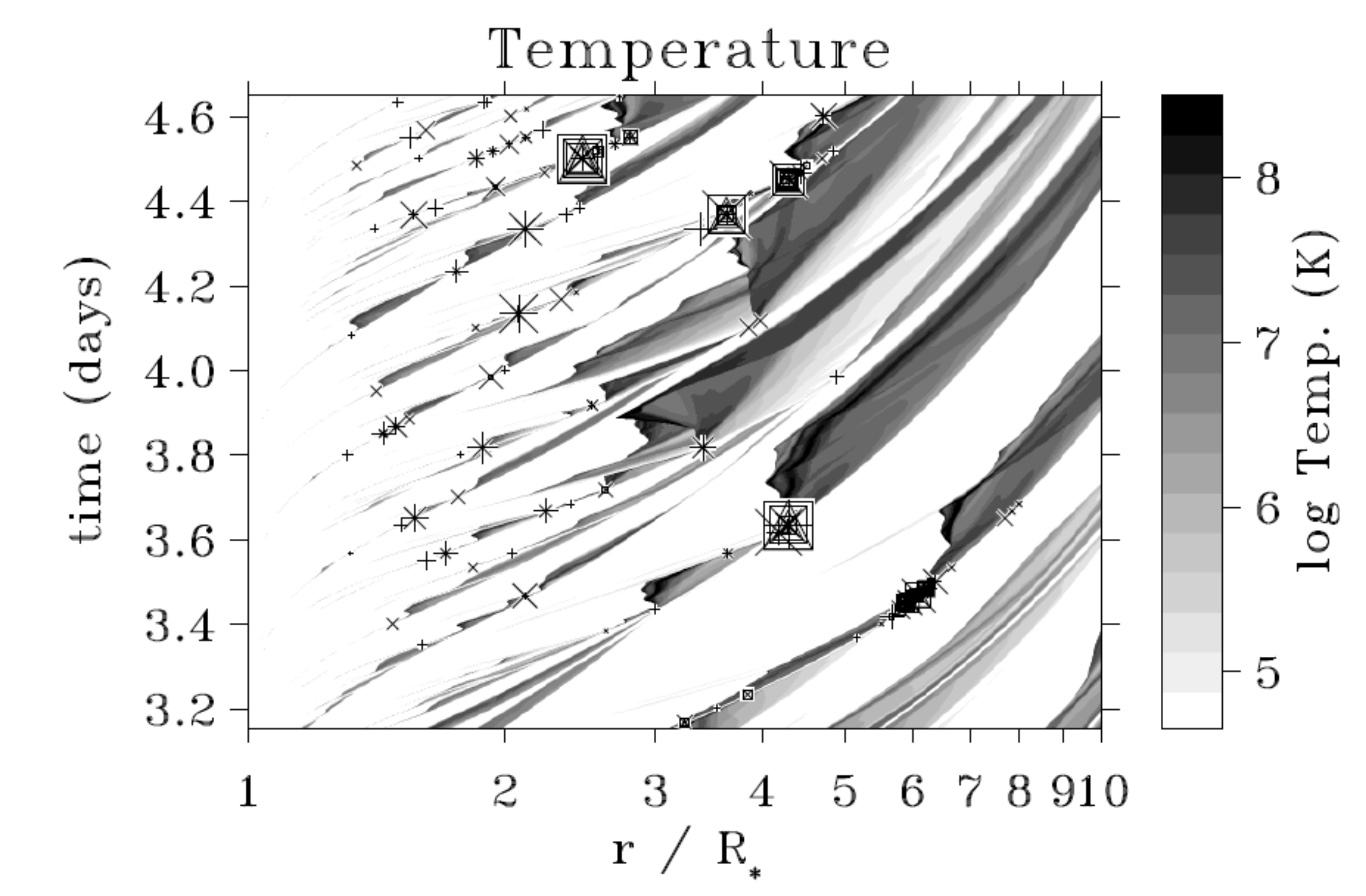

Feldmeier, Puls, & Pauldrach 1997

shock jump velocities ~ few 100 km/s

Numerical simulations of the line-driving instability (LDI)

self-excited instability

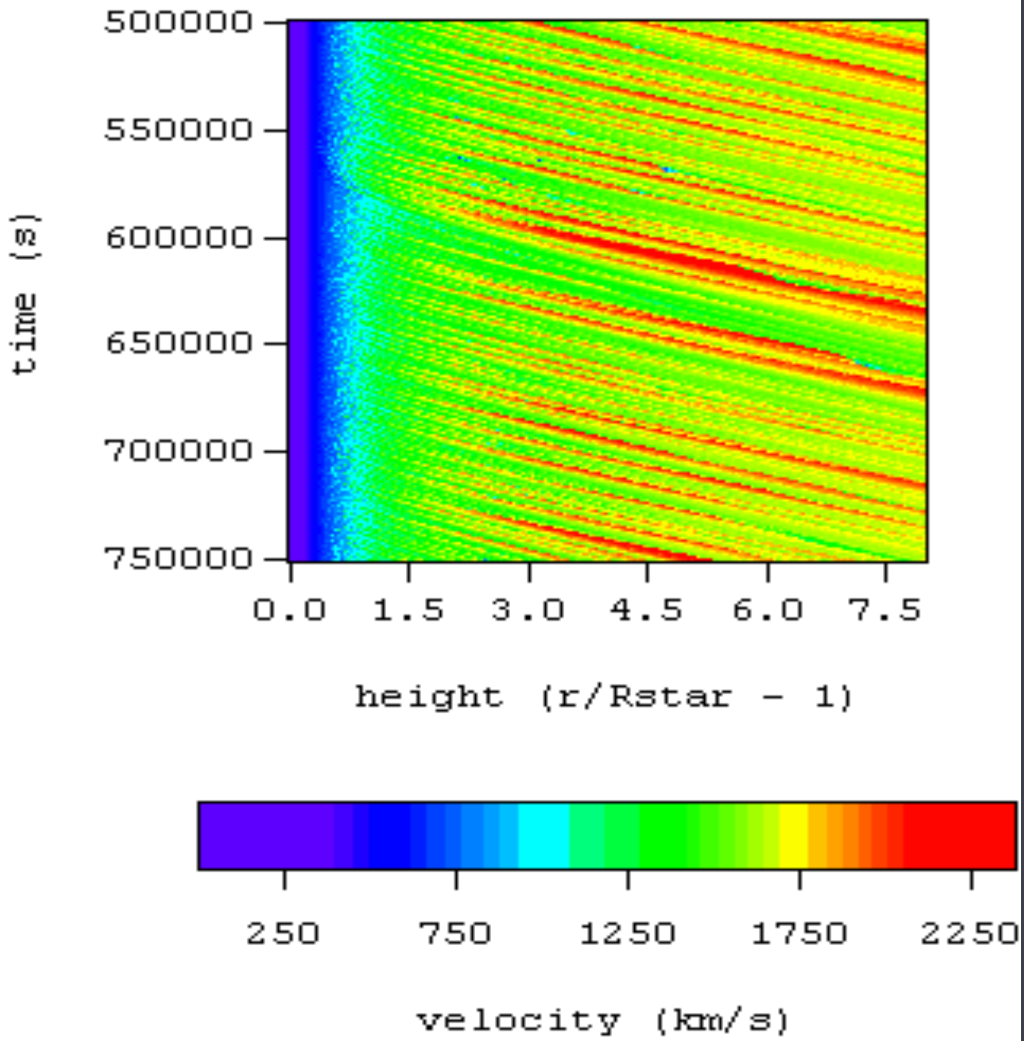

Owocki, Cooper, Cohen 1999

excited by turbulence at the wind base

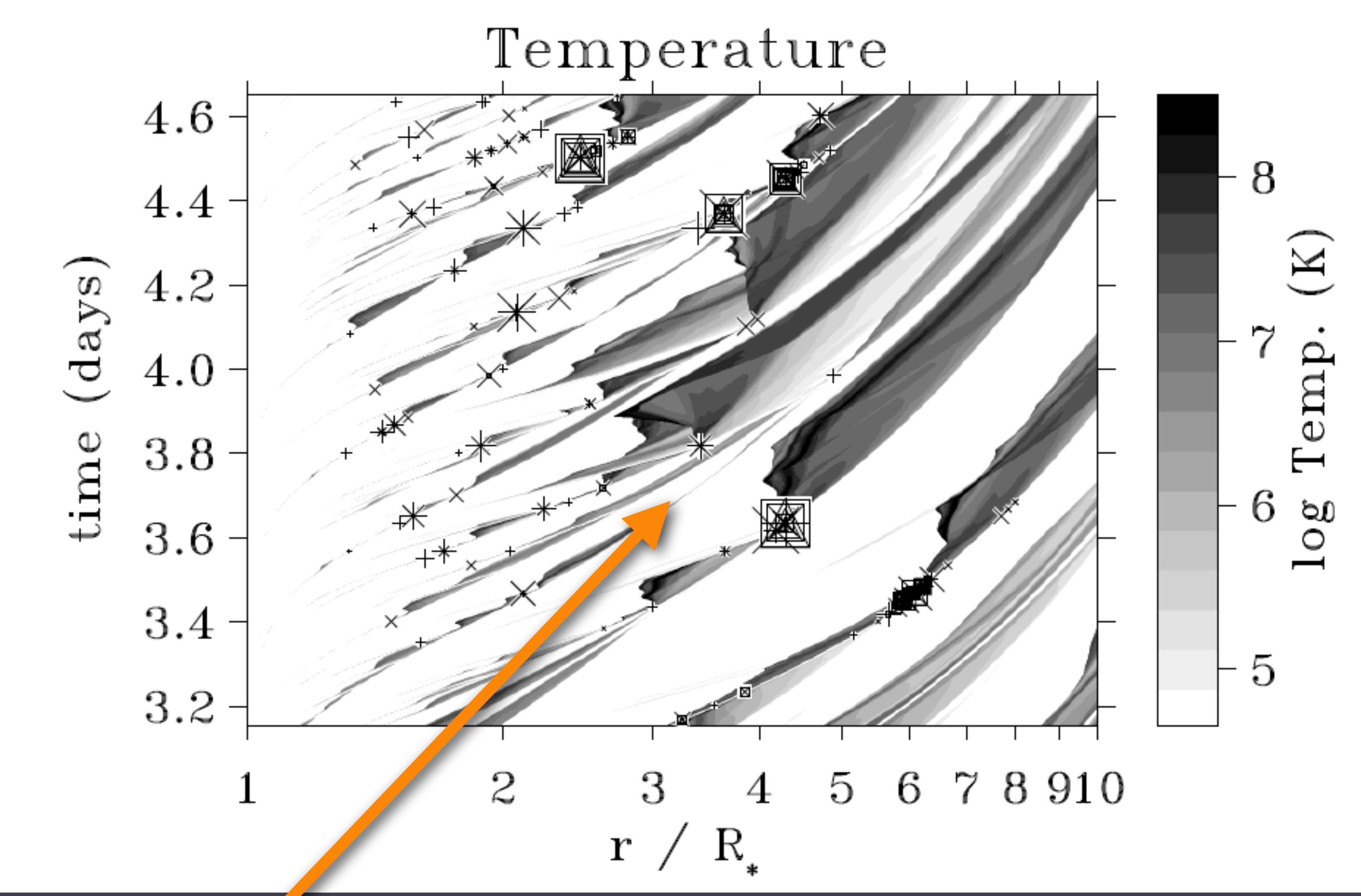

Feldmeier, Puls, & Pauldrach 1997

shock jump temperatures ~ few 10^6 K

Numerous shock structures distributed above $r \sim 1.5\ R_\star$

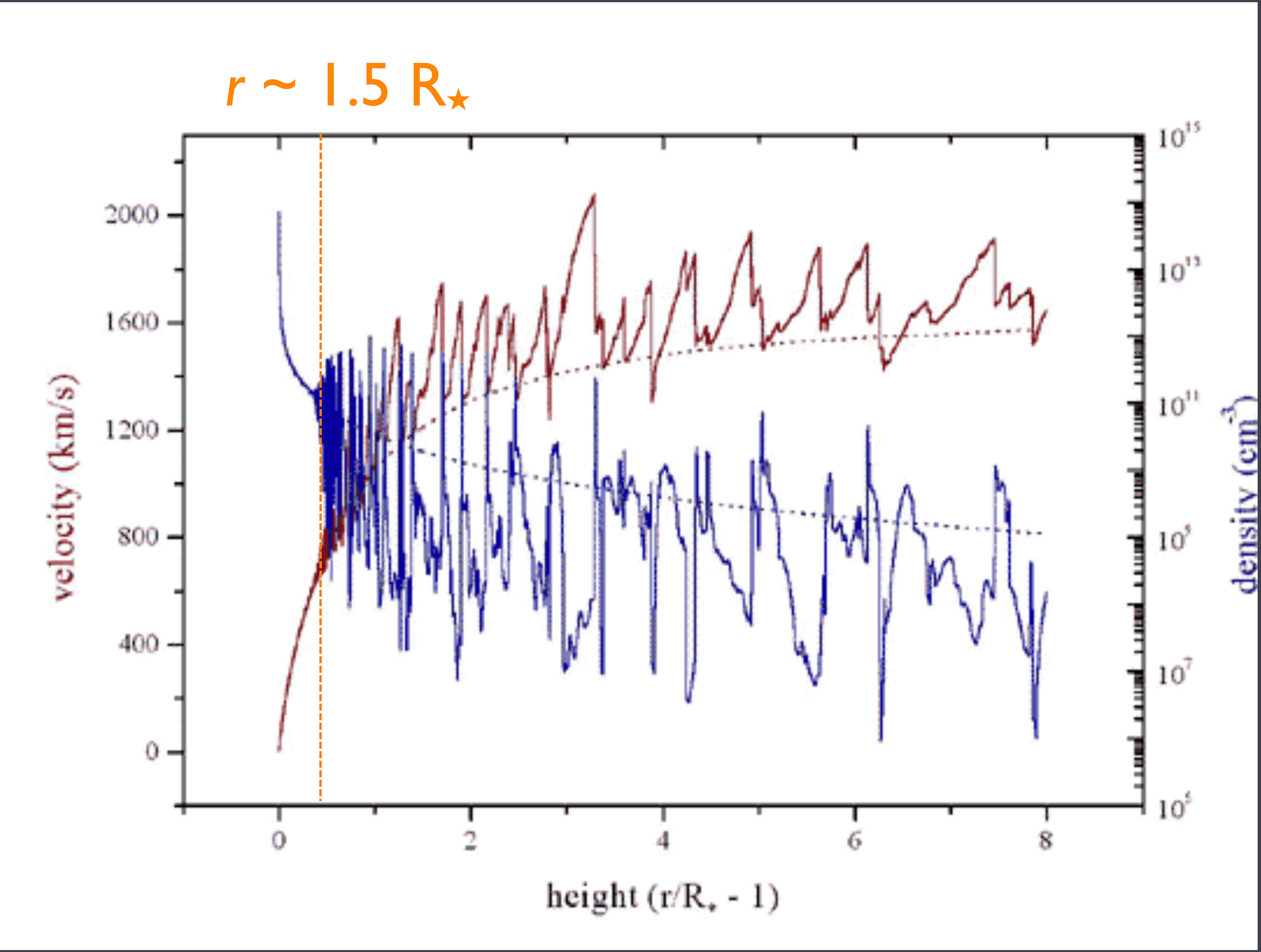

$V_{shock} \sim 300$ km/s : $T \sim 10^6$ K

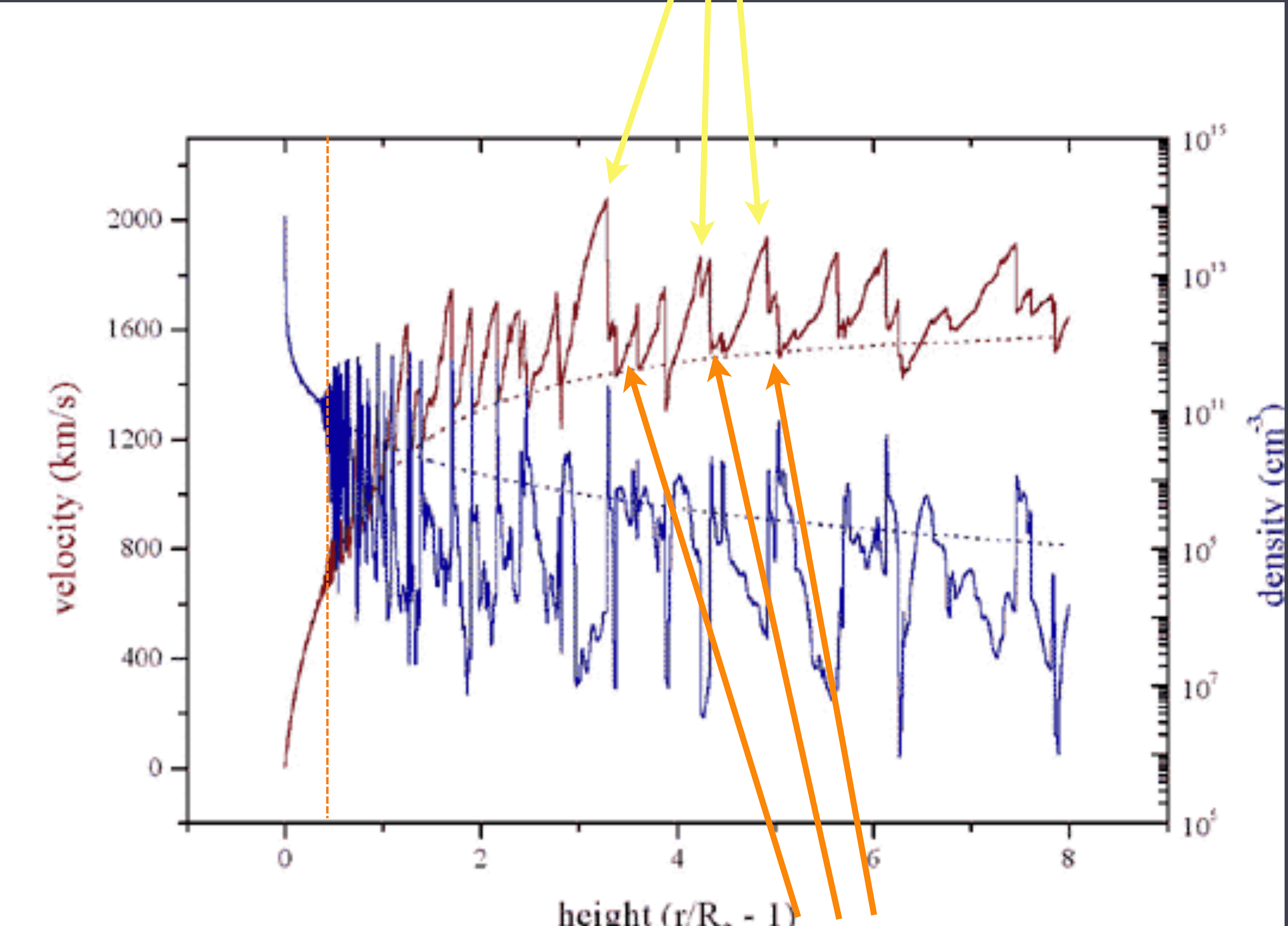

shocked wind plasma is decelerated back down to the local CAK wind velocity

Shocked plasma is moving at $v \sim 1000$ km/s

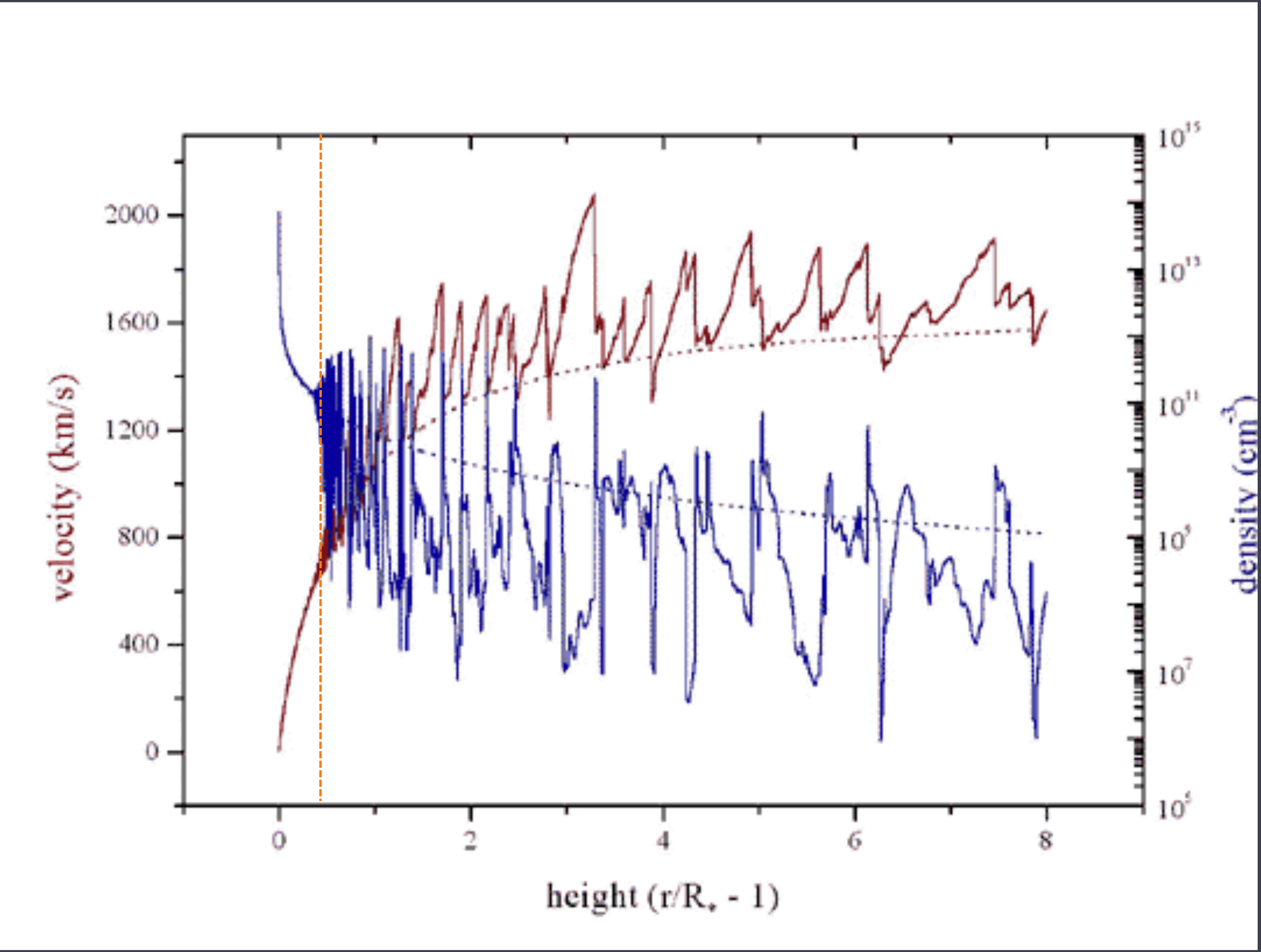

X-ray emission lines should be **Doppler broadened**

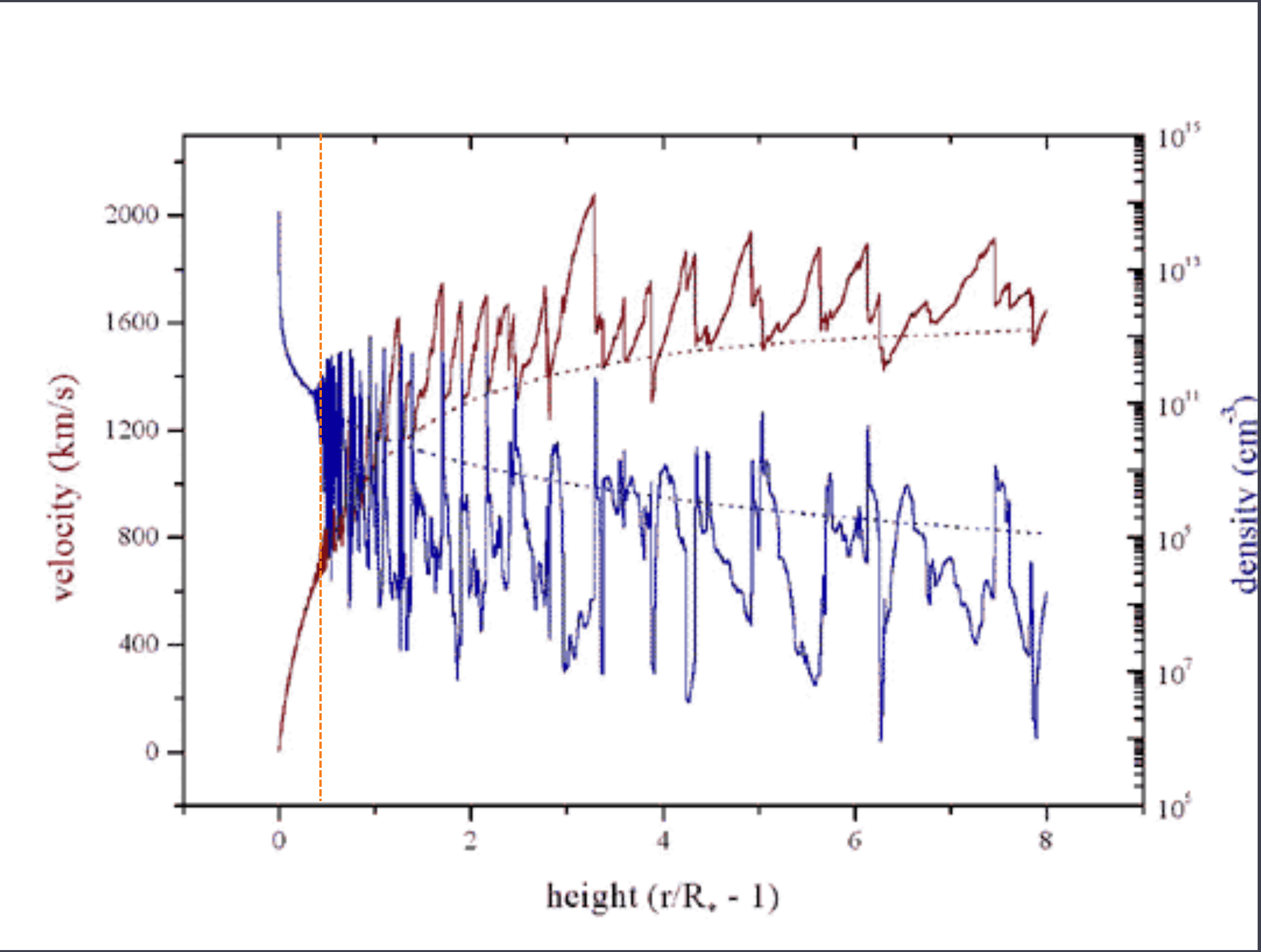

Less than 1% of the wind is emitting X-rays

>99% of the wind is cold and X-ray *absorbing*

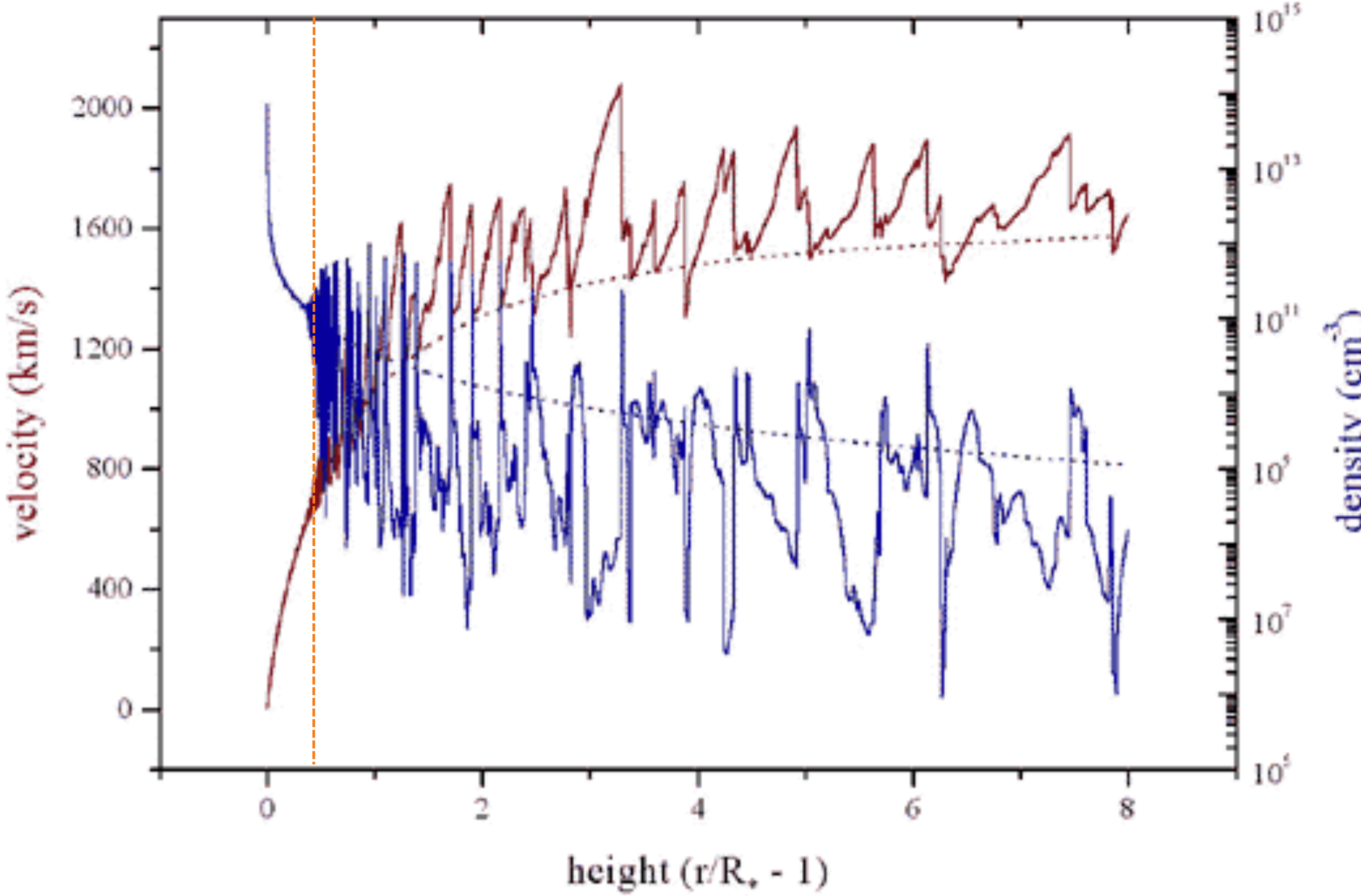

Data

O supergiant X-ray emission lines are **broad**

Chandra grating spectrum

ζ Pup (O4If)

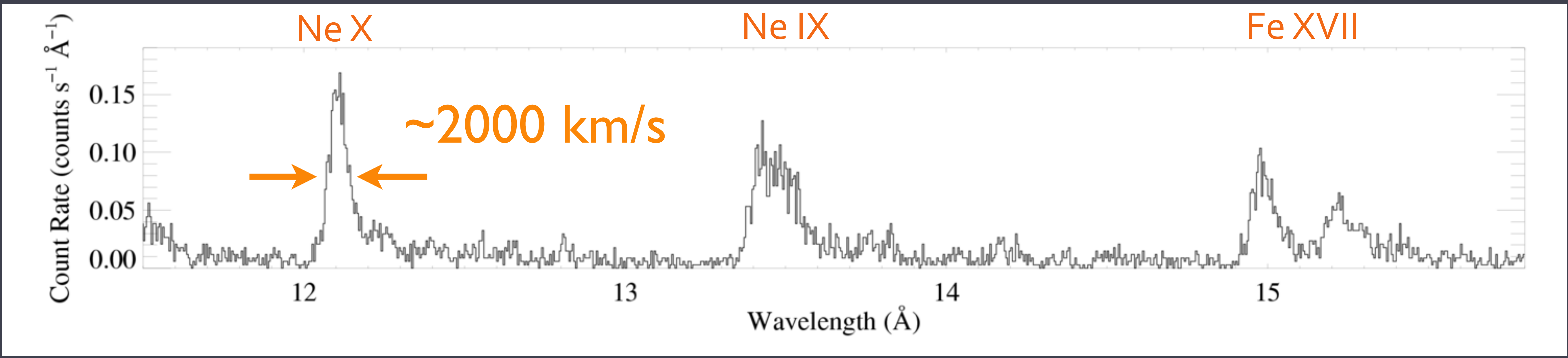

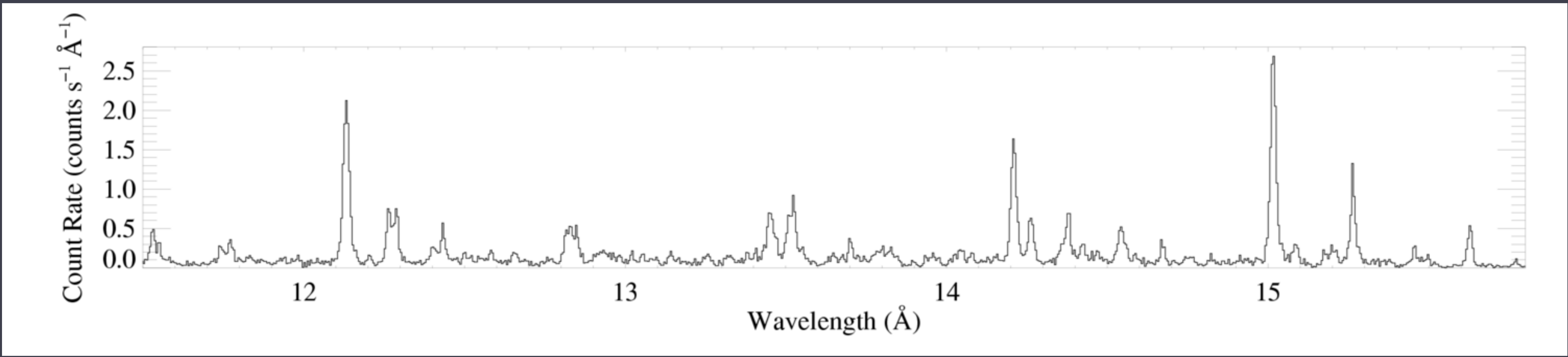

Capella: G star for comparison (narrow lines)

lines are asymmetric

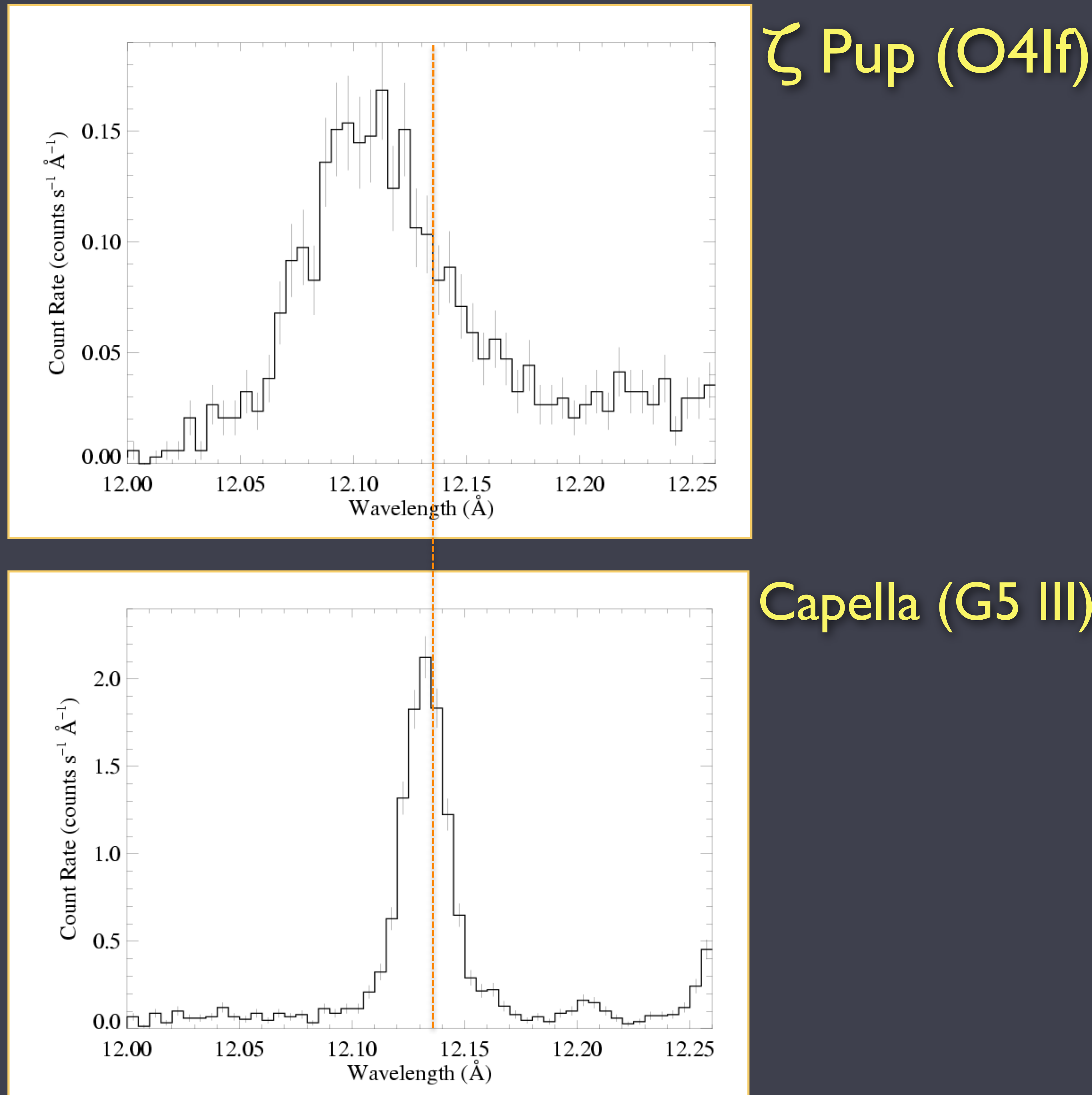

Simple, empirical line-profile model: for extracting physically meaningful parameters from spectral data

Line Asymmetry

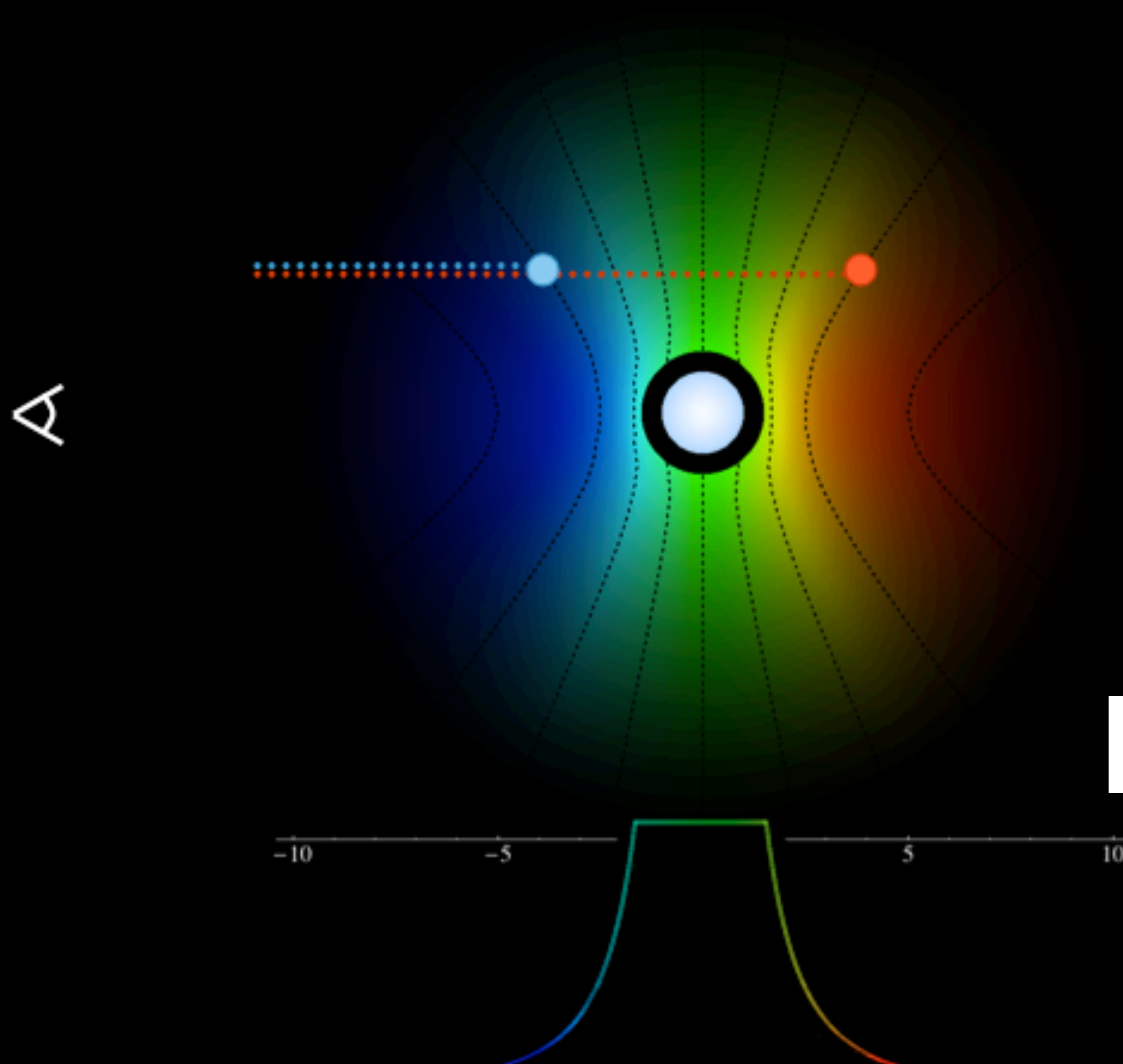

$$v = v_{\infty}(1 - r/R_{\star})^{\beta}$$

Line Asymmetry

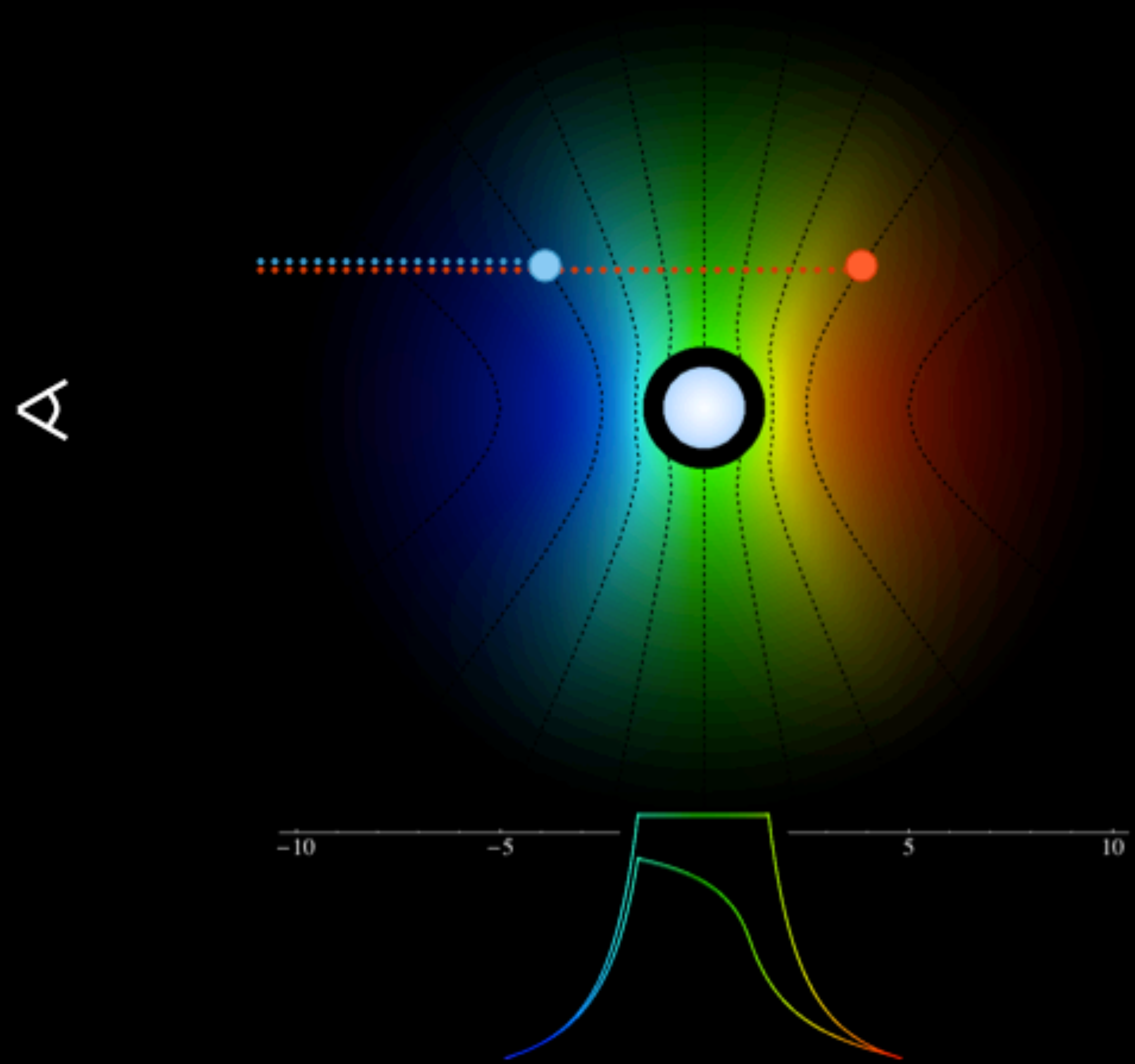

Line Asymmetry

$$\tau = \tau_* \int_z^\infty \frac{R_* dz'}{r'^2 (1 - R_*/r')^\beta}$$

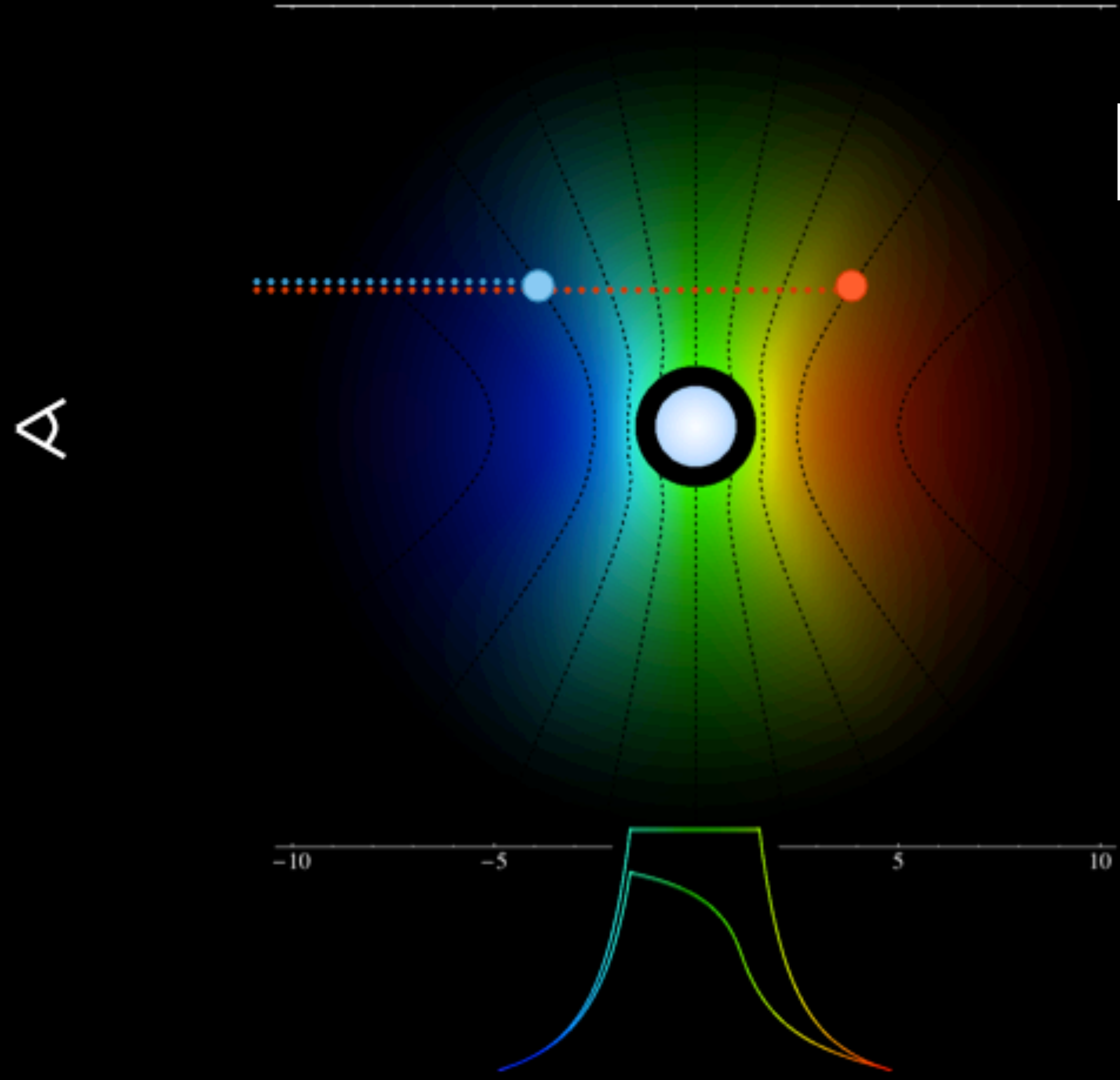

Wind Profile Model

$$\tau_* = \frac{\kappa \dot{M}}{4\pi R_* v_\infty}$$

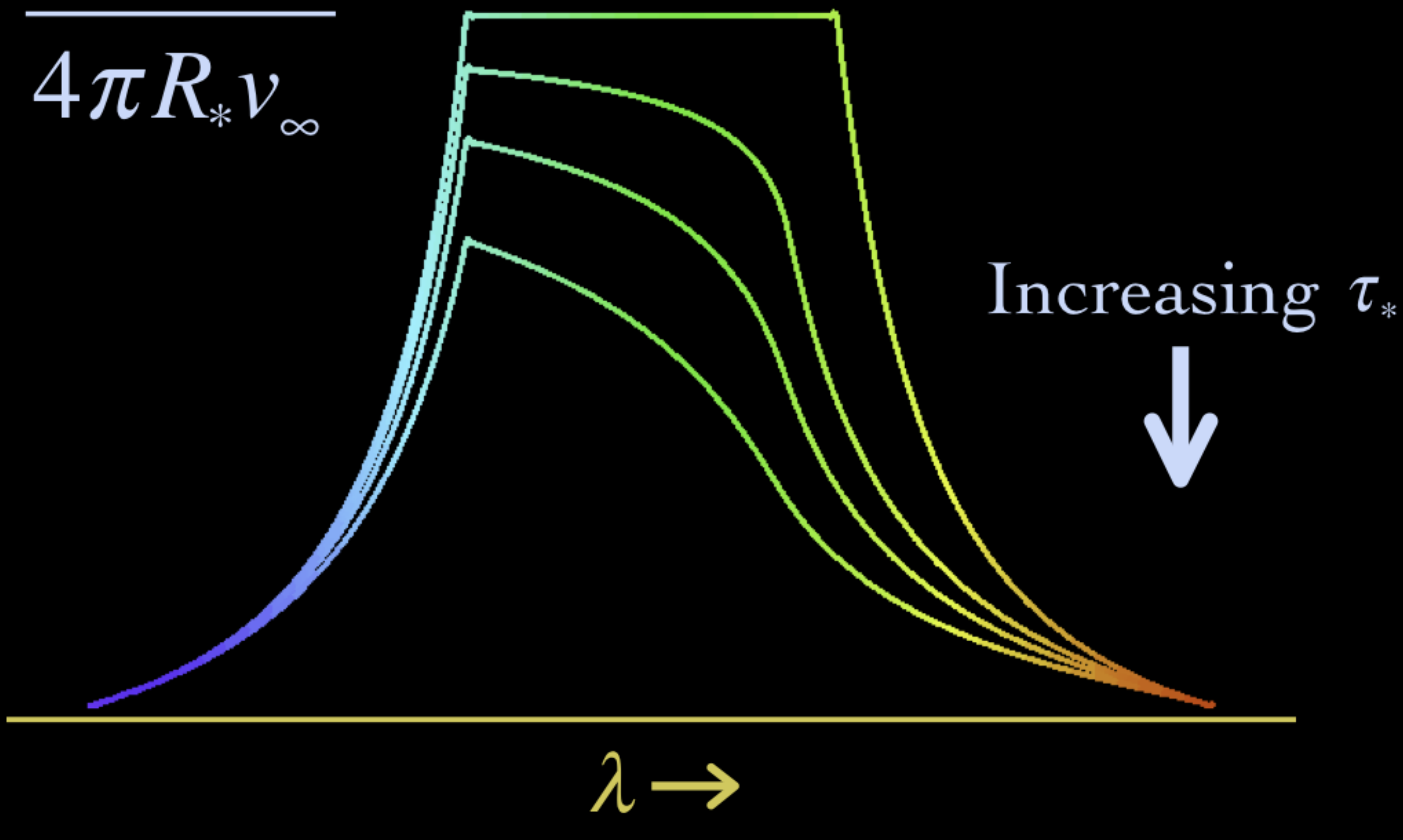

Quantifying the wind optical depth

opacity of the cold wind component (due to bound-free transitions in C, N, O, Ne, Fe)

wind mass-loss rate

$$\dot{M} = 4\pi r^2 v \rho$$

$$\tau_* \equiv \frac{\kappa \dot{M}}{4\pi R_* v_\infty}$$

stellar radius

wind terminal velocity

soft X-ray wind opacity

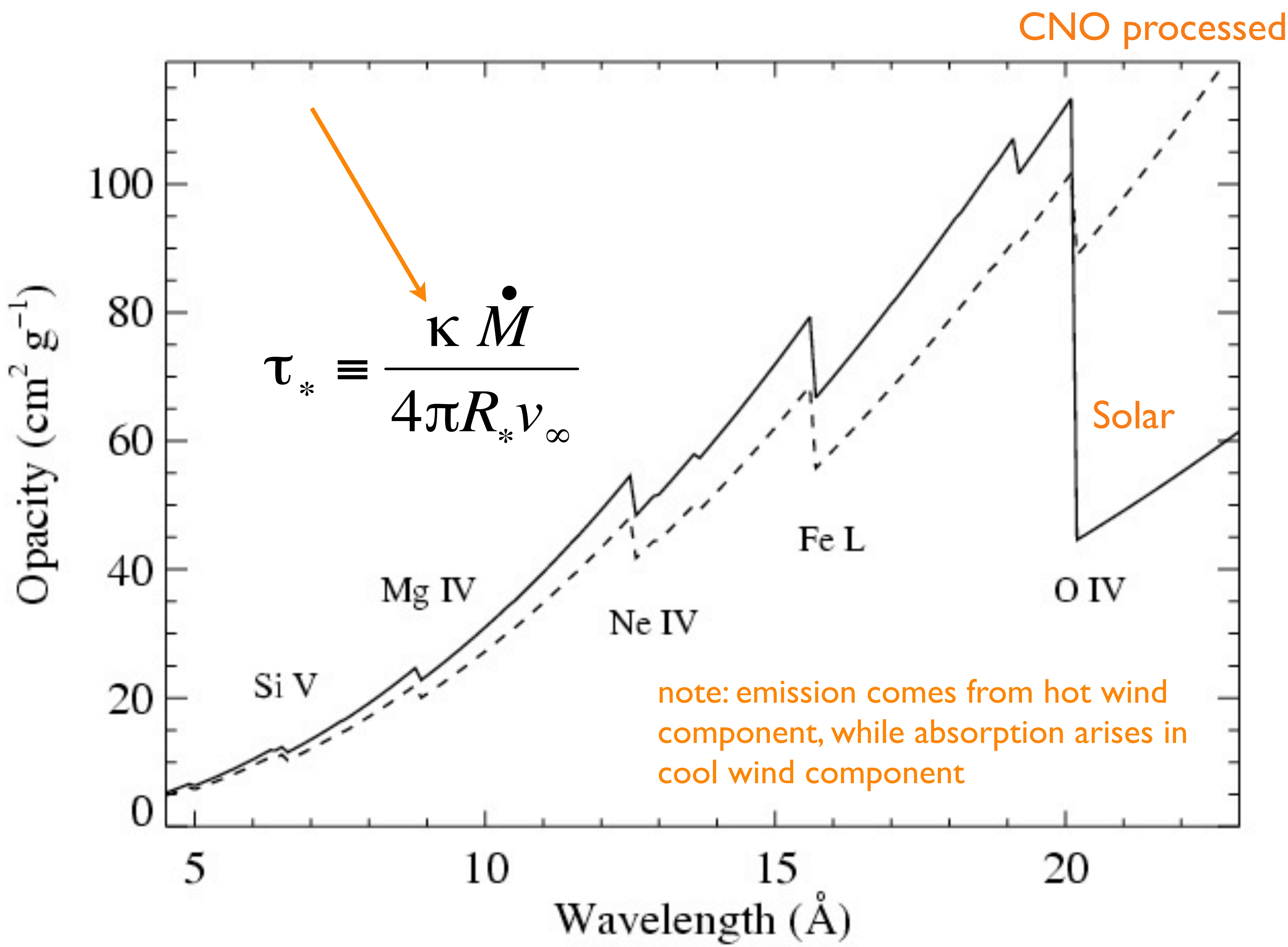

$$\tau_* \equiv \frac{\kappa \dot{M}}{4\pi R_* v_\infty}$$

note: emission comes from hot wind component, while absorption arises in cool wind component

Line profile shapes

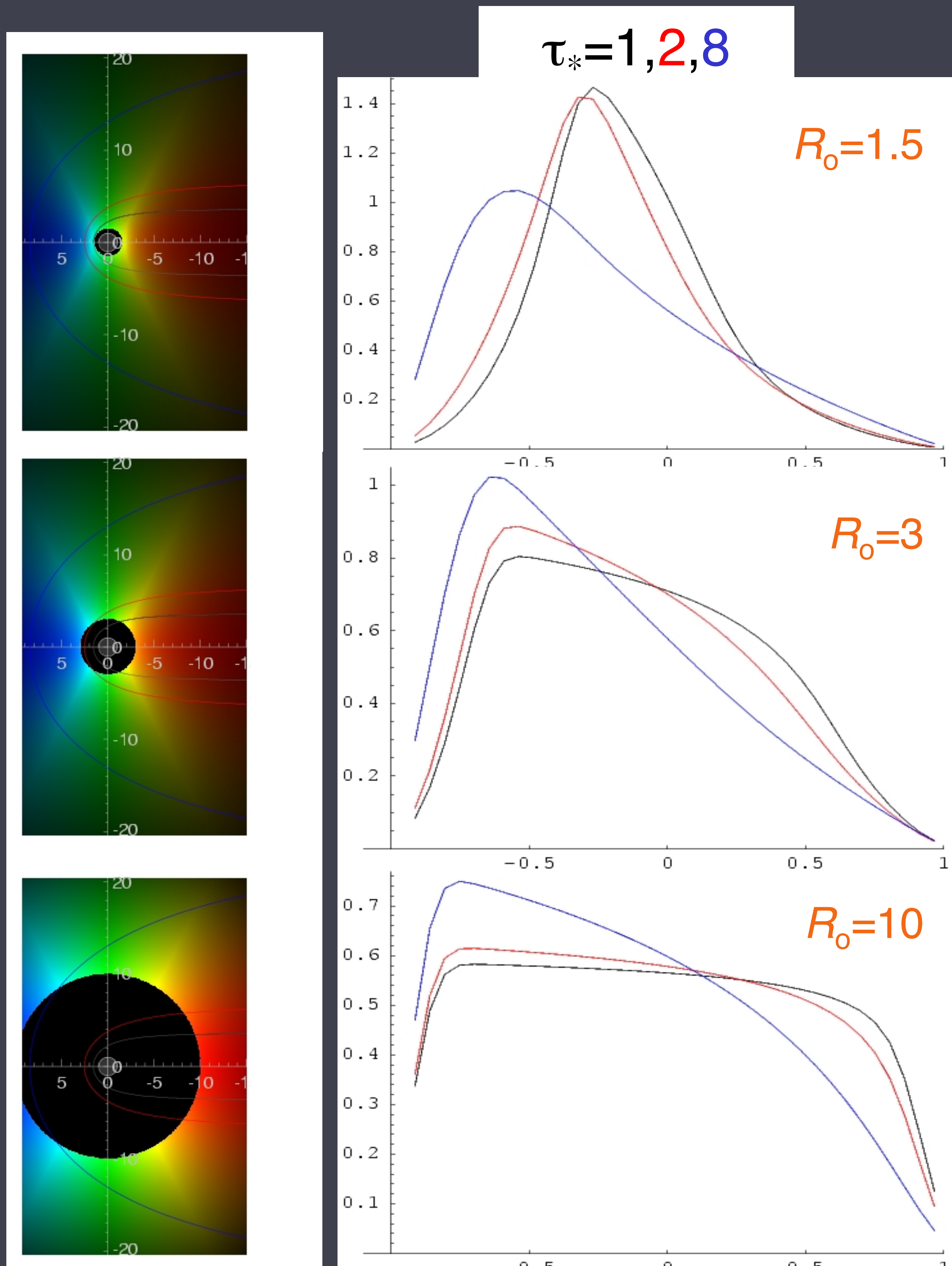

key parameters: R_o & $\tau_\star$

$$v = v_\infty(1 - r/R_\star)^\beta$$

$$j \sim \rho^2 \text{ for } r/R_* > R_o, \quad = 0 \text{ otherwise}$$

$$\tau = \tau_* \int_z^\infty \frac{R_* dz'}{r'^2 (1 - {R_*}/{r'})^\beta}$$

$$\tau_* \equiv \frac{\kappa \dot{M}}{4\pi R_* v_\infty}$$

$V_{shock} \sim 300$ km/s : $T \sim 10^6$ K

X-ray emission: we assume hot plasma follows beta-velocity law

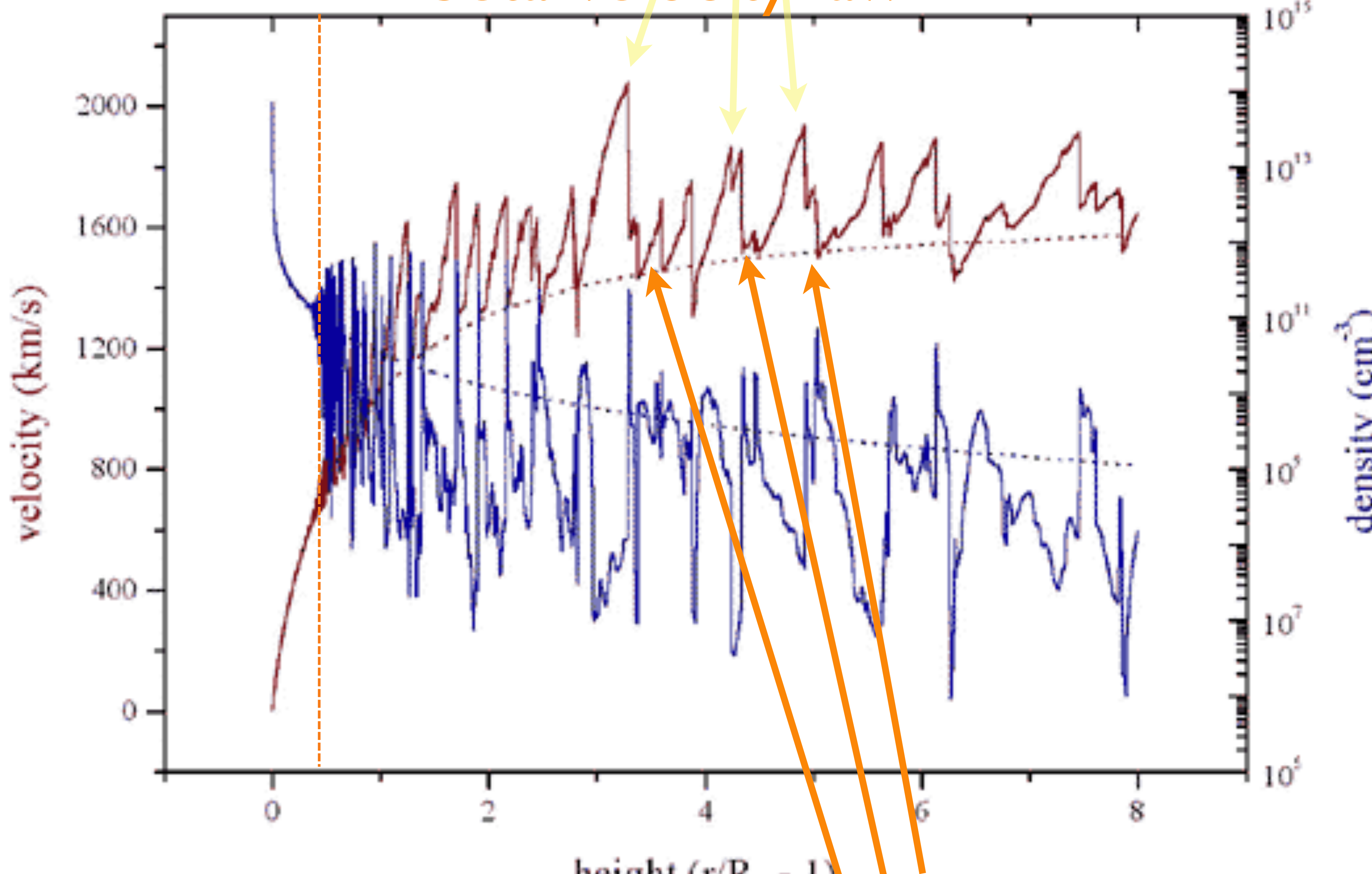

shocked wind plasma is decelerated back down to the local CAK wind velocity

ζ Pup: *Chandra* MEG

Fe XVII

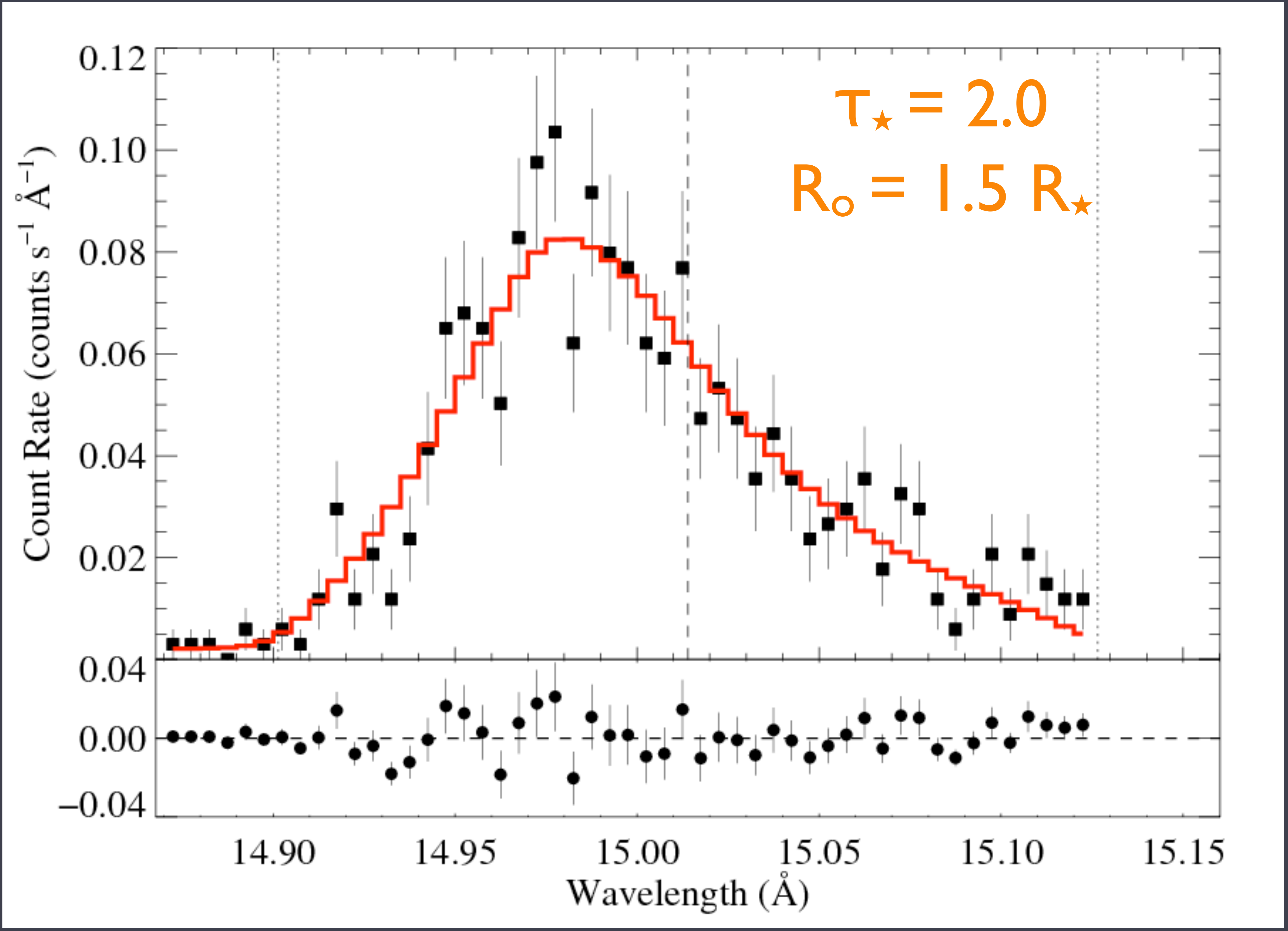

ζ Pup *Chandra*: three emission lines

Mg Lyα: 8.42 Å　　Ne Lyα: 12.13 Å　　O Lyα: 18.97 Å

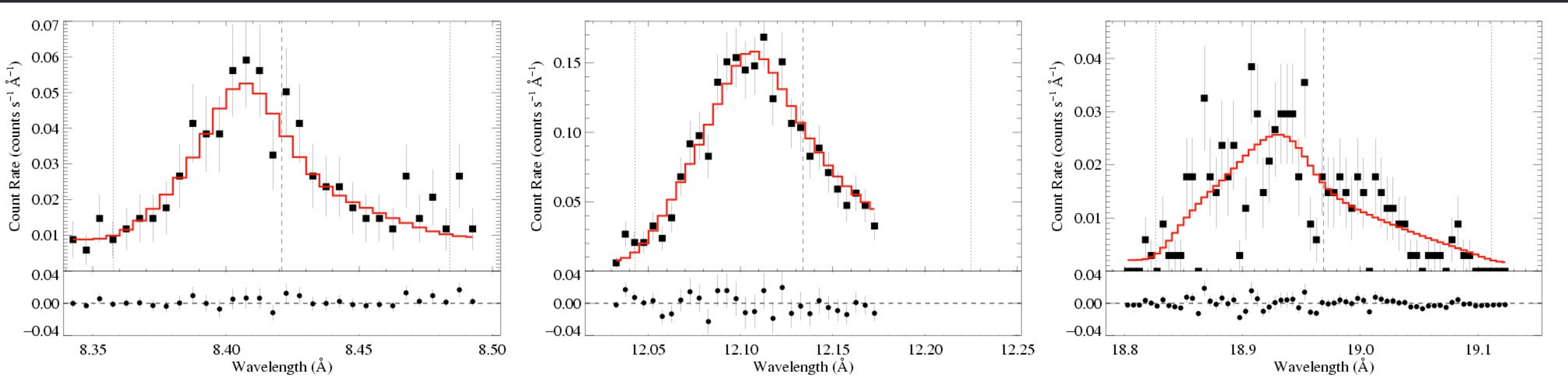

$\tau_* = 1$　　$\tau_* = 2$　　$\tau_* = 3$

Recall:

$$\tau_* \equiv \frac{\kappa \dot{M}}{4\pi R_* v_\infty}$$

Results from the 3 line fits shown previously

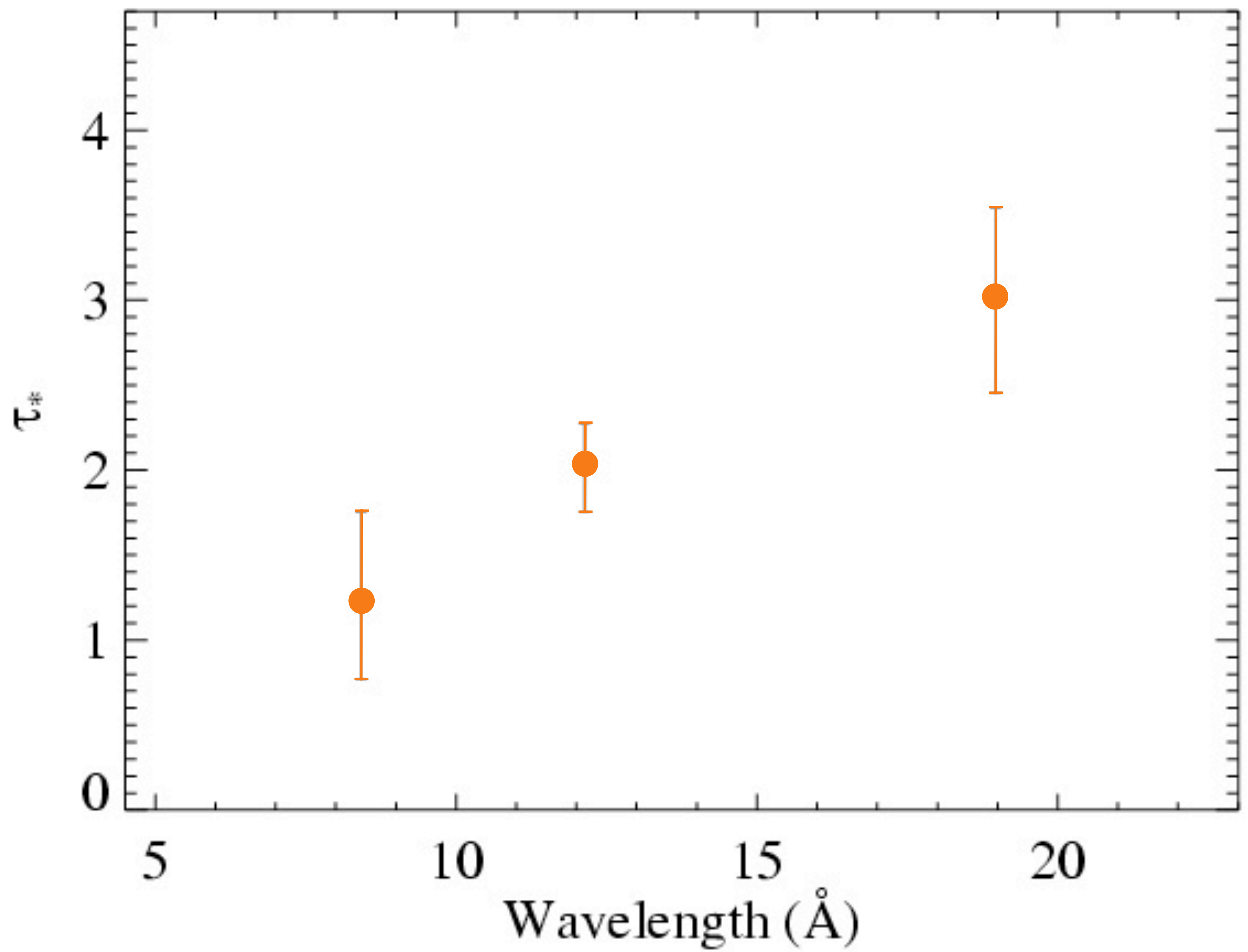

Fits to 16 lines in the *Chandra* spectrum of ζ Pup

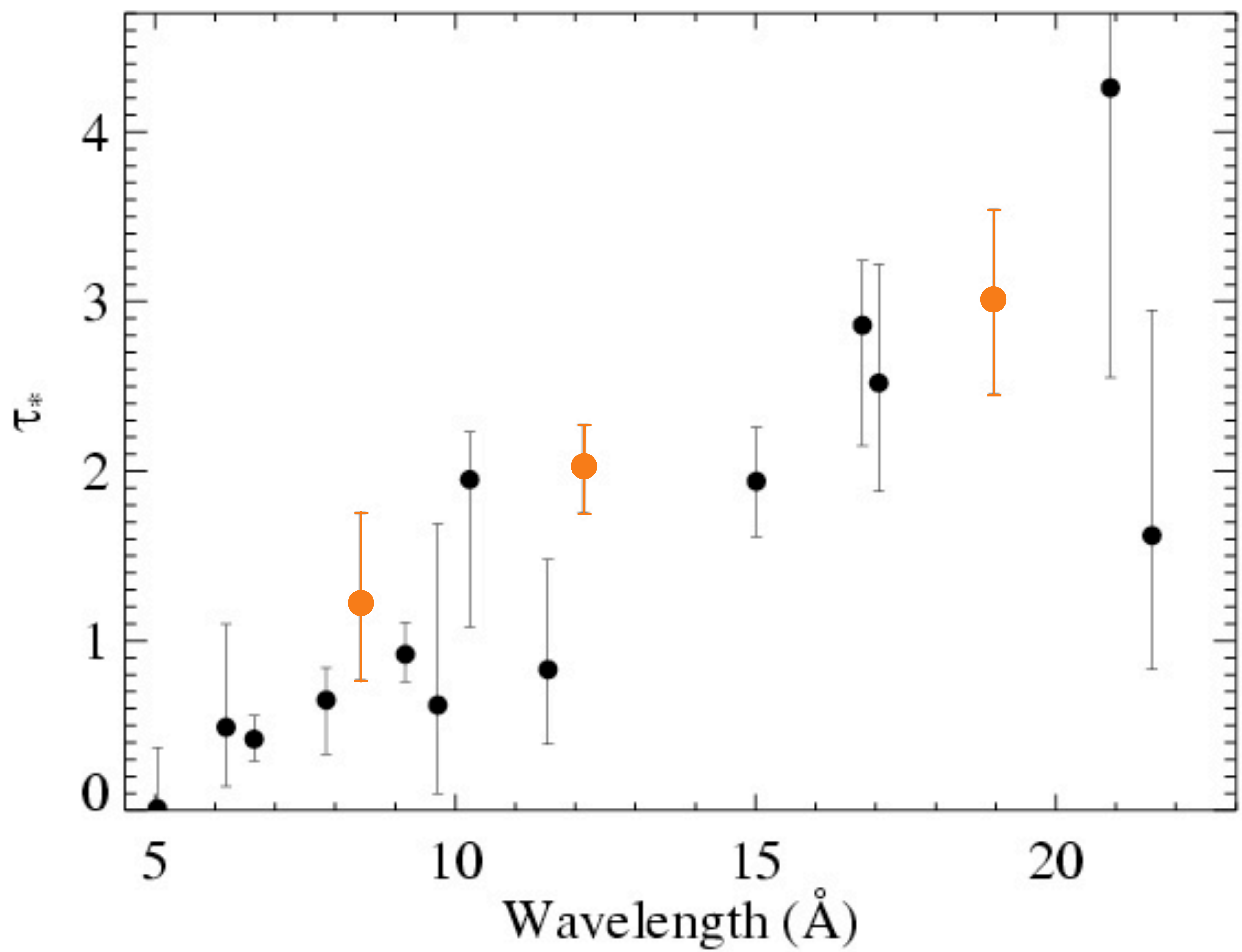

Fits to 16 lines in the *Chandra* spectrum of ζ Pup

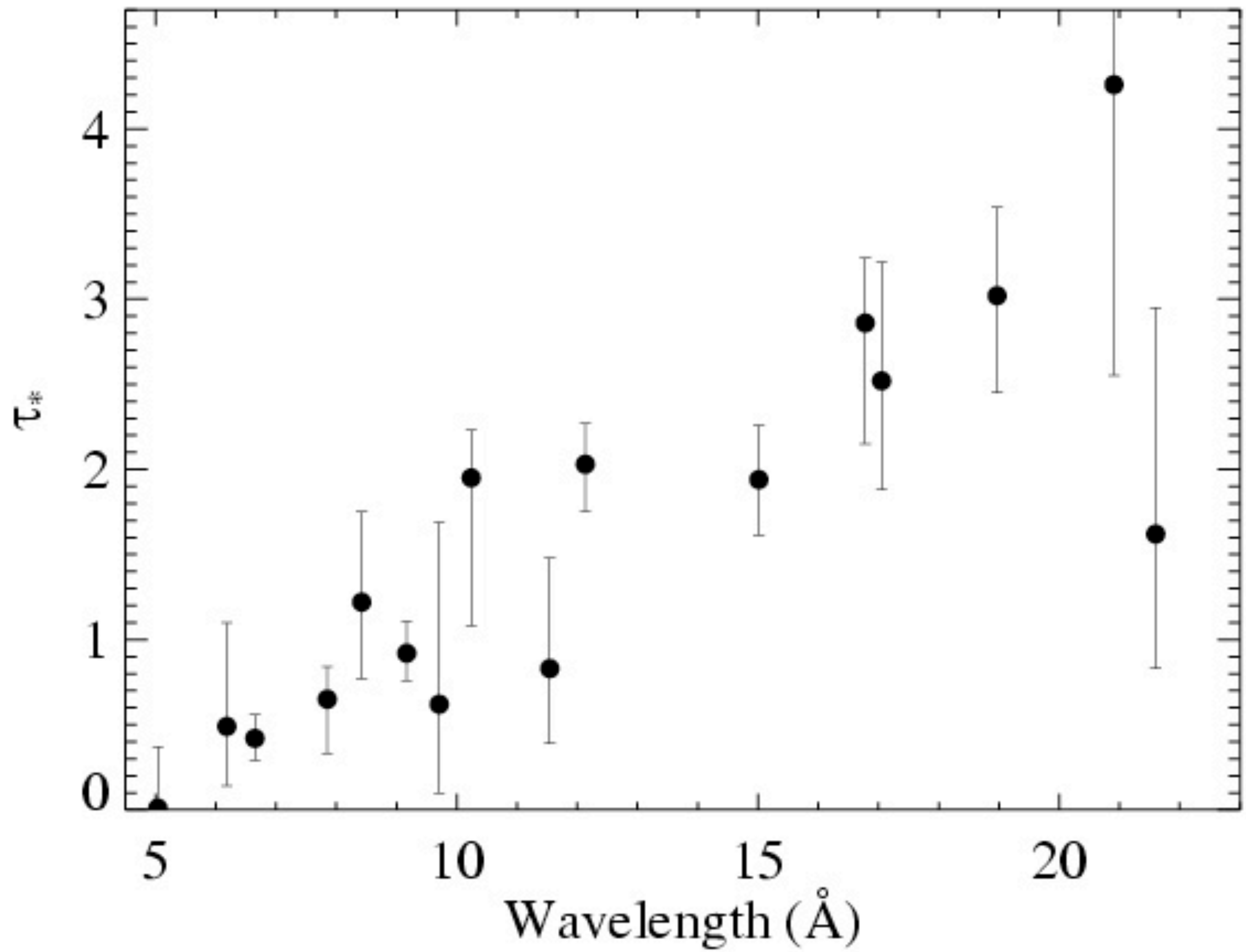

Fits to 16 lines in the *Chandra* spectrum of ζ Pup

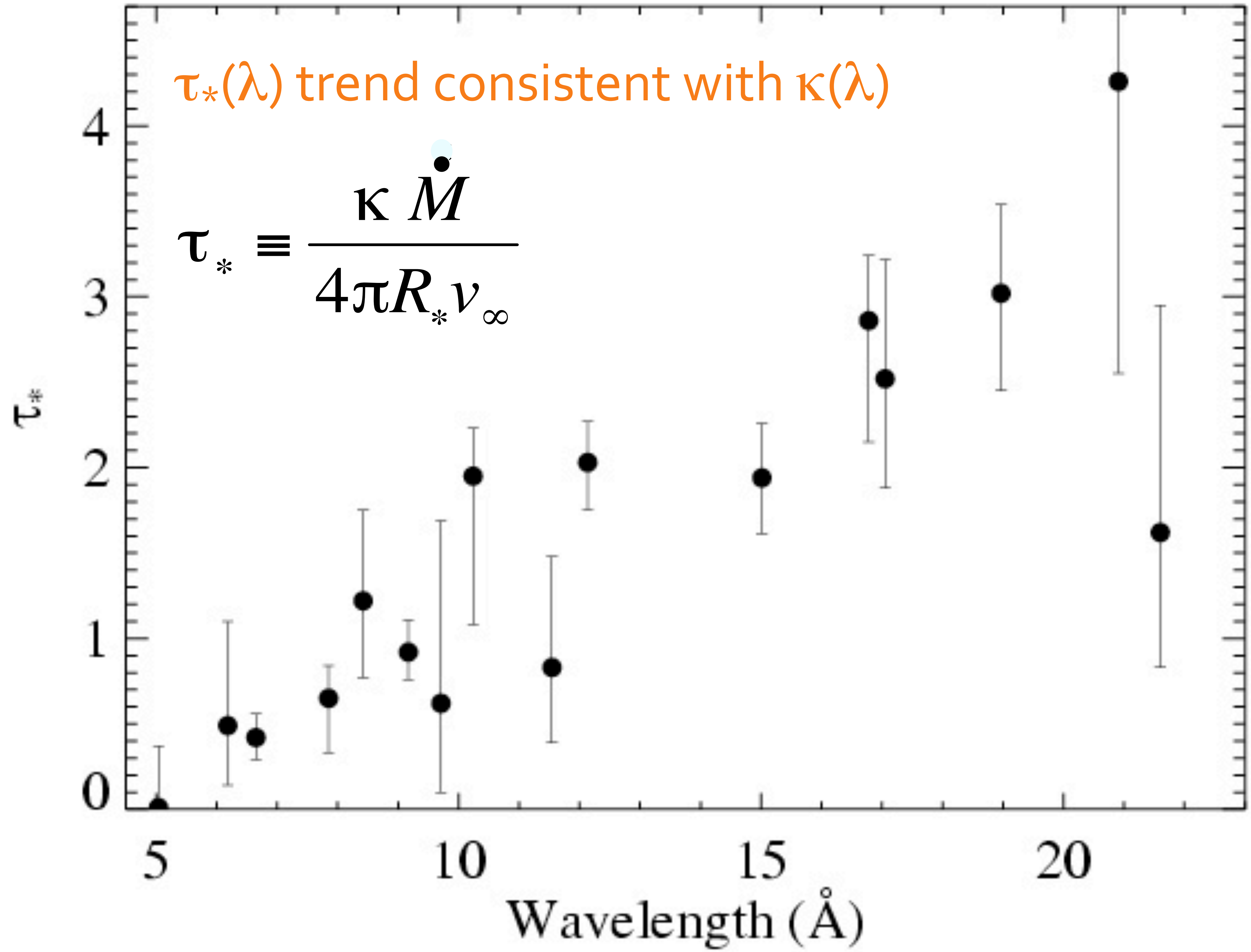

soft X-ray wind opacity

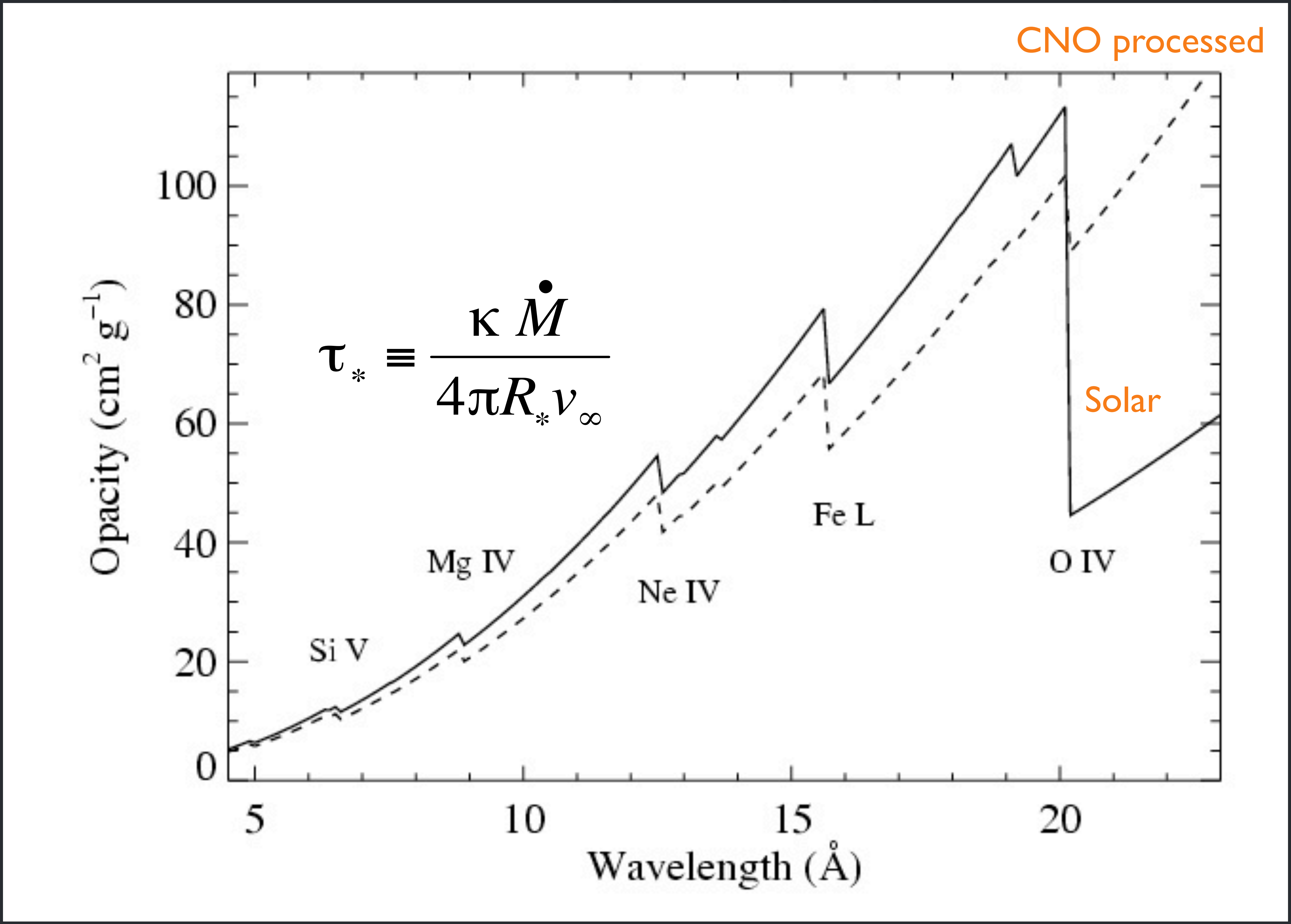

$$\tau_* \equiv \frac{\kappa \dot{M}}{4\pi R_* v_\infty}$$

$\dot{M}$ becomes the free parameter of the fit to the $\tau_*(\lambda)$ trend

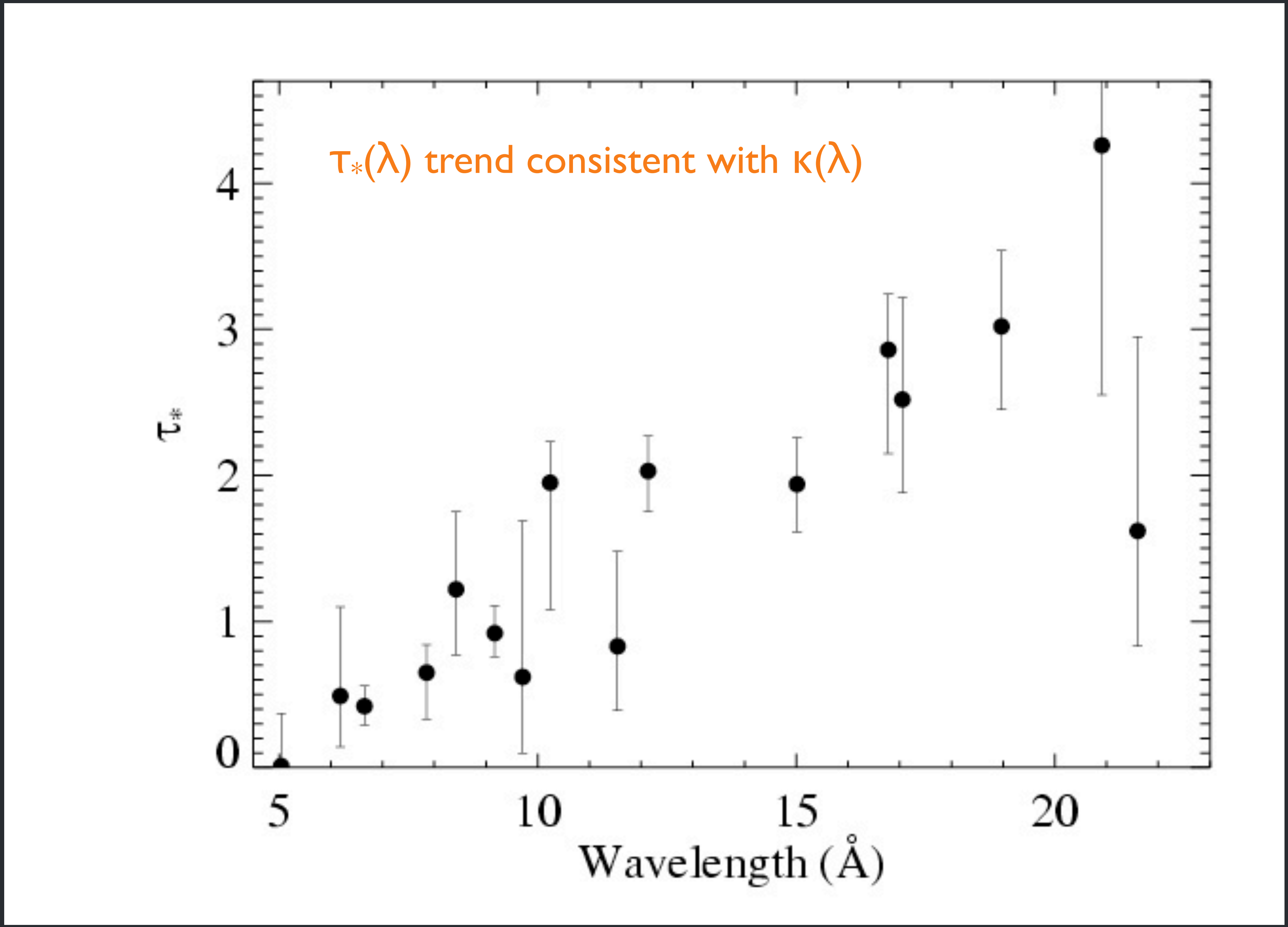

$$\tau_* \equiv \frac{\kappa \dot{M}}{4\pi R_* v_\infty}$$

$\dot{M}$ becomes the free parameter of the fit to the $\tau_*(\lambda)$ trend

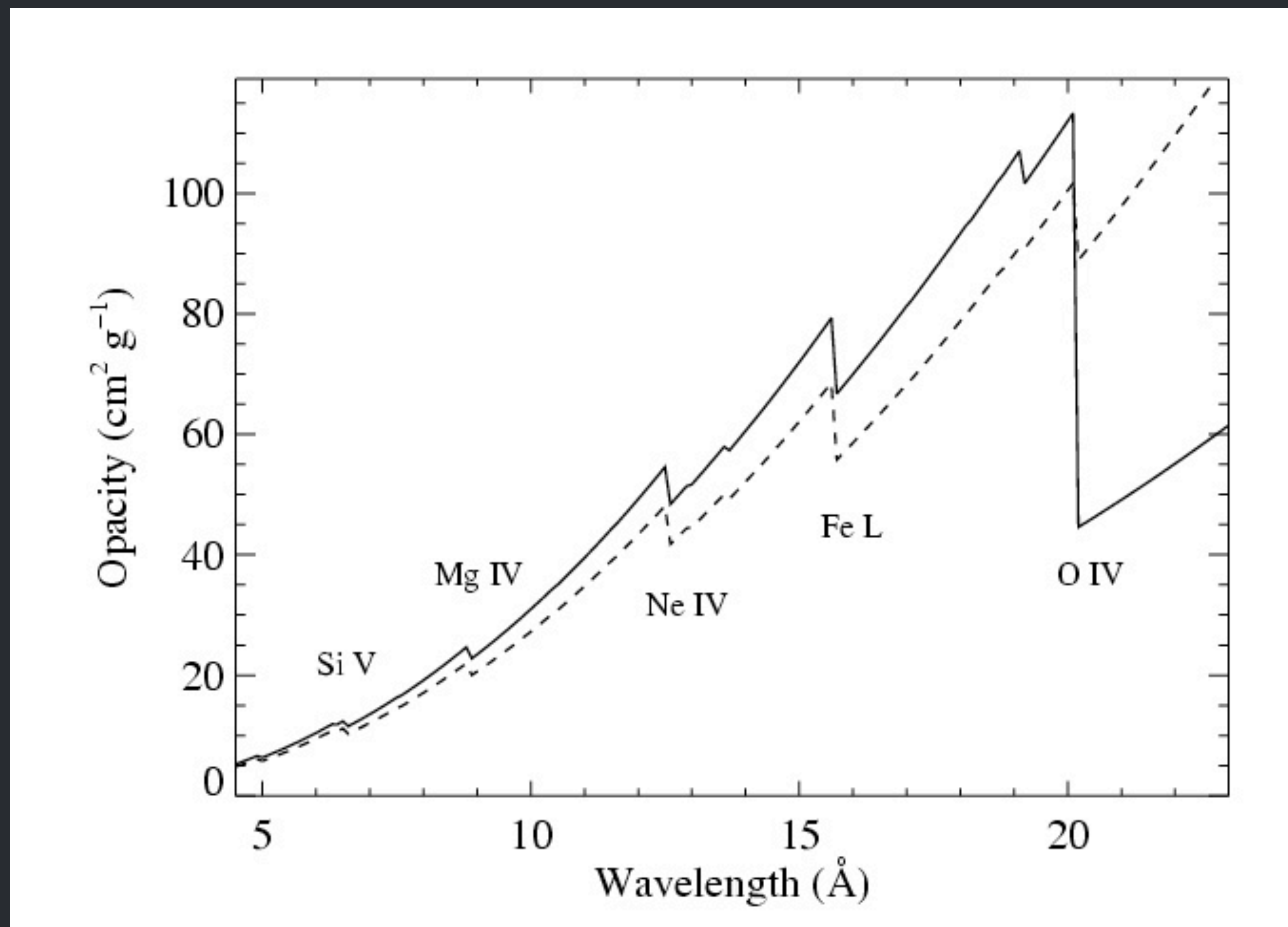

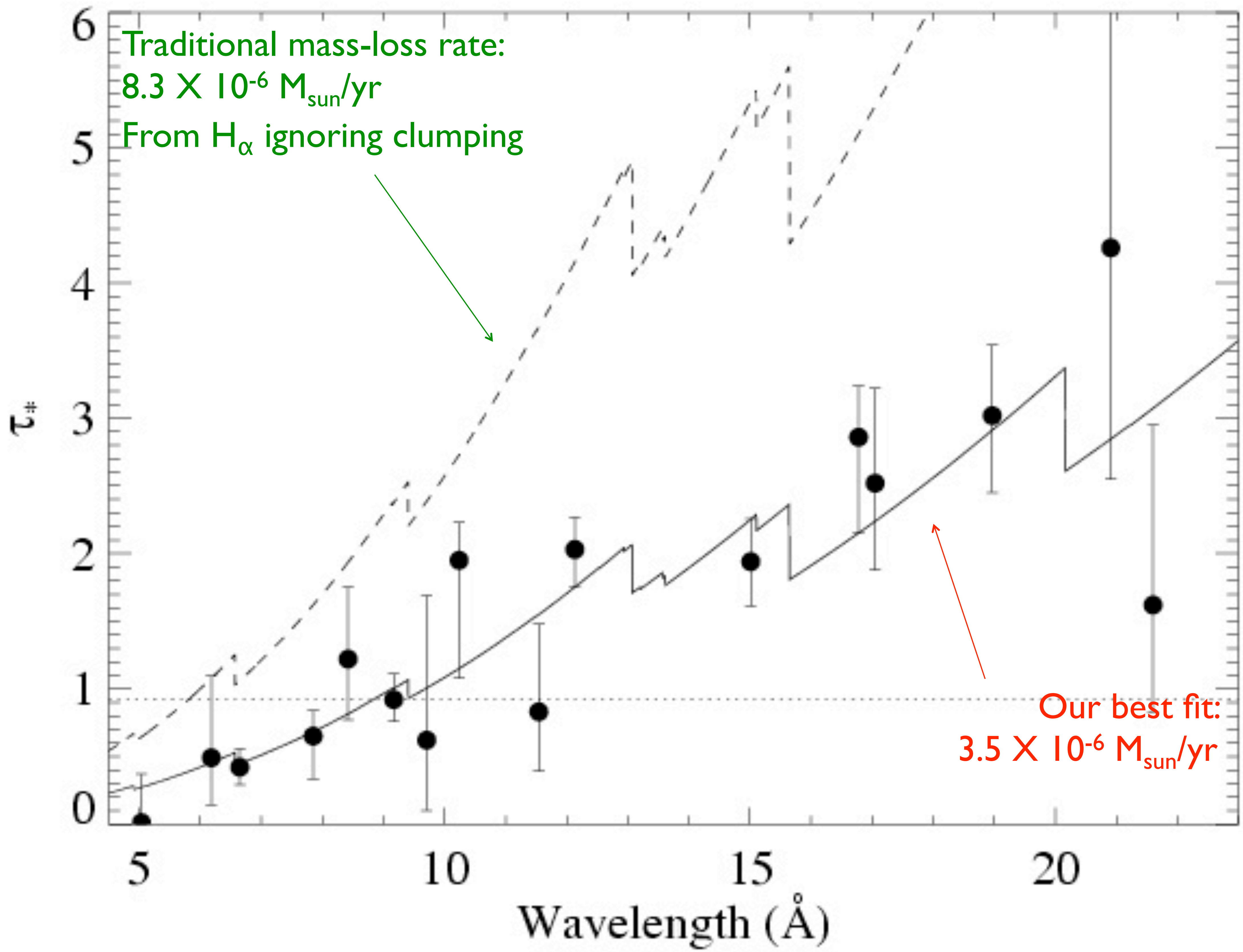
Traditional mass-loss rate:
8.3 X 10-6 Msun/yr
From Hα ignoring clumping
Our best fit:
3.5 X 10-6 Msun/yr
τ*
Wavelength (Å)
0
1
2
3
4
5
6
5
10
15
20

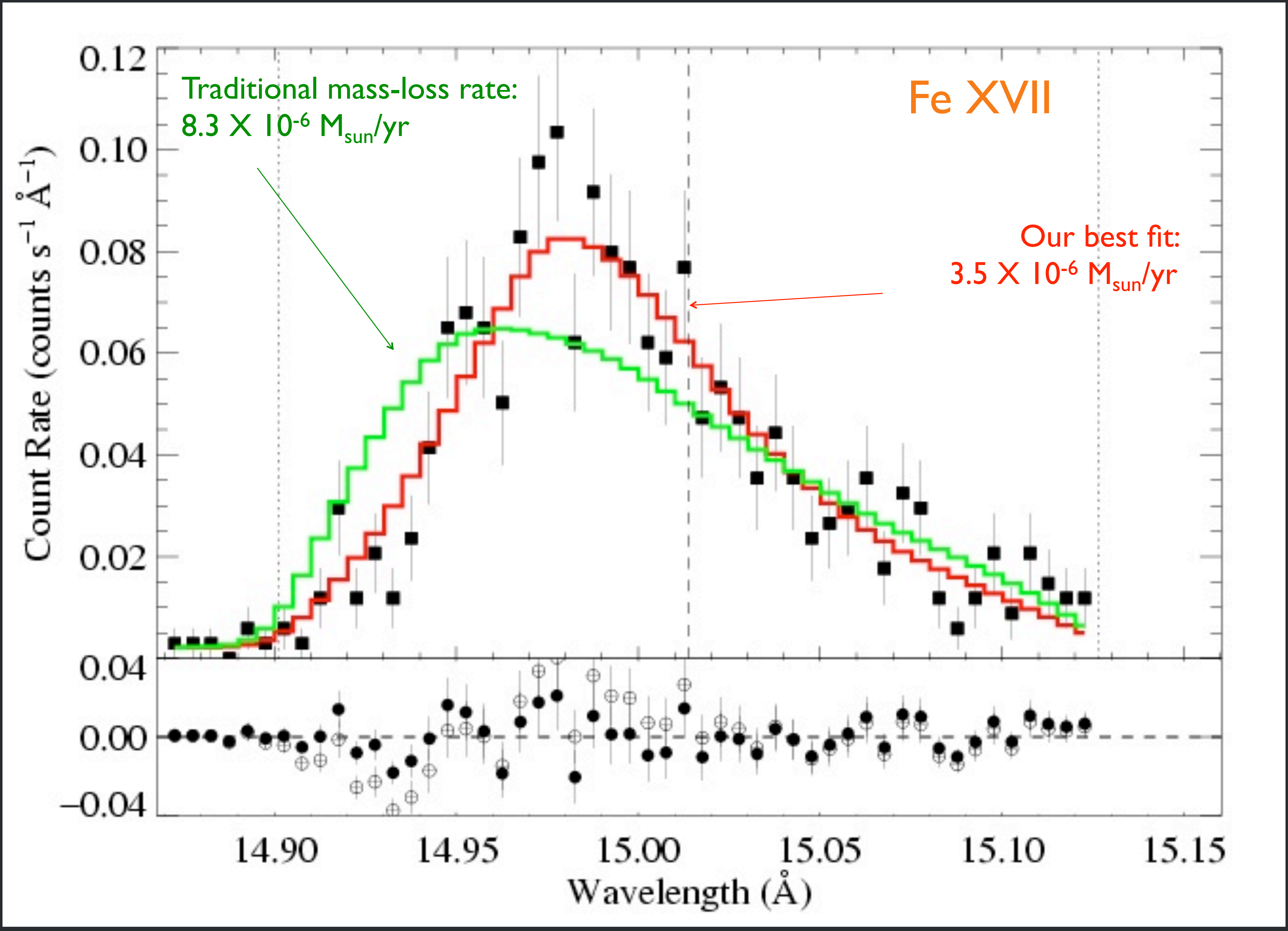
Traditional mass-loss rate:
8.3 X 10-6 Msun/yr
Fe XVII
Our best fit:
3.5 X 10-6 Msun/yr
Count Rate (counts s−1 Å−1)
0.12
0.10
0.08
0.06
0.04
0.02
0.04
0.00
−0.04
14.90
14.95
15.00
15.05
15.10
15.15
Wavelength (Å)

ζ Pup mass-loss rate < 4.2 x 10^{-6} M_{sun}/yr

Bright OB stars in the Galaxy

III. Constraints on the radial stratification of the clumping factor in hot star winds from a combined H_α, IR and radio analysis*

J. Puls[1], N. Markova[2], S. Scuderi[3], C. Stanghellini[4], O. G. Taranova[5], A. W. Burnley[6] and I. D. Howarth[6]

[1] Universitäts-Sternwarte München, Scheinerstr. 1, D-81679 München, Germany, e-mail: uh101aw@usm.uni-muenchen.de
[2] Institute of Astronomy, Bulgarian National Astronomical Observatory, P.O. Box 136, 4700 Smoljan, Bulgaria, e-mail: nmarkova@astro.bas.bg
[3] INAF - Osservatorio Astrofisico di Catania, Via S. Sofia 78, I-95123 Catania, Italy, e-mail: scuderi@oact.inaf.it
[4] INAF - Istituto di Radioastronomia, Via P. Gobetti 101, I-40129 Bologna, Italy, e-mail: c.stanghellini@ira.inaf.it
[5] Sternberg Astronomical Institute, Universitetski pr. 13, Moscow, 119992, Russia, e-mail: taranova@sai.msu.ru
[6] Department of Physics and Astronomy, University College London, Gower Street, London WC1E 6BT, UK, e-mail: awxb@star.ucl.ac.uk, idh@star.ucl.ac.uk

Received; accepted

Abstract. Recent results strongly challenge the canonical picture of massive star winds: various evidence indicates that currently accepted mass-loss rates, $\dot{M}$, may need to be revised downwards, by factors extending to one magnitude or even more. This is because the most commonly used mass-loss diagnostics are affected by "clumping" (small-scale density inhomogeneities), influencing our interpretation of observed spectra and fluxes.
Such downward revisions would have dramatic consequences for the evolution of, and feedback from, massive stars, and thus robust determinations of the clumping properties and mass-loss rates are urgently needed. We present a first attempt concerning this objective, by means of constraining the radial stratification of the so-called clumping factor.
To this end, we have analyzed a sample of 19 Galactic O-type supergiants/giants, by combining our own and archival data for H_α, IR, mm and radio fluxes, and using approximate methods, calibrated to more sophisticated models. Clumping has been included into our analysis in the "conventional" way, by assuming the inter-clump matter to be void. Because (almost) all our diagnostics depends on the square of density, we cannot derive absolute clumping factors, but only factors normalized to a certain minimum.
This minimum was usually found to be located in the outermost, radio-emitting region, i.e., the radio mass-loss rates are the lowest ones, compared to $\dot{M}$ derived from H_α and the IR. The radio rates agree well with those predicted by theory, but are only upper limits, due to unknown clumping in the outer wind. H_α turned out to be a useful tool to derive the clumping properties inside $r < 3 \ldots 5 R_\star$. Our most important result concerns a (physical) difference between denser and thinner winds: for denser winds, the innermost region is more strongly clumped than the outermost one (with a normalized clumping factor of 4.1 ± 1.4), whereas thinner winds have similar clumping properties in the inner and outer regions.
Our findings are compared with theoretical predictions, and the implications are discussed in detail, by assuming different scenarios regarding the still unknown clumping properties of the outer wind.

ζ Pup: radially varying clumping

for $\dot{M} = 3.5 \times 10^{-6}\ M_{sun}/yr$

$f_{cl} \equiv \langle\rho^2\rangle/\langle\rho\rangle^2$

f_{cl} = 1.3 @ r < 1 .12 R_*
f_{cl} = 6.0 @ 1.12 < r < 1.5 R_*
f_{cl} = 3.7 @ 1.5 < r < 2 R_*
f_{cl} = 2.6 @ 2 < r < 15 R_*
f_{cl} = 1.3 @ r > 15 R_*

Hα IR radio

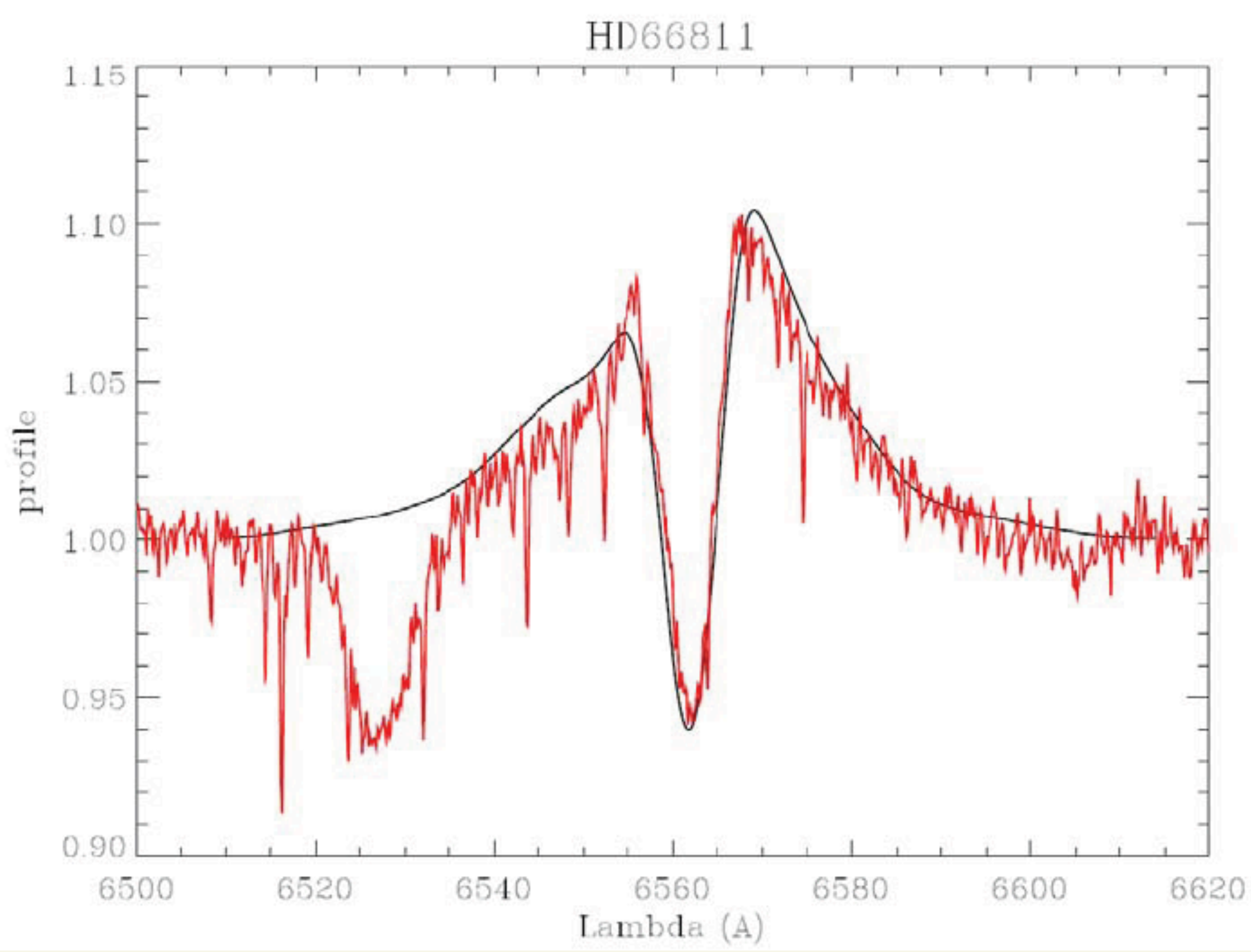

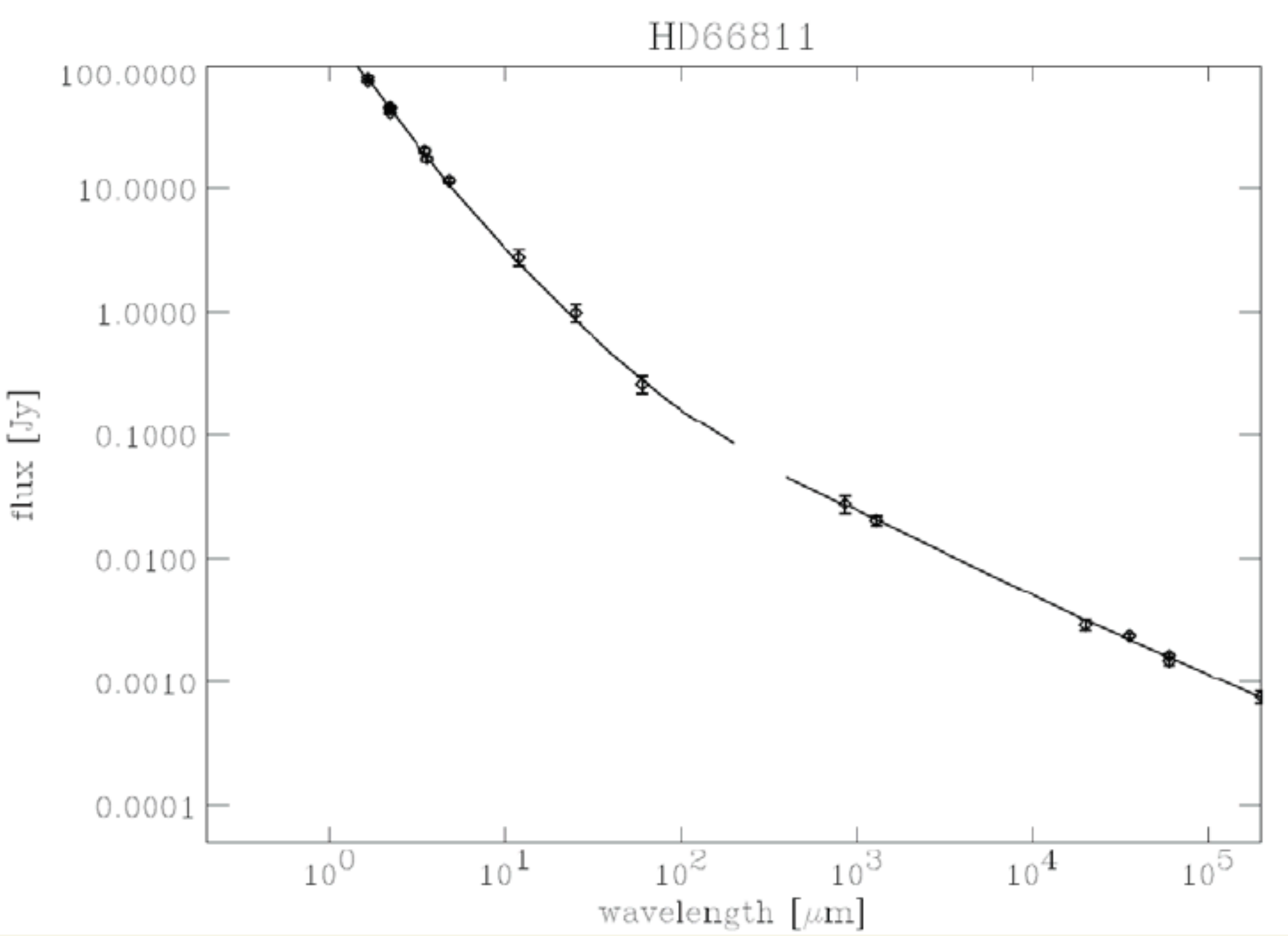

ζ Pup: radially varying clumping

for $\dot{M} = 3.5 \times 10^{-6}\ M_{sun}/yr$

$f_{cl} = 1.3$ @ $r < 1.12\ R_*$
$f_{cl} = 6.0$ @ $1.12 < r < 1.5\ R_*$
$f_{cl} = 3.7$ @ $1.5 < r < 2\ R_*$
$f_{cl} = 2.6$ @ $2 < r < 15\ R_*$
$f_{cl} = 1.3$ @ $r > 15\ R_*$

$f_{cl} \equiv \langle\rho^2\rangle / \langle\rho\rangle^2$

$$\dot{M}_{cl} \equiv \dot{M}_{smooth} / f_{cl}^{0.5}$$

ignoring clumping overestimates mass-loss rates by a factor of $\sqrt{f_{cl}}$

ζ Pup: radially varying clumping

for $\dot{M} = 3.5 \times 10^{-6}\ M_{sun}/yr$

consistent multi-wavelength fit with a single mass-loss rate

$f_{cl} = 1.3$ @ $r < 1.12\ R_*$
$f_{cl} = 6.0$ @ $1.12 < r < 1.5\ R_*$
$f_{cl} = 3.7$ @ $1.5 < r < 2\ R_*$
$f_{cl} = 2.6$ @ $2 < r < 15\ R_*$
$f_{cl} = 1.3$ @ $r > 15\ R_*$

Hα IR radio

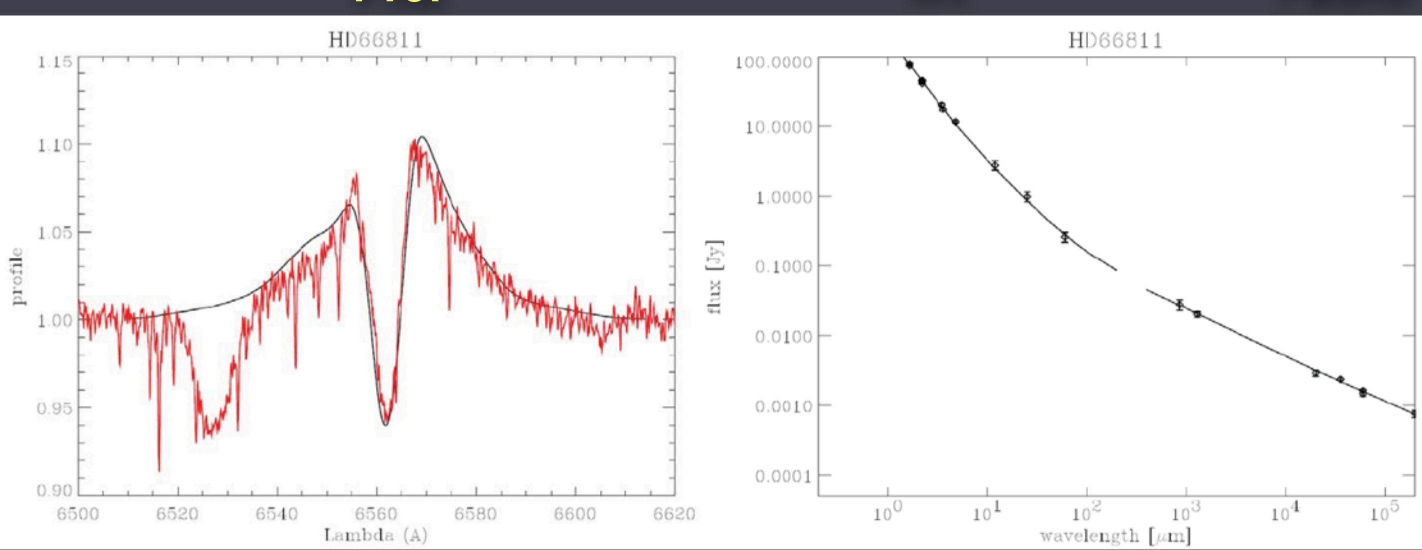

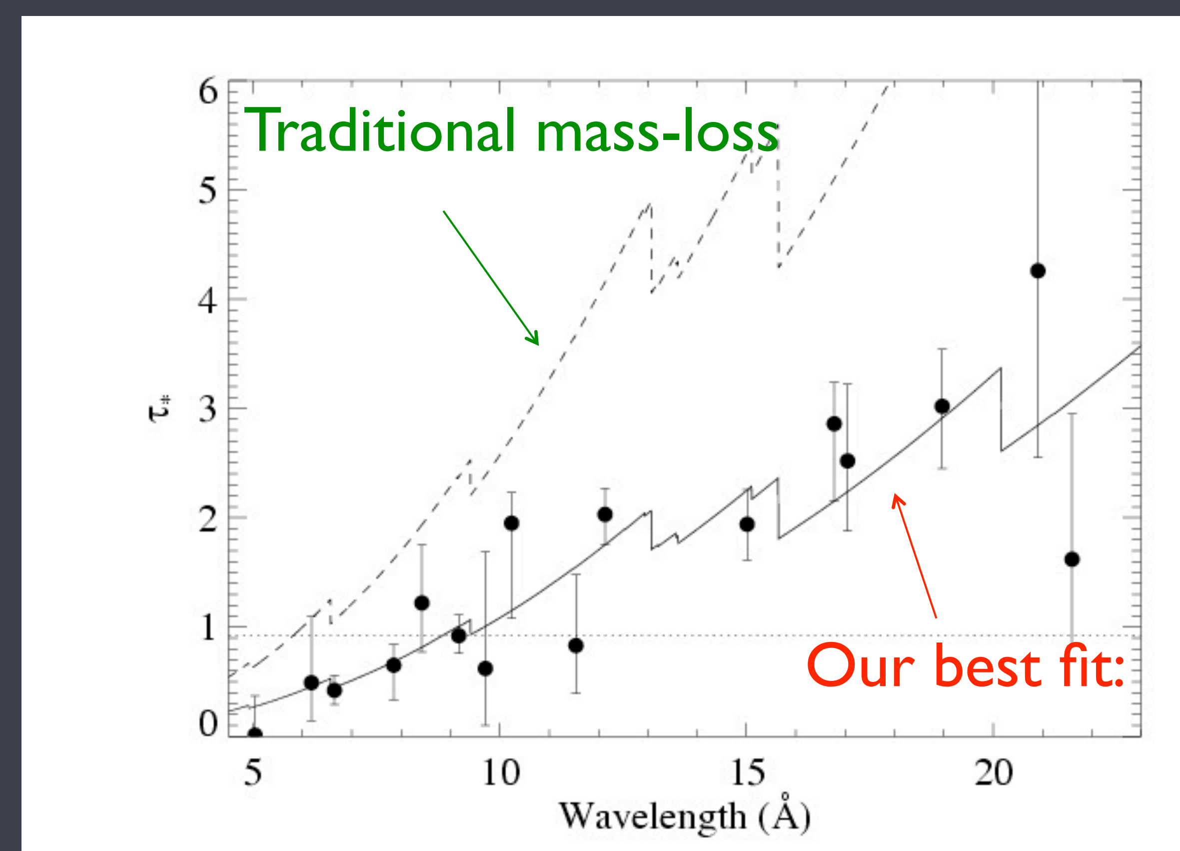

Hot plasma kinematics and location

R_o controls the line width via v(r)

$R_o = 1.5\ R_\star$

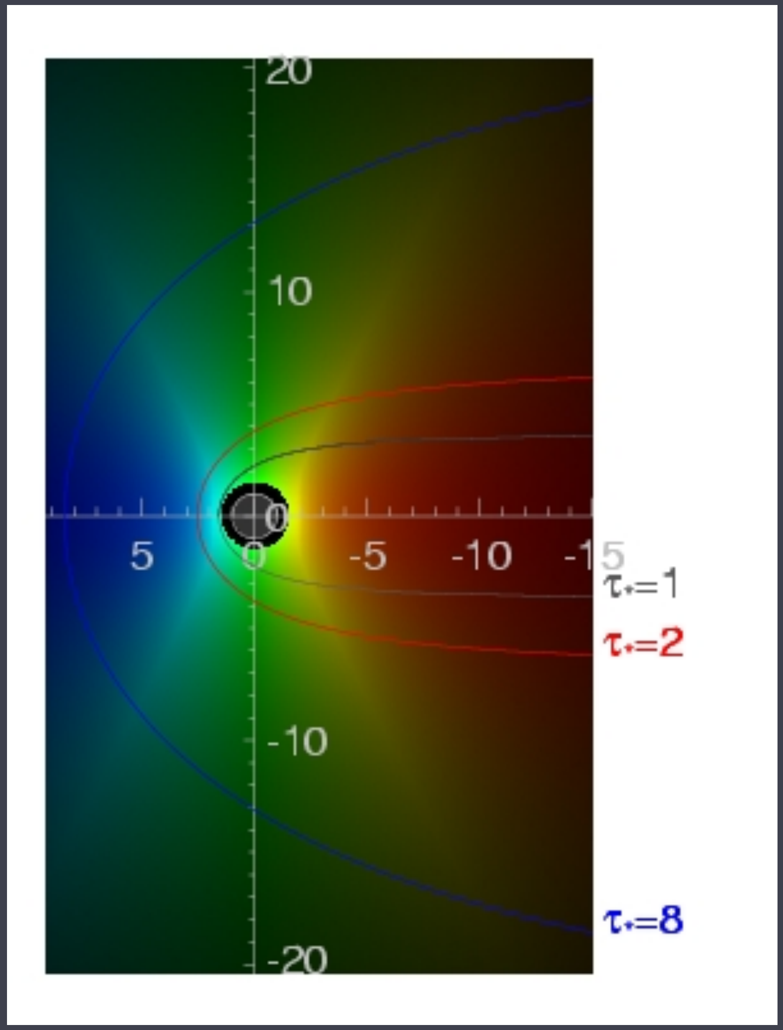

$R_o = 3\ R_\star$

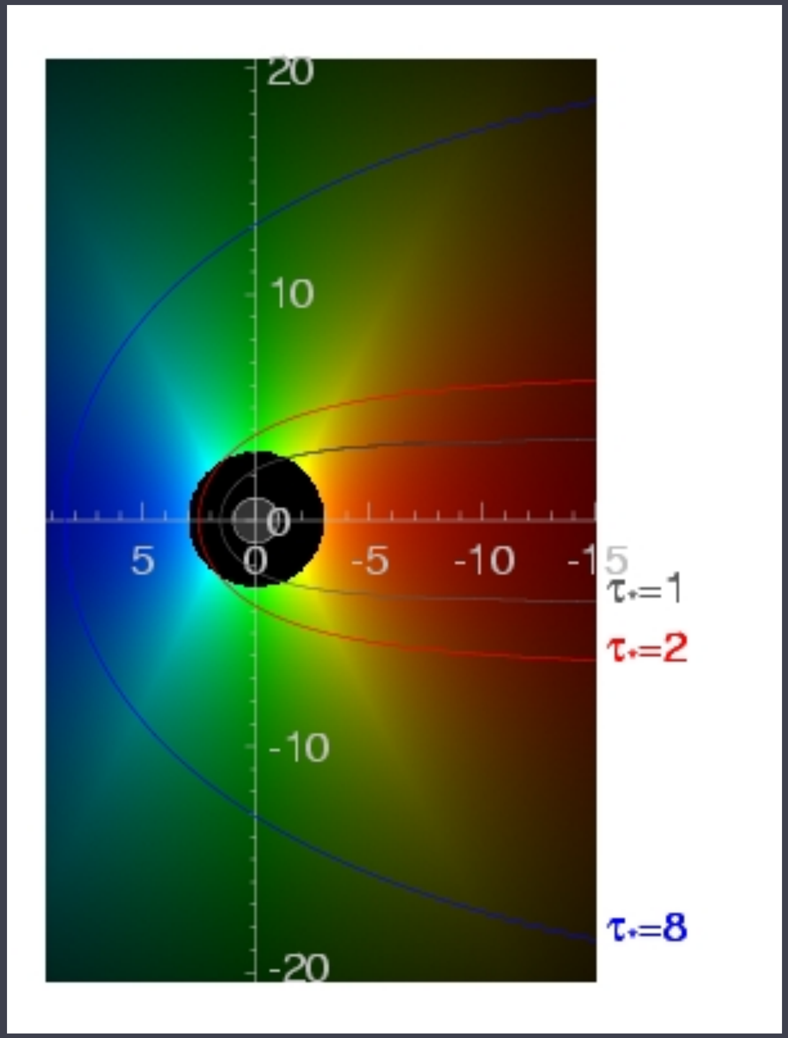

$R_o = 10\ R_\star$

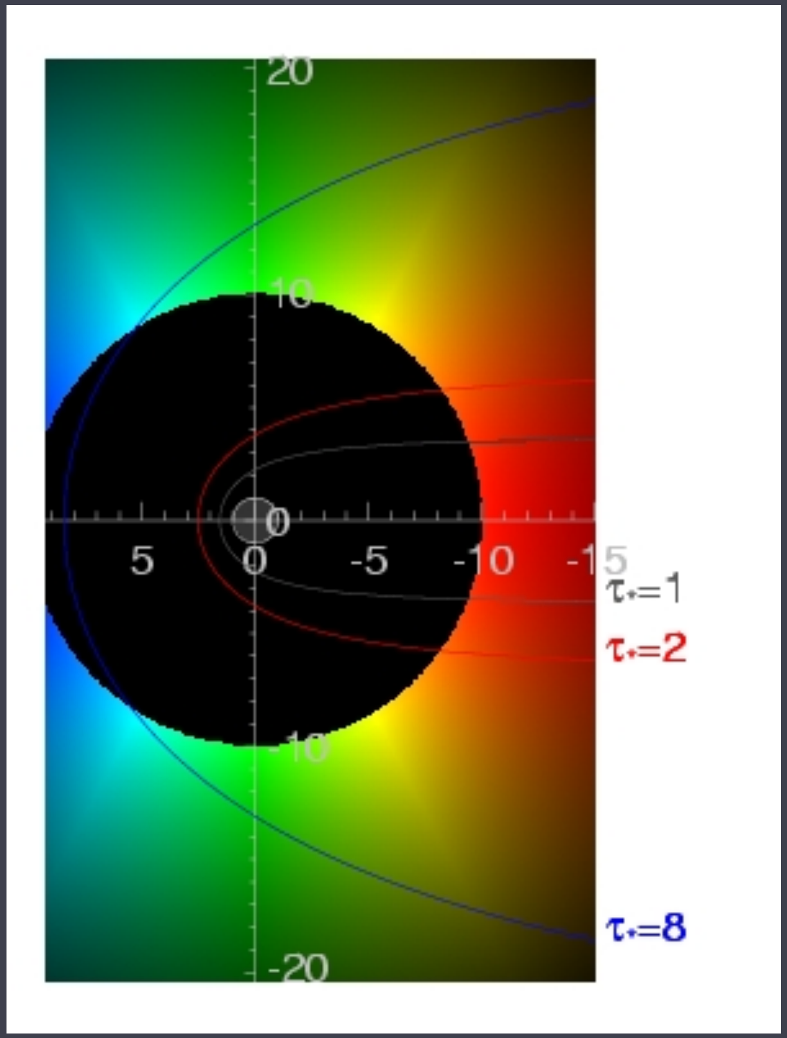

Distribution of R_o values for ζ Pup

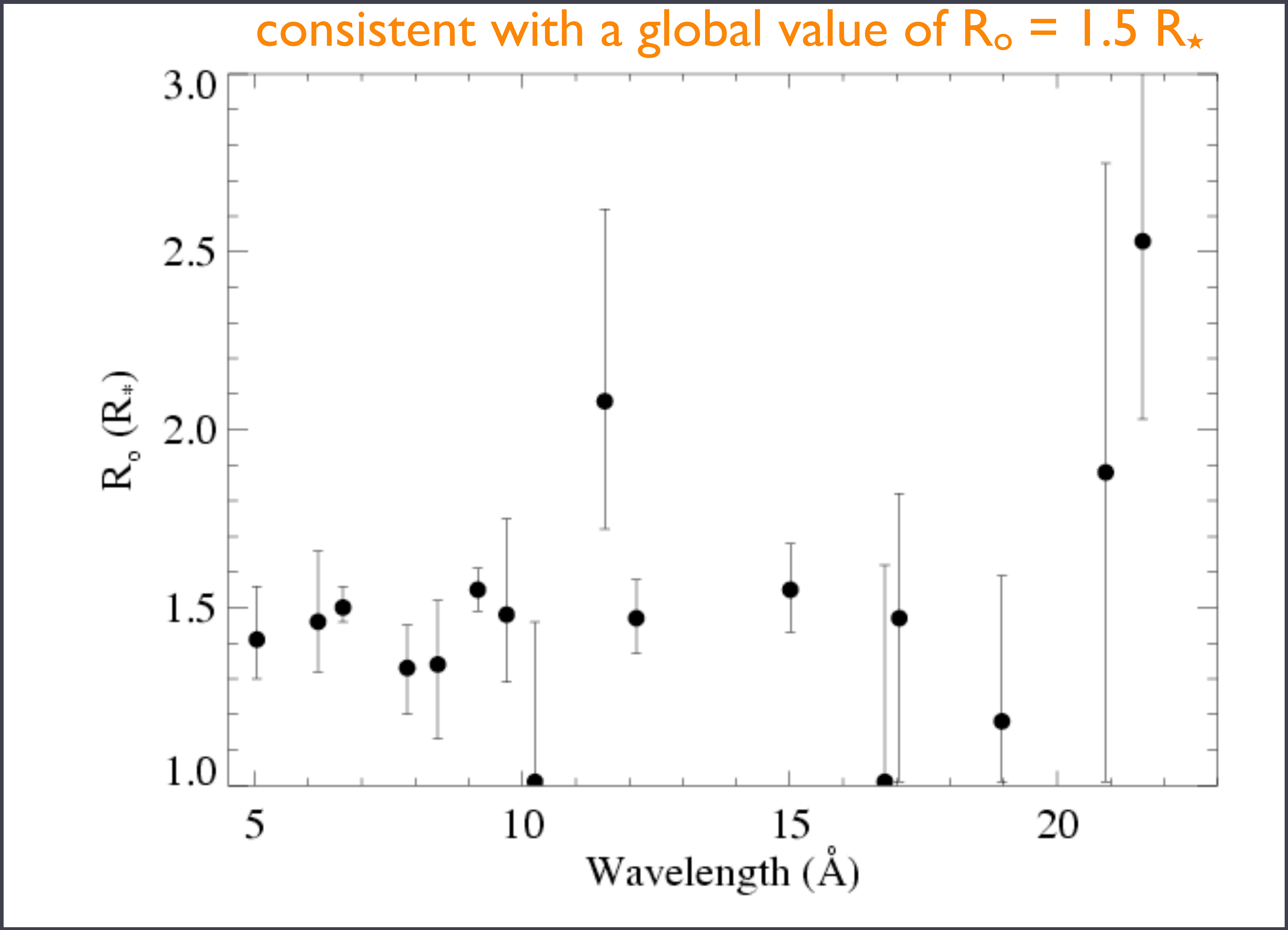

v_∞ can be constrained by the line fitting too

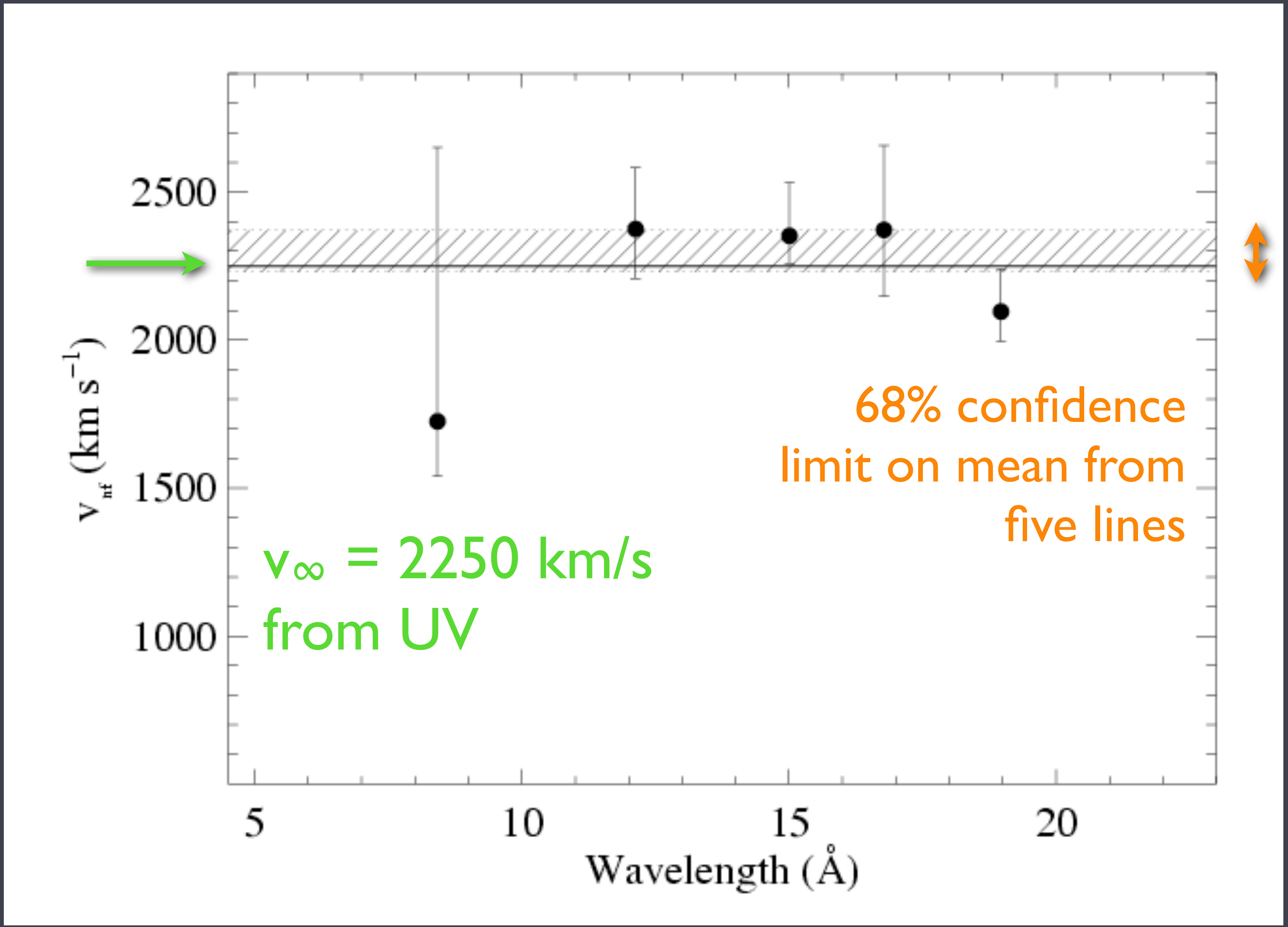

X-ray plasma and mean wind have same kinematics

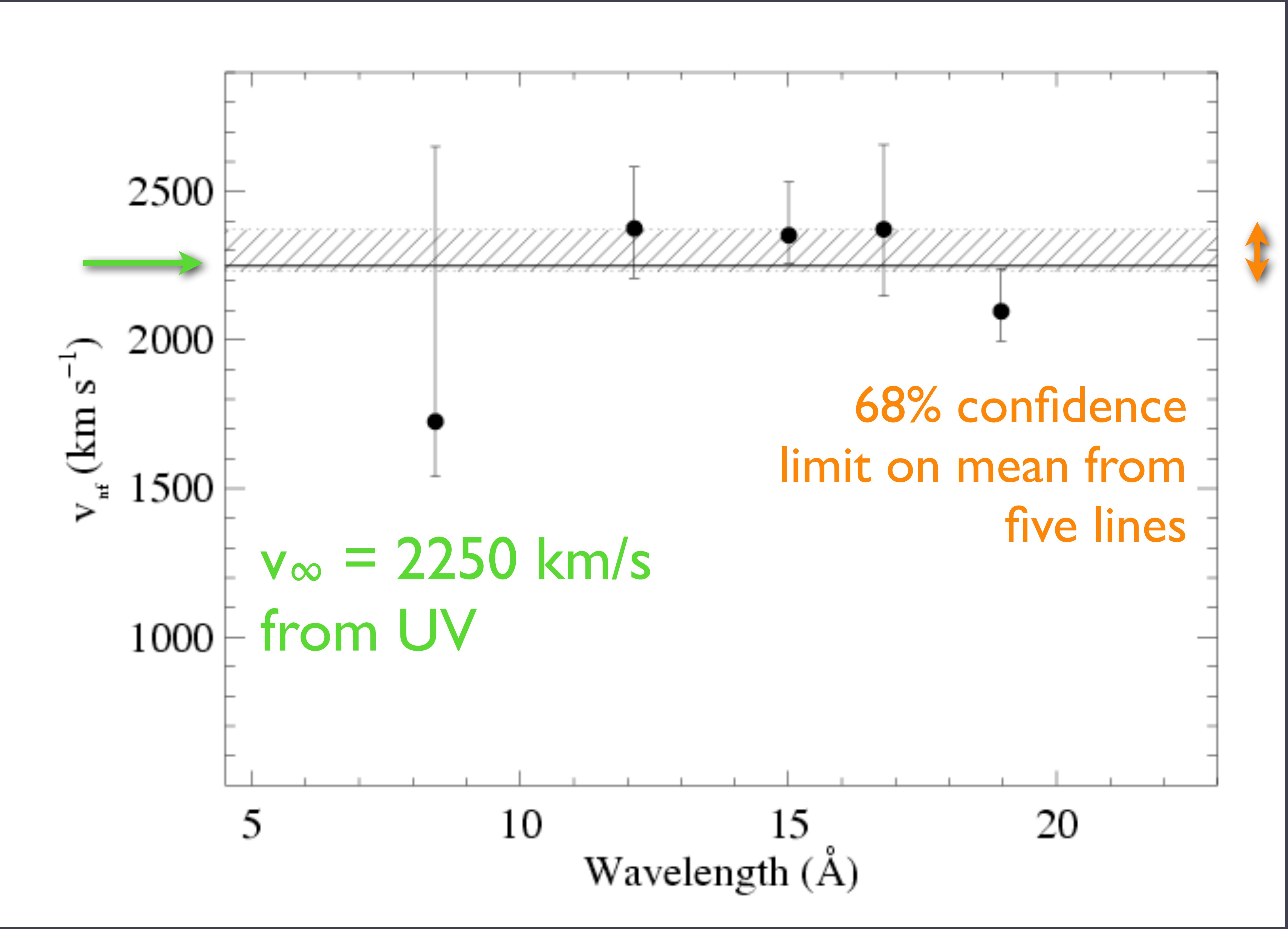

Other Stars?

HD 93129A

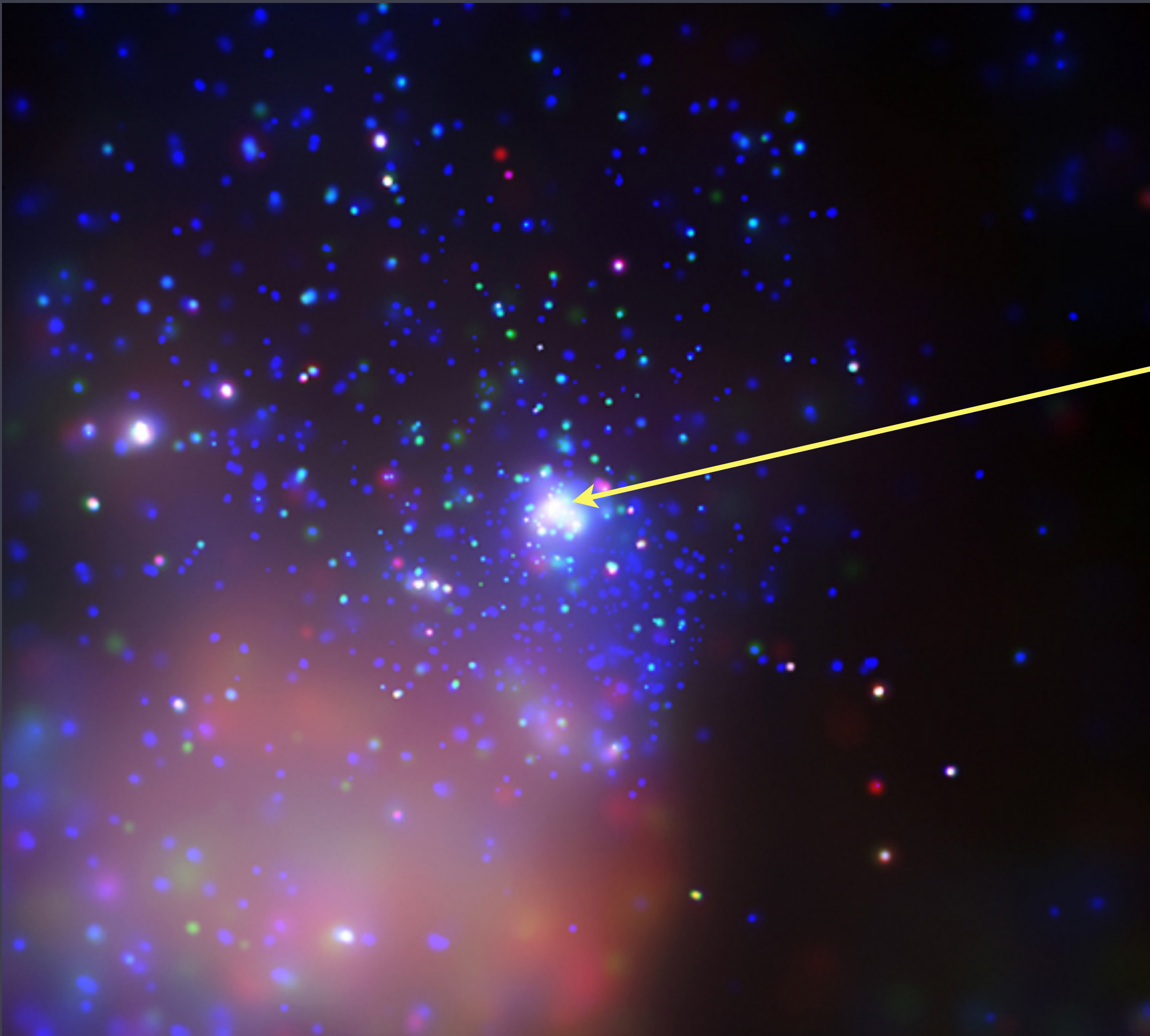

Tr 14: *Chandra*

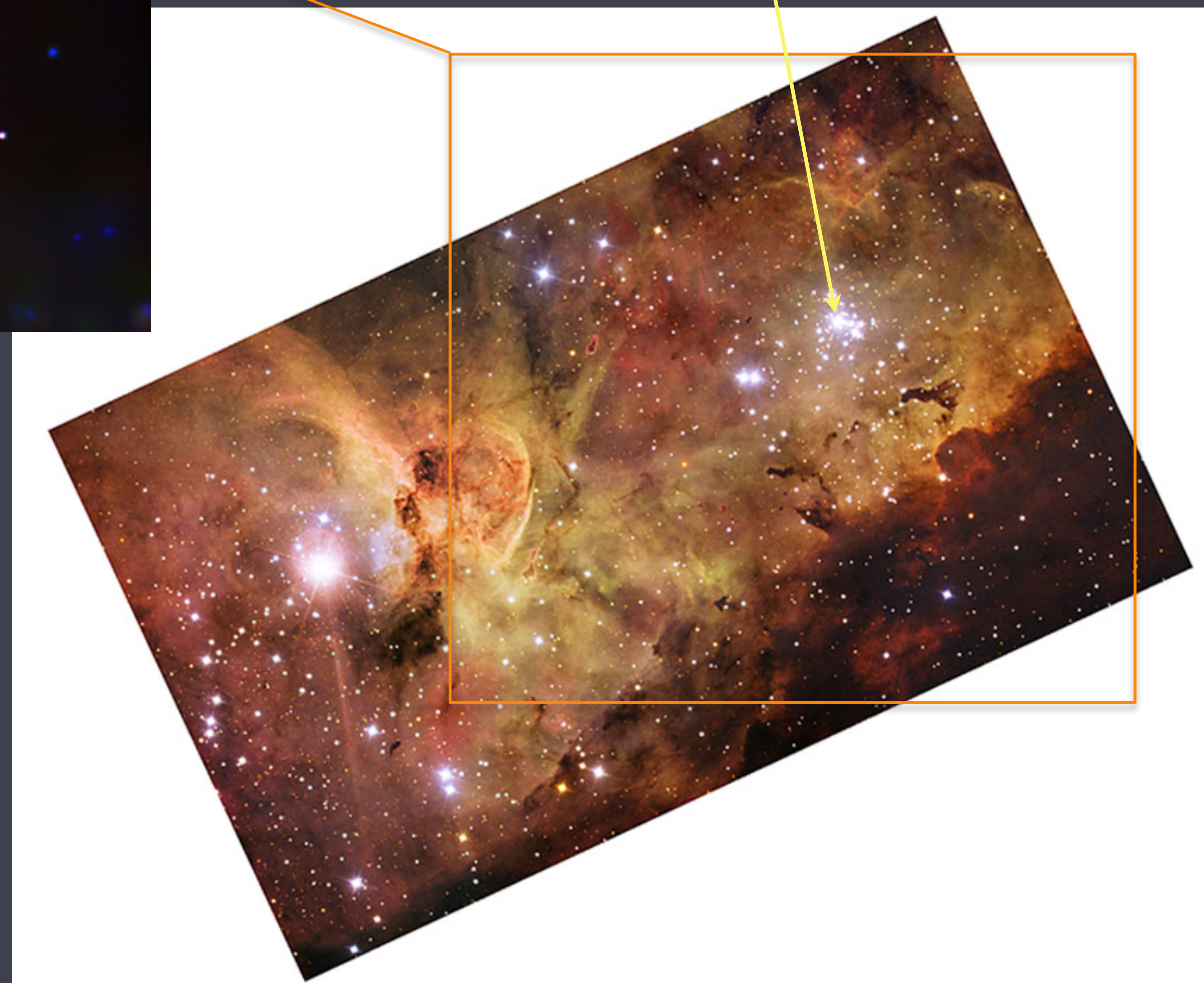

Carina: ESO

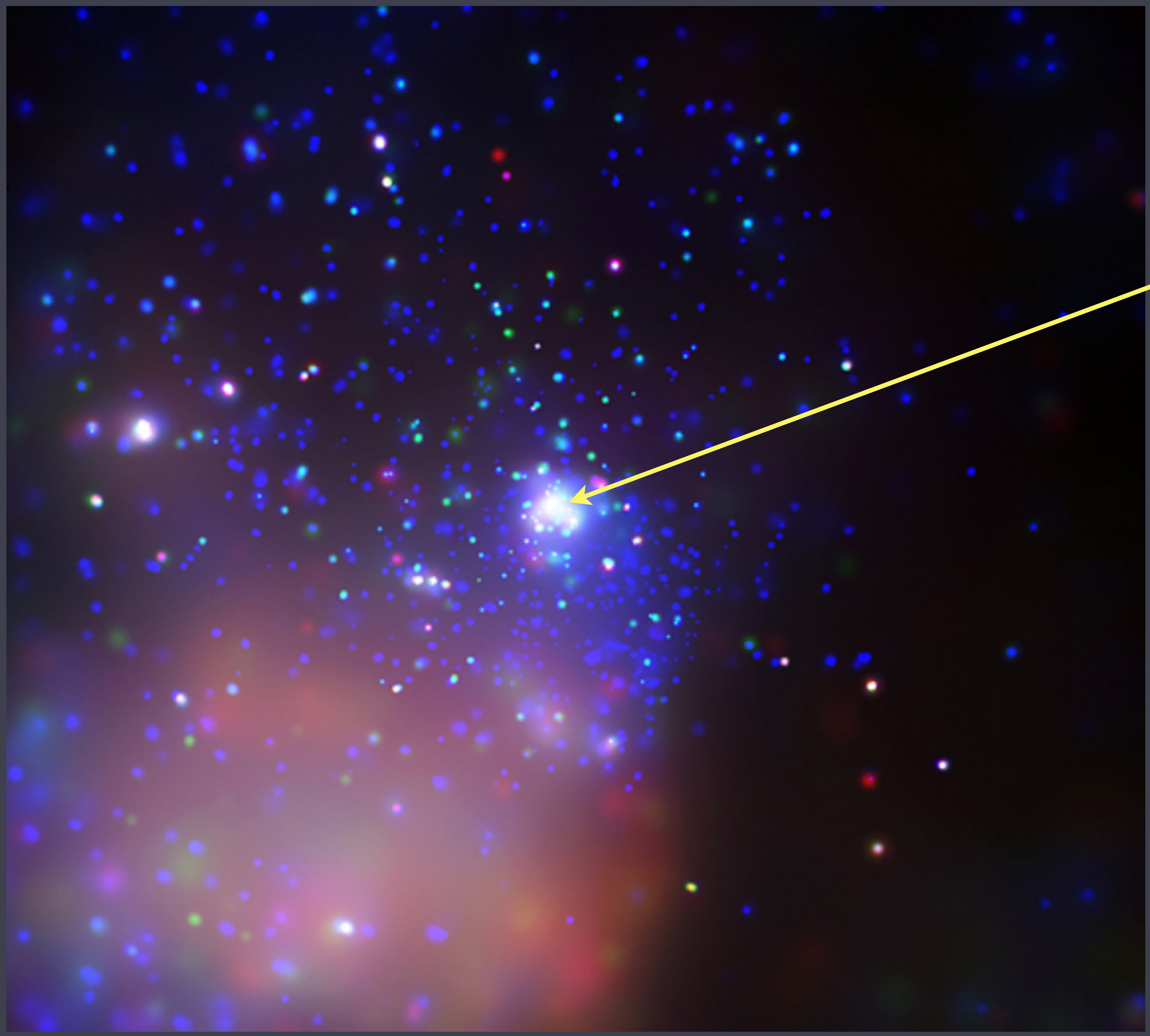

Tr 14: *Chandra*

$L_X \sim 7 \times 10^{32}$

$\langle h\nu \rangle \sim 1$ keV

: $kT \sim 10^7$ K

$L_{bol} \sim 2 \times 10^6 L_{sun}$ so $\mathbf{L_X/L_{bol} \sim 10^{-7}}$

Strong stellar winds: traditional diagnostics

UV

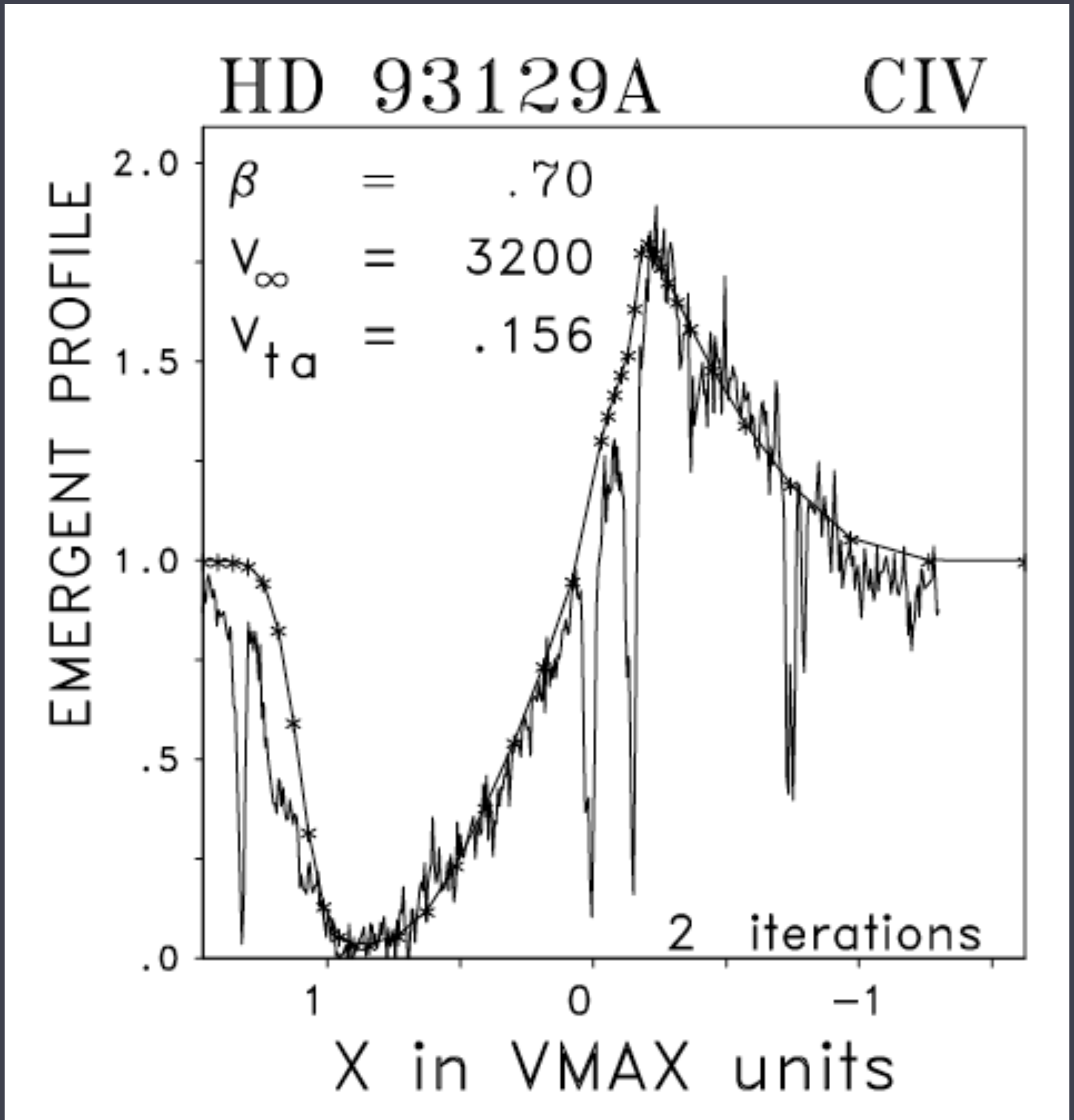

Taresch et al. (1997)

$\dot{M} = 2 \times 10^{-5}\ M_{sun}/yr$

$v_\infty = 3200$ km/s

Hα

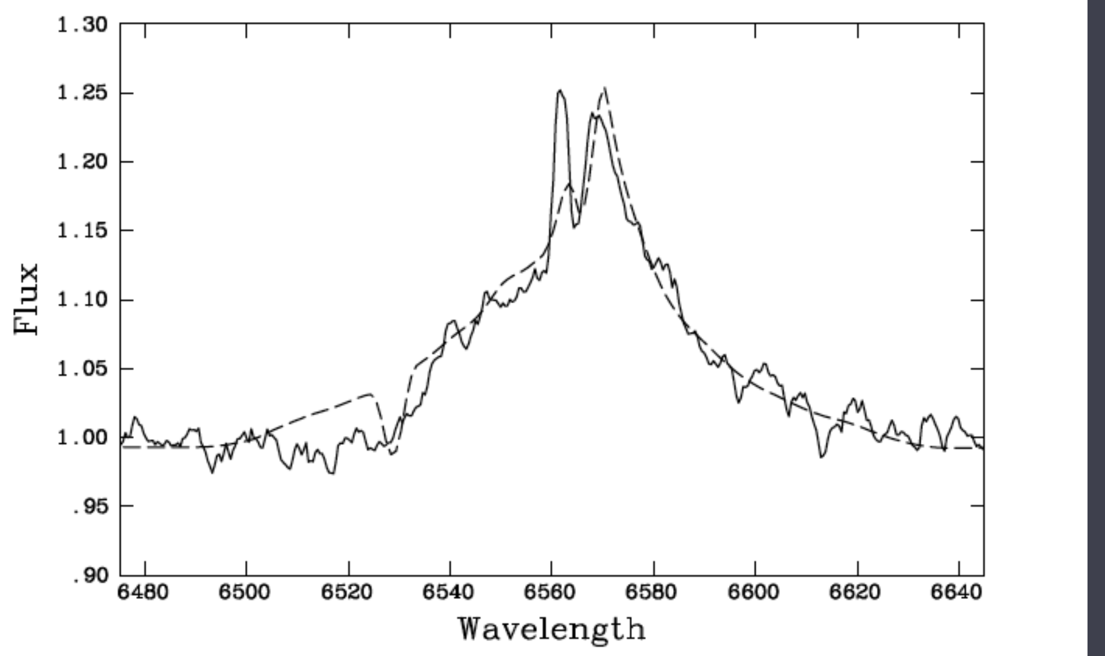

Fig. 13. Observed Hα profile (**solid**) compared with the calculation assuming a mass loss of $18 \times 10^{-6}\ M_\odot$/yr (dashed). Note that the blue narrow emission peak originates from the H II-region emission.

HD 93129A: strongest wind measured in an O star

Hα

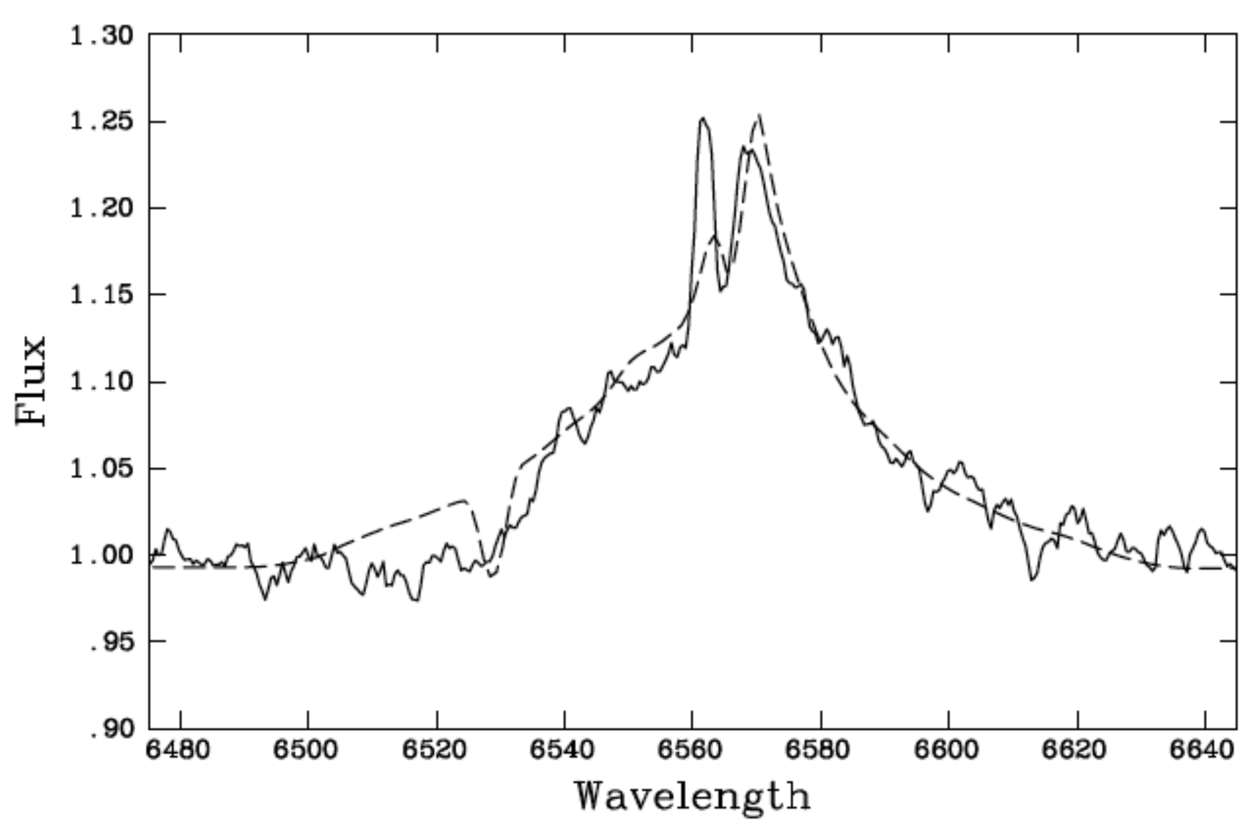

Fig. 13. Observed Hα profile (**solid**) compared with the calculation assuming a mass loss of $18 \times 10^{-6}\ M_{\odot}$/yr (dashed). Note that the blue narrow emission peak originates from the H II-region emission.

Taresch et al. (1997)

$\dot{M} = 2 \times 10^{-5}\ M_{sun}/yr$

assuming a *smooth* wind

↑

i.e. no clumping

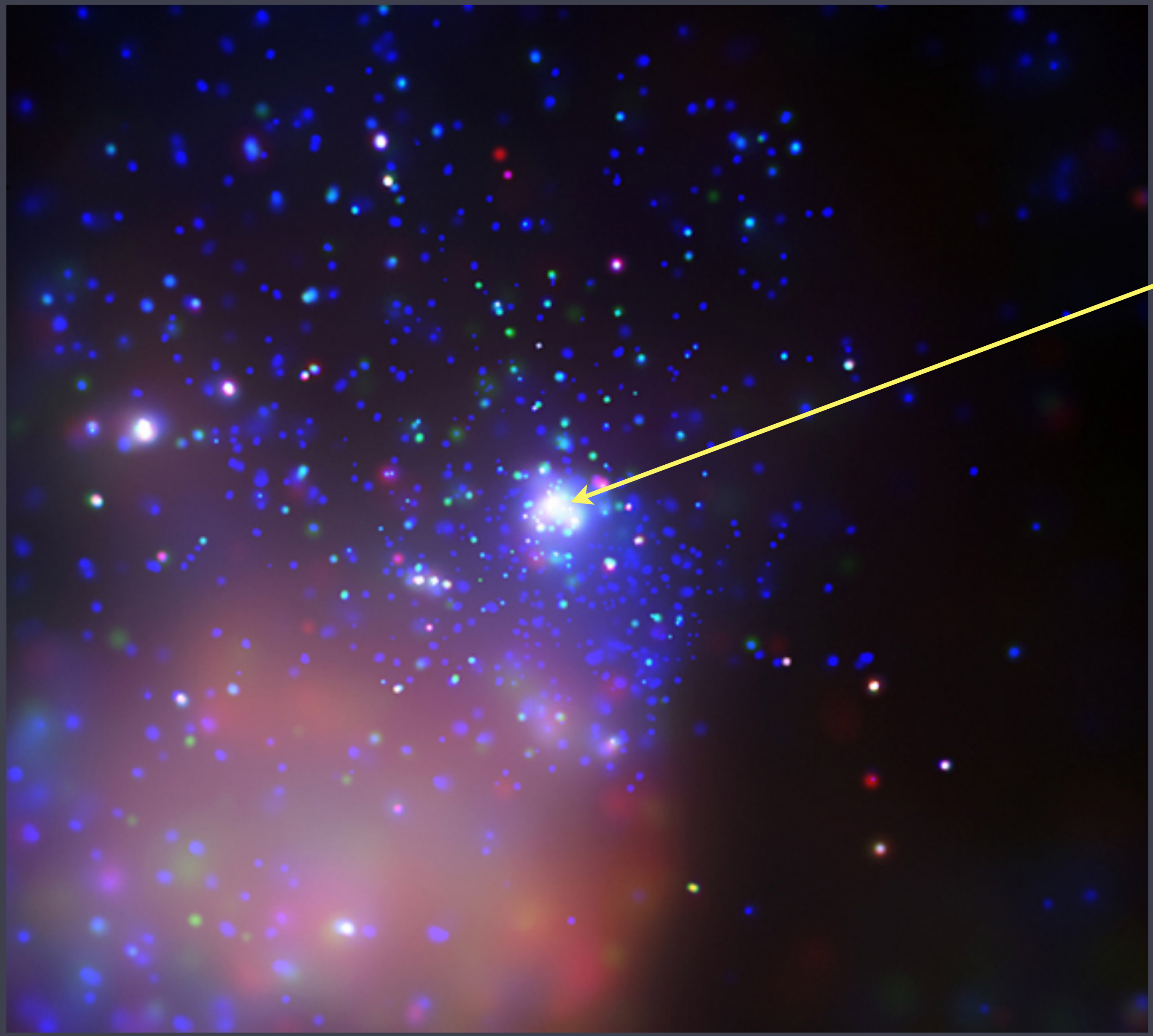

Tr 14: *Chandra*

HD 93129A

$L_X \sim 7 \times 10^{32}$

$\langle h\nu \rangle \sim 1$ keV

: $kT \sim 10^7$ K

$L_{bol} \sim 2 \times 10^6\ L_{sun}$ so $\mathbf{L_X/L_{bol} \sim 10^{-7}}$

components A & B separated by 2.7″ (5500 AU)

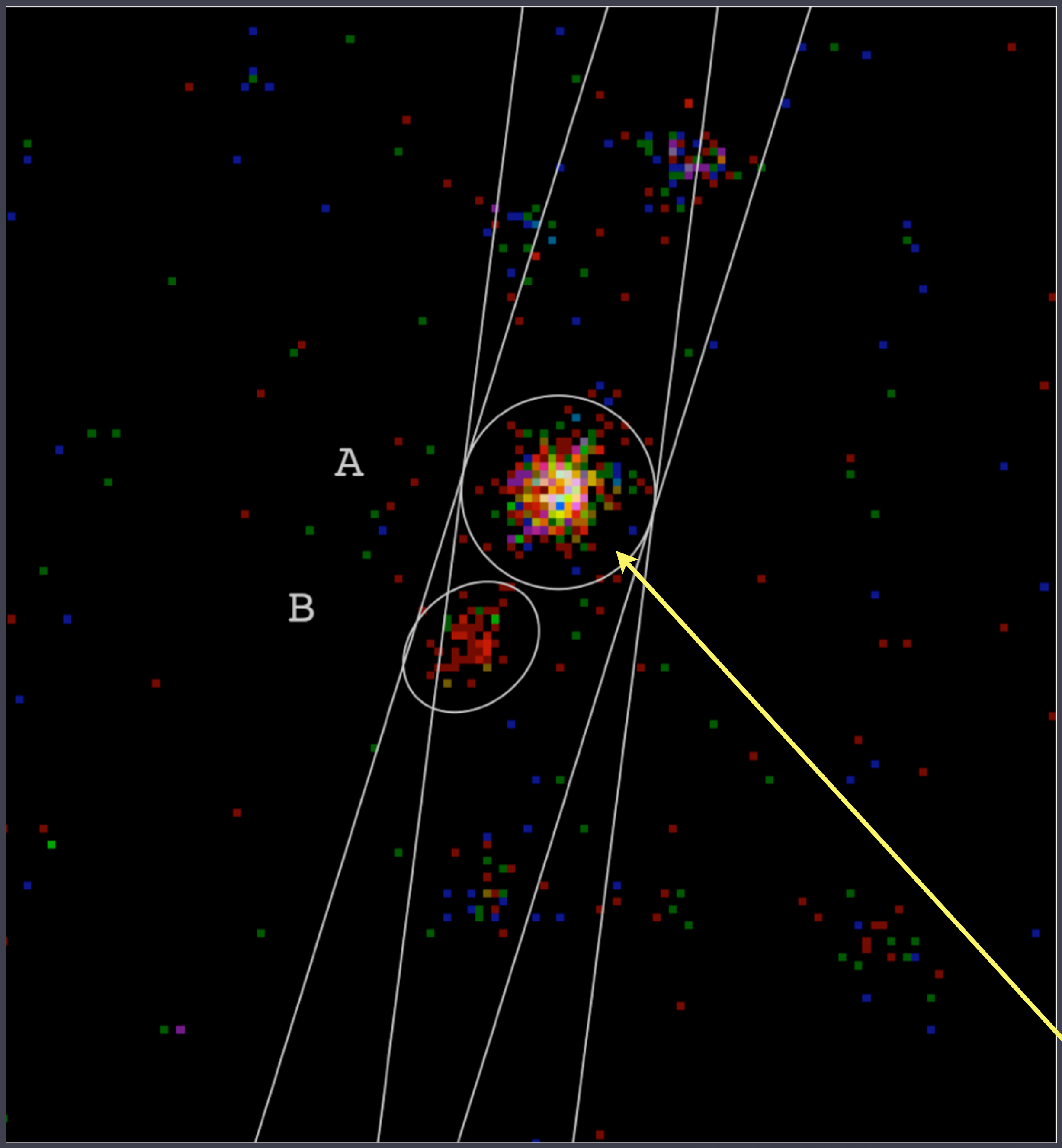

Nelan et al. , 2004, AJ, 128, 323

a ~ 100 AU (~ 1000 R_*)

O2If* + ~O3.5V

component A is actually a binary itself:

sep. 0.05″

$\Delta m = 0^m.9$

Chandra High Energy Transmission Grating Spectrometer

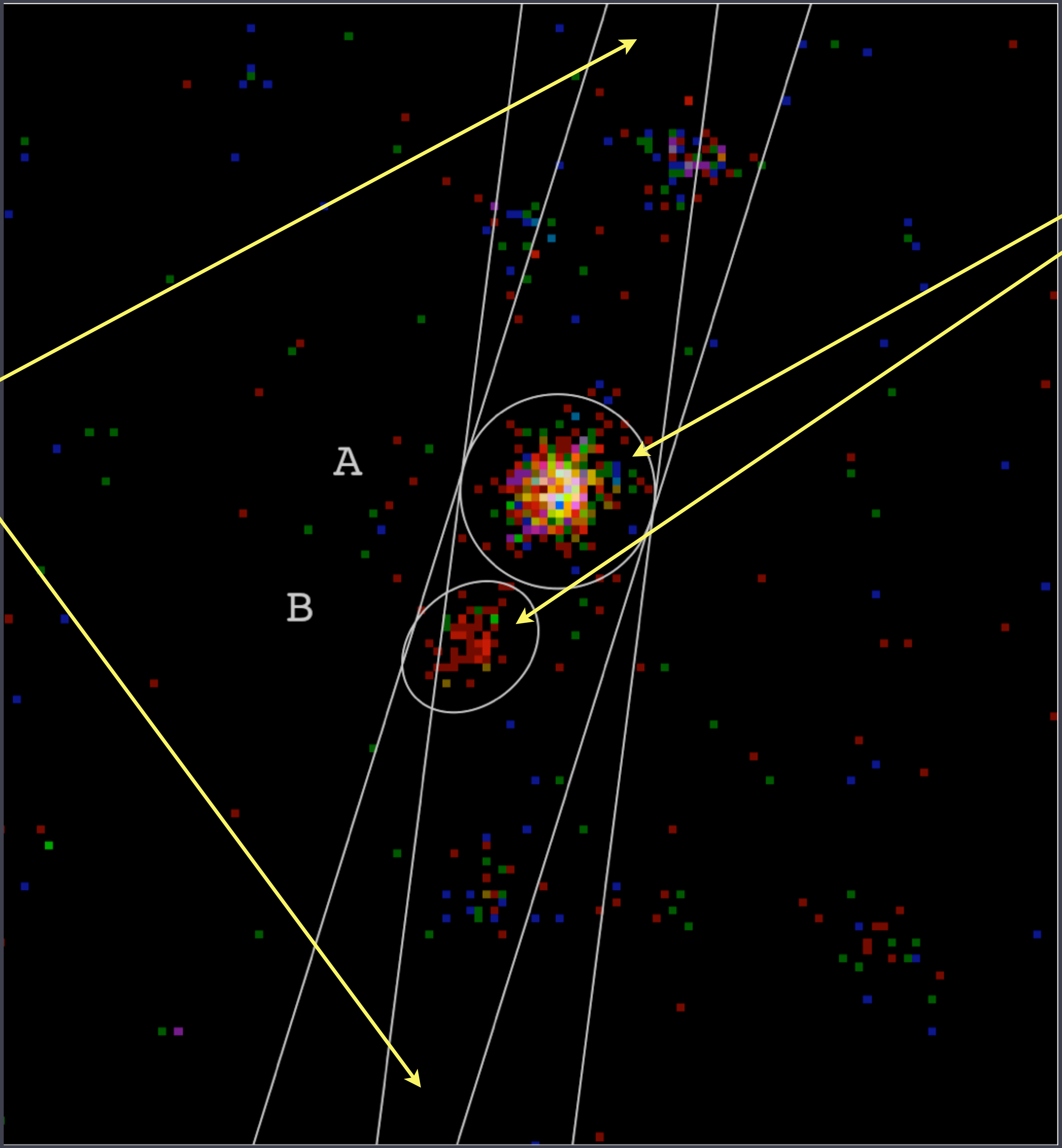

dispersed spectrum: *high-resolution*

“zeroth order spectrum”: *low-resolution*

H-like vs. He-like soft emission absent: wind attenuation

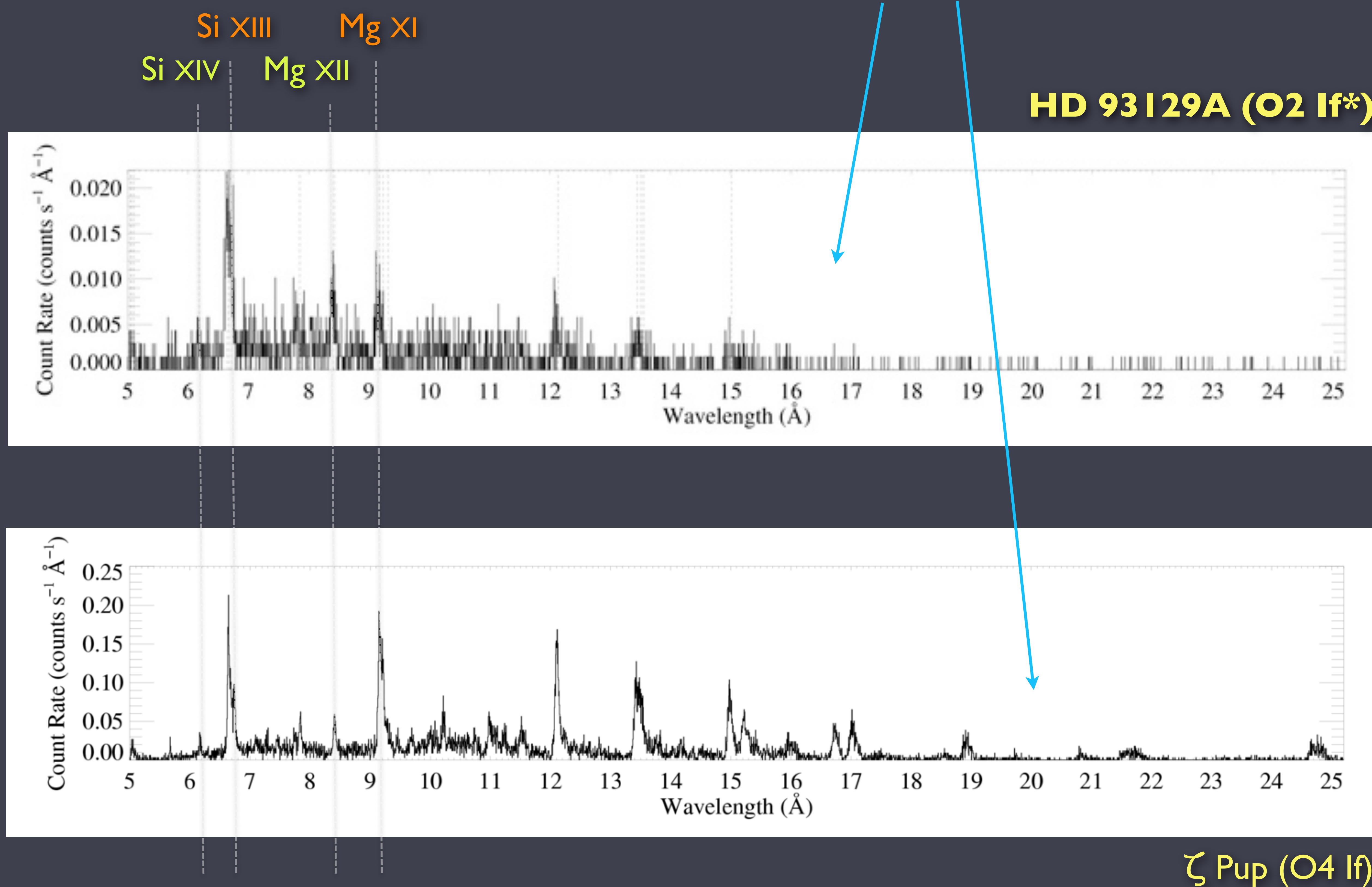

HD 93129A

Mg XII Lyman-alpha

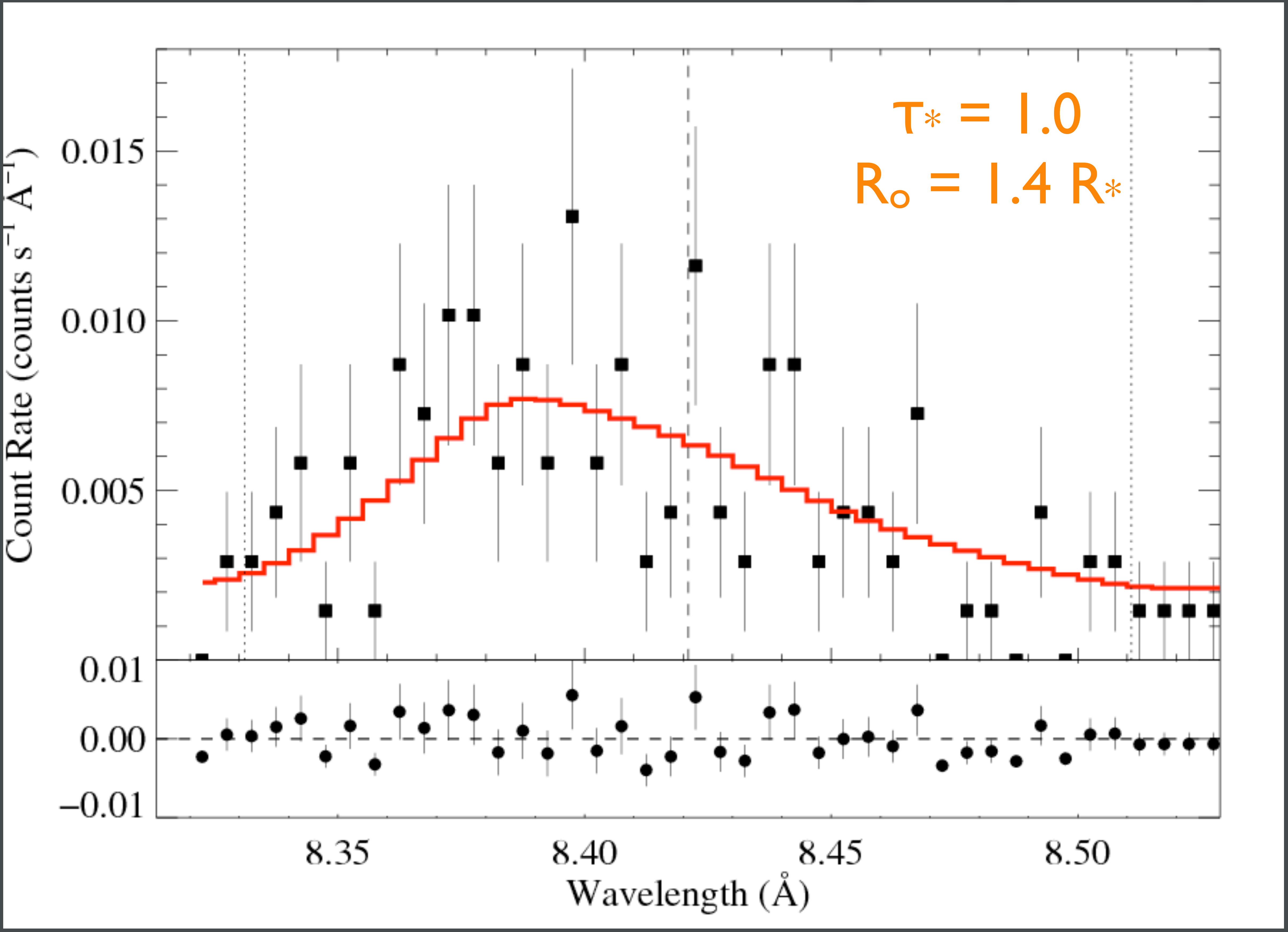

R_o = onset radius of X-ray emission

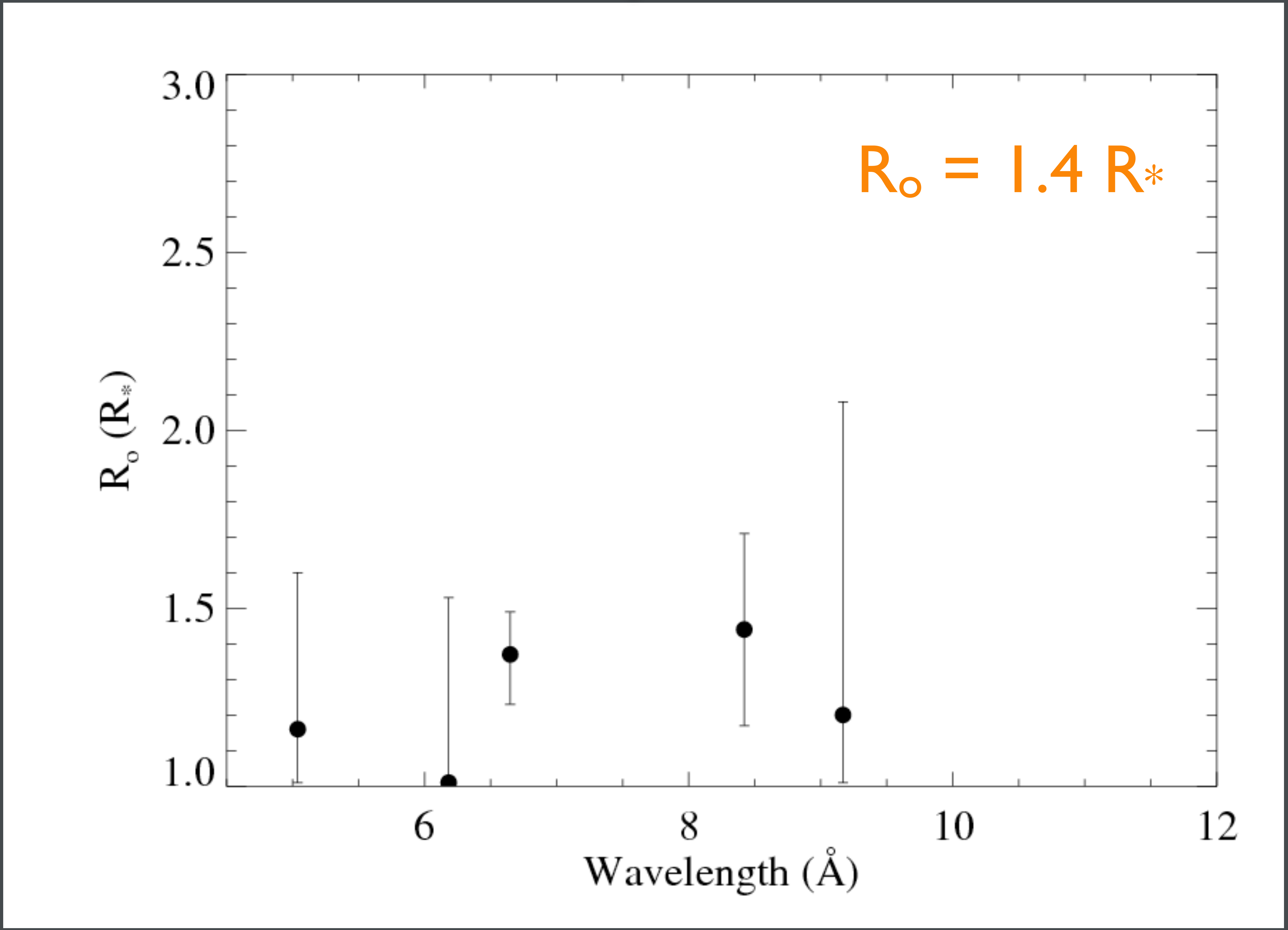

HD 93129A

τ_* from five emission lines

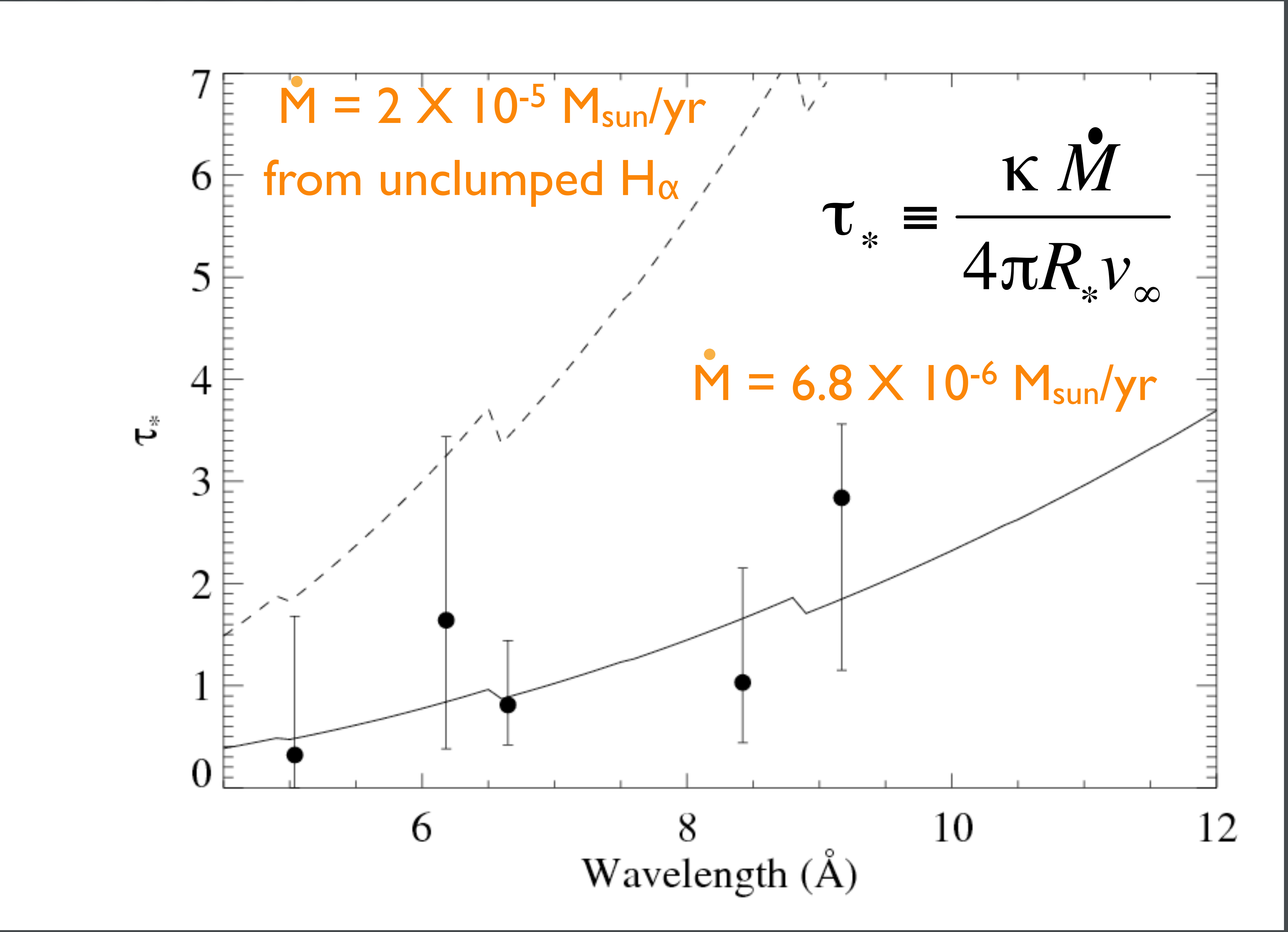

$\tau_* = \kappa(\lambda)\dot{M}/4\pi R_* v_\infty$

Chandra High Energy Transmission Grating Spectrometer

dispersed spectrum: high-resolution

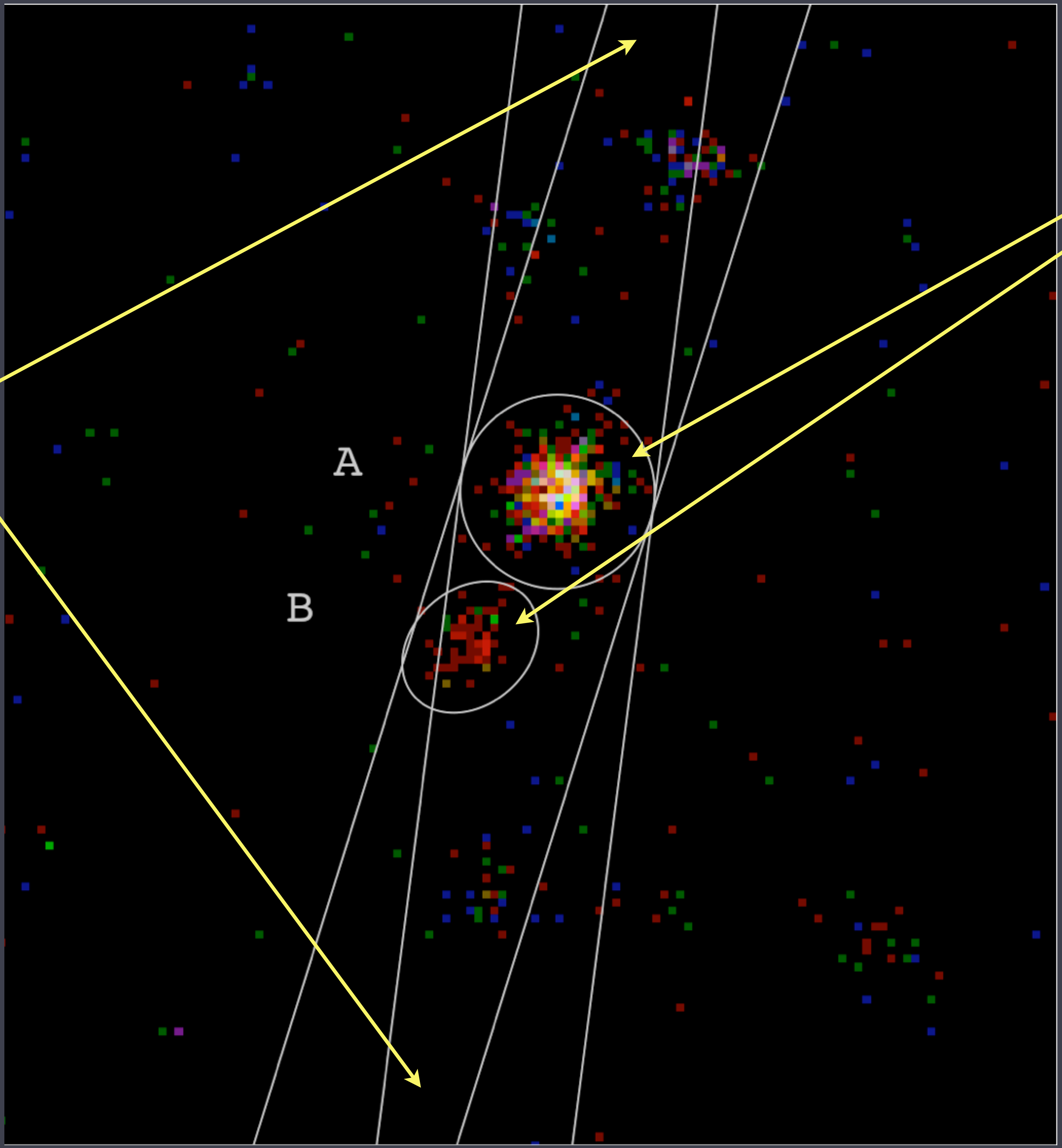

"zeroth order spectrum": low-resolution

HD 93129A: *Chandra* ACIS spectrum

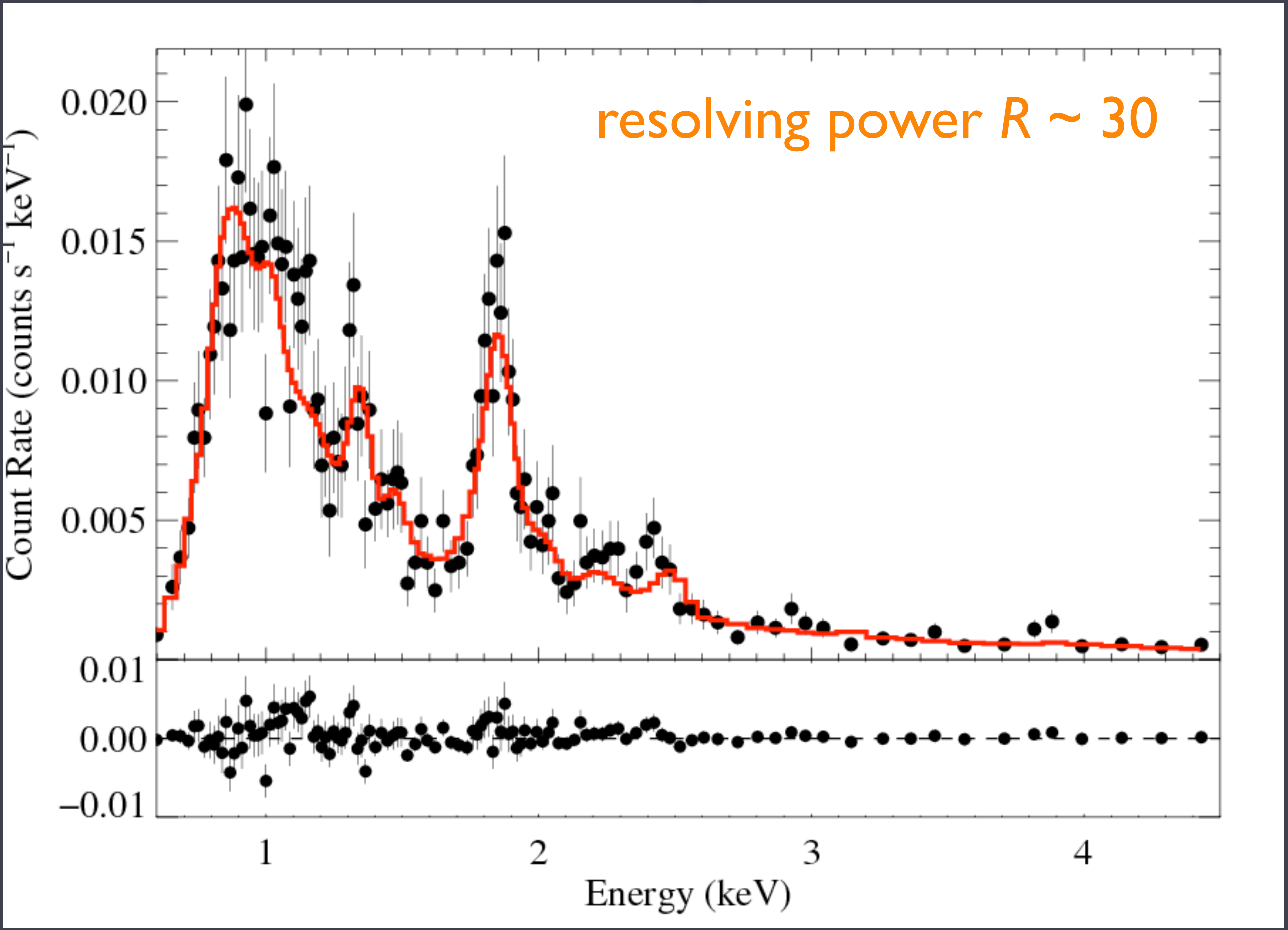

HD 93129A: *Chandra* ACIS spectrum

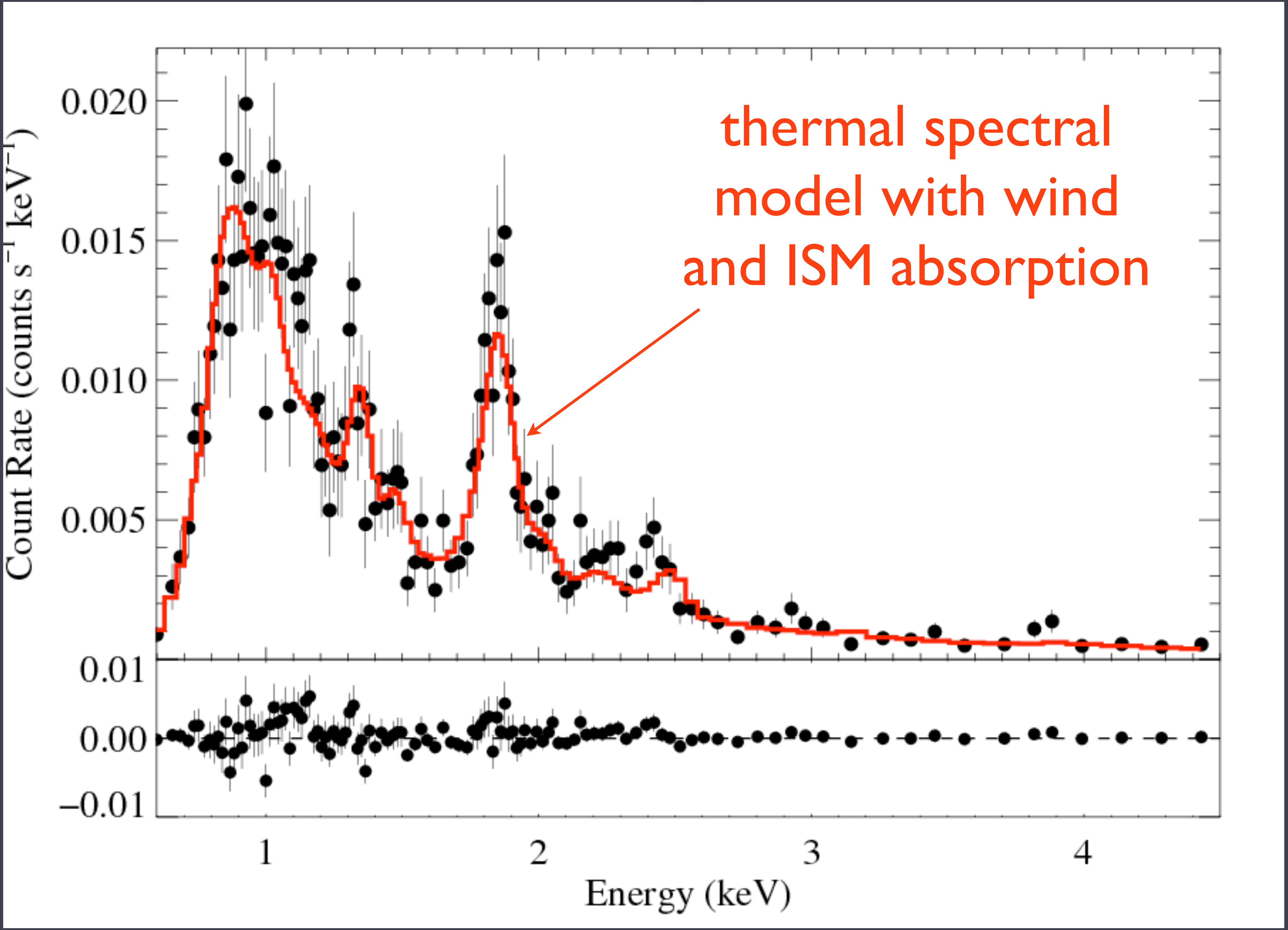

The Spectral Model

*(apec*windtabs + apec)*tbabs*

ISM attenuation

wind attenuation

thermal emission (bremsstrahlung + emission lines)

HD 93129A: *Chandra* ACIS spectrum

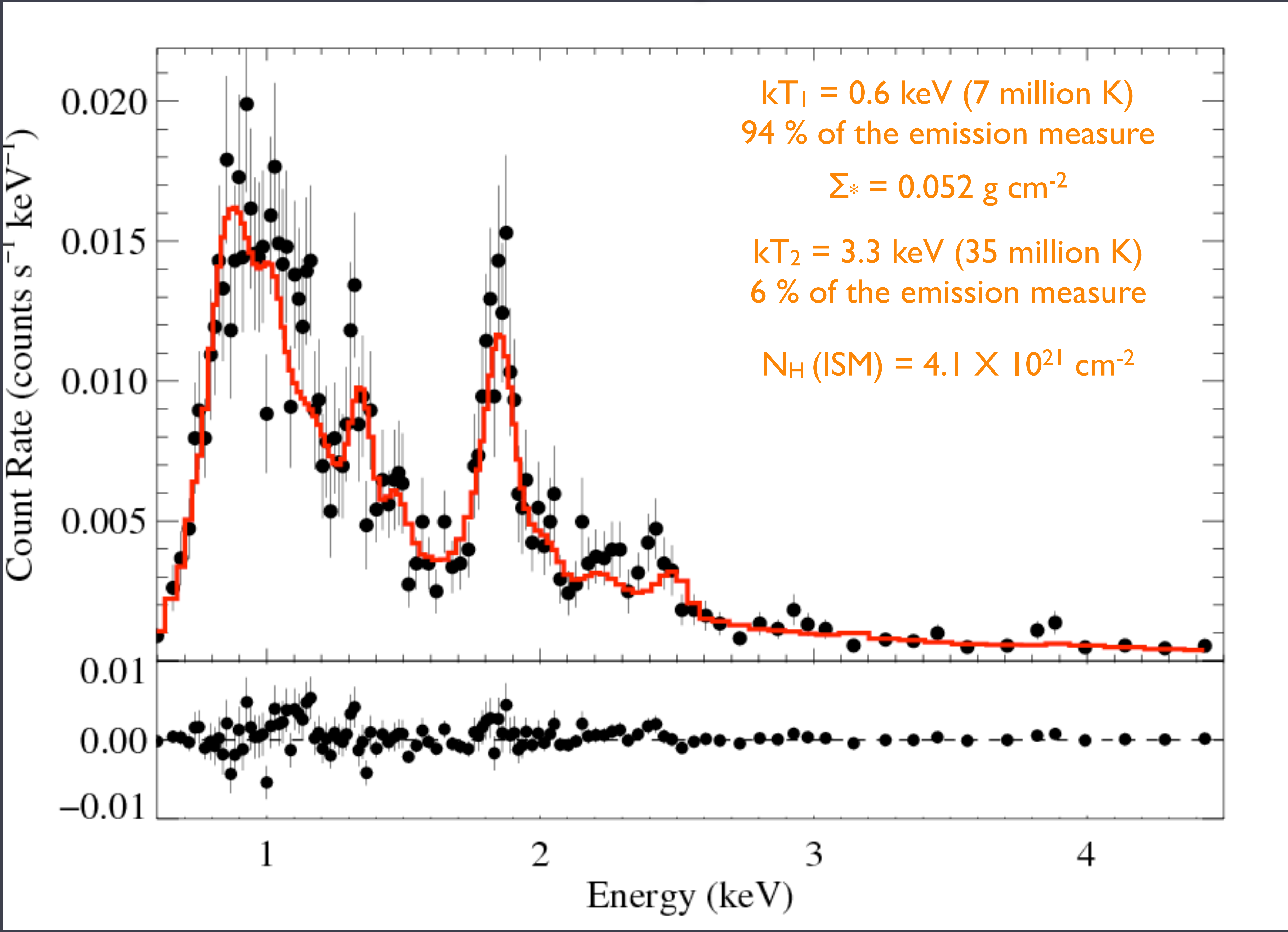

HD 93129A: *Chandra* ACIS spectrum

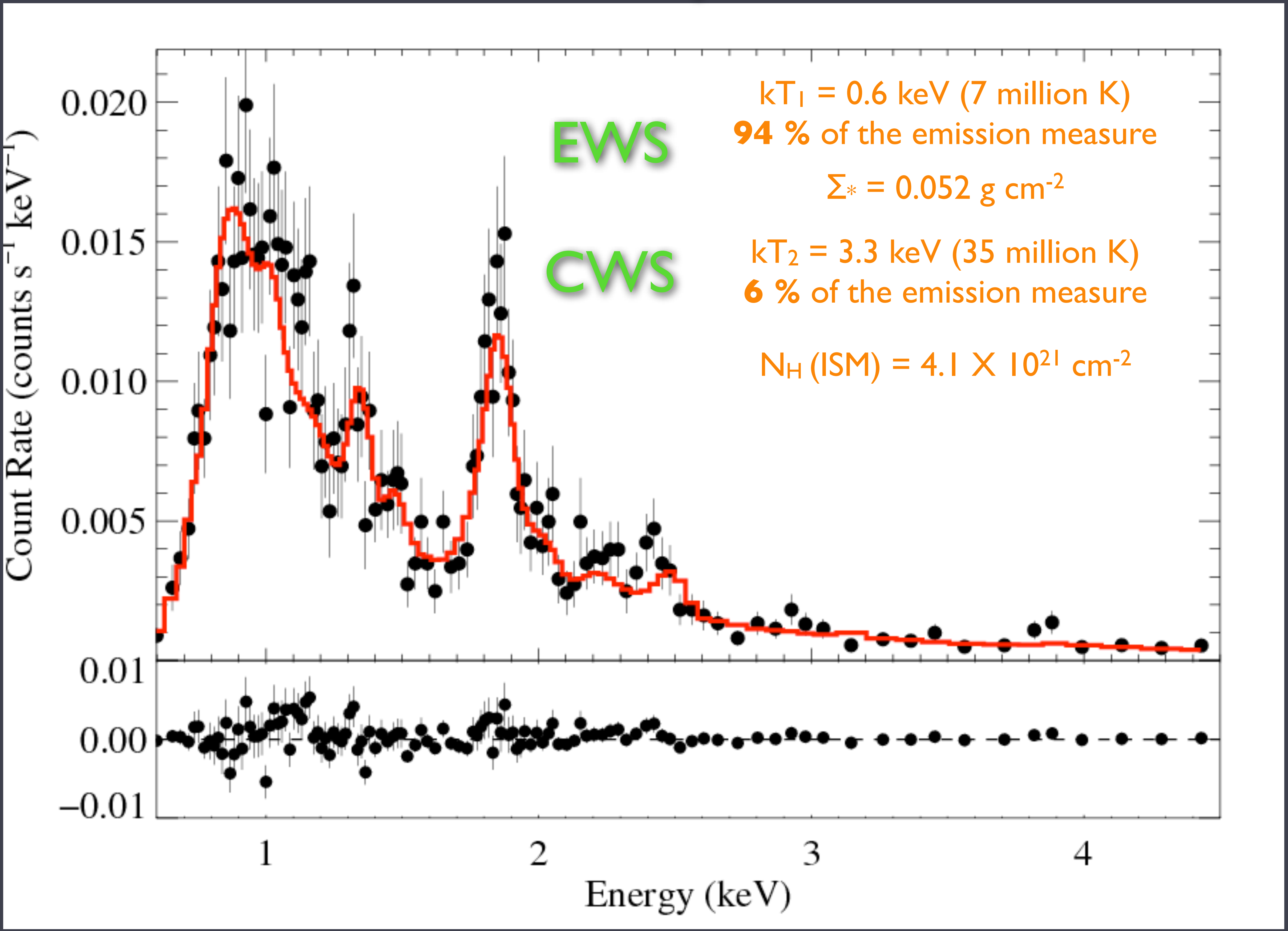

HD 93129A: *Chandra* ACIS spectrum

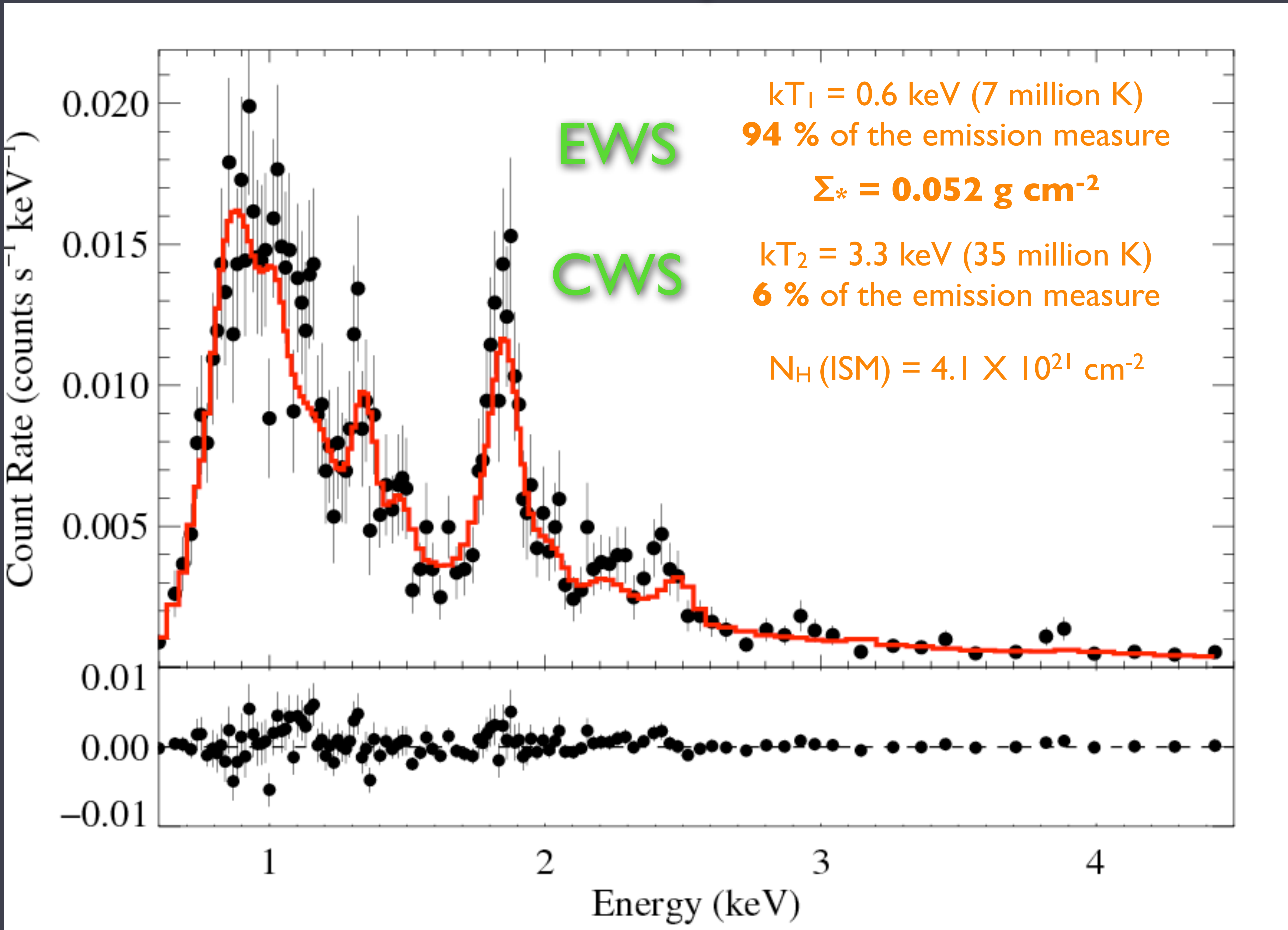

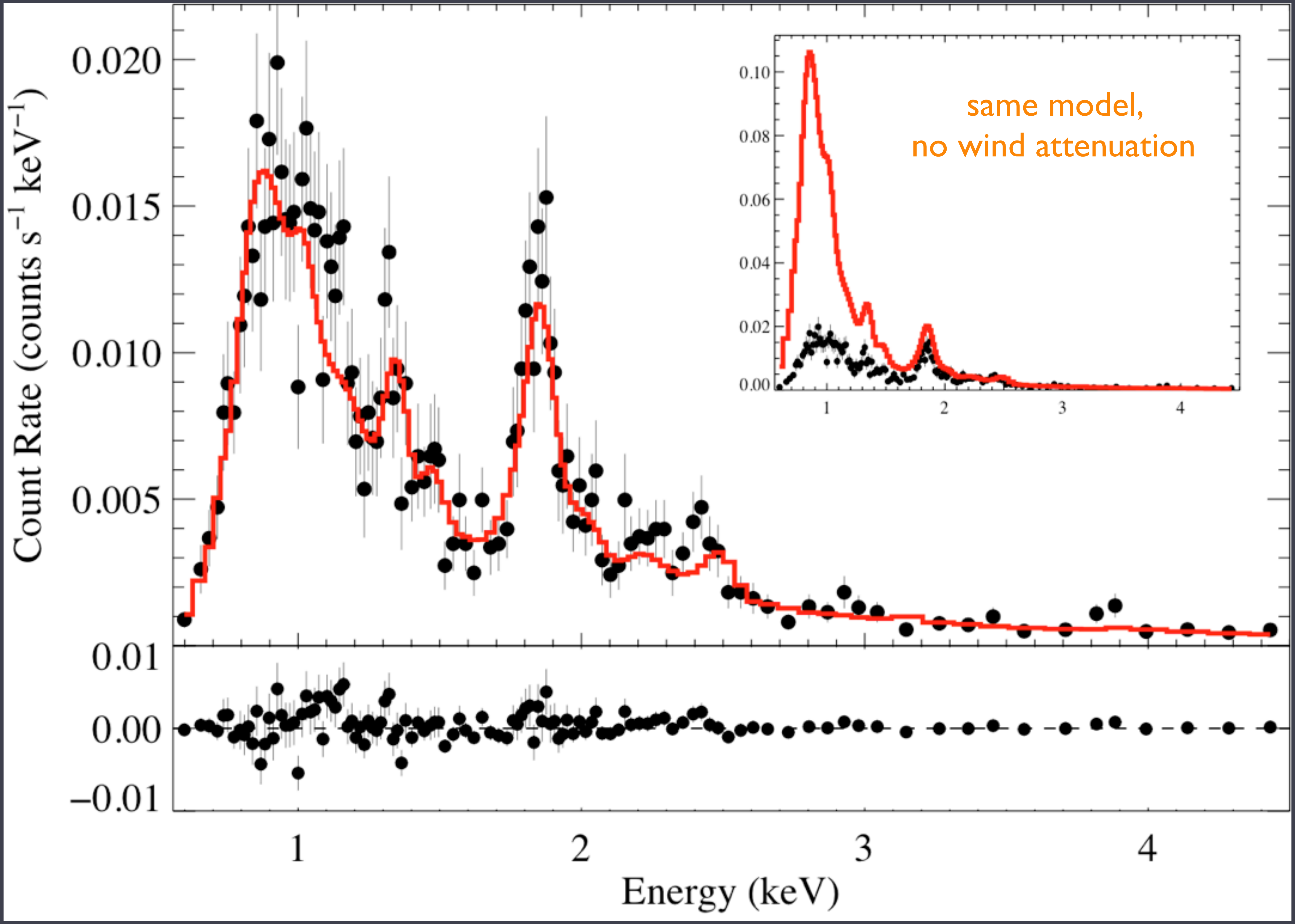

0.020
0.015
0.010
0.005
Count Rate (counts s^{-1} keV^{-1})
0.01
0.00
−0.01
1
2
3
4
Energy (keV)
0.10
0.08
0.06
0.04
0.02
0.00
same model,
no wind attenuation

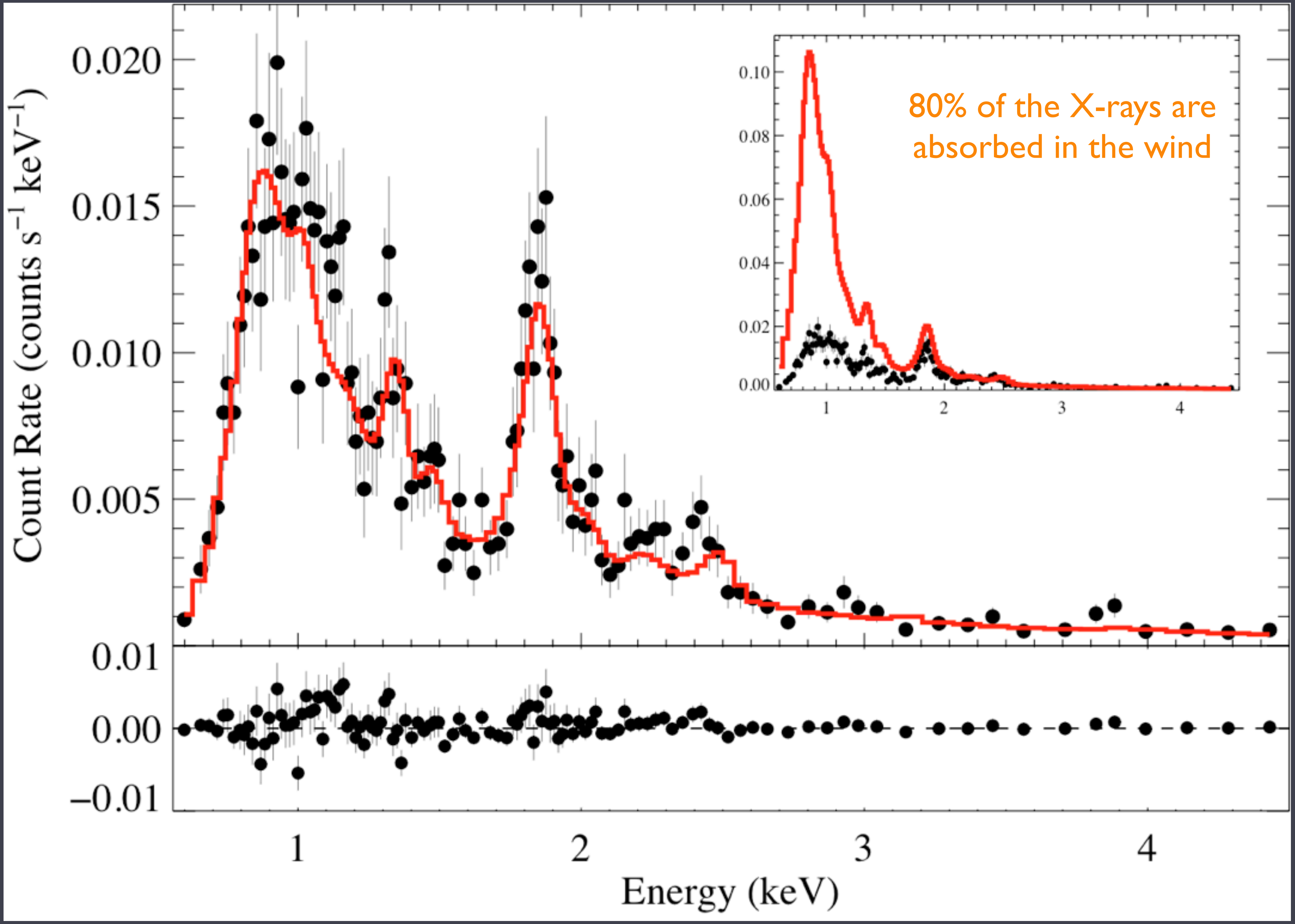

80% of the X-rays are absorbed in the wind
Count Rate (counts s^{-1} keV^{-1})
Energy (keV)
0.020
0.015
0.010
0.005
0.01
0.00
–0.01
1
2
3
4
0.10
0.08
0.06
0.04
0.02
0.00

$\Sigma_* = 0.052\ \mathrm{g\ cm^{-2}}$

where this mass column parameter

$\Sigma_\star = \dot{M}/4\pi R_\star v_\infty$

this fitted value corresponds to:

$\dot{M} = 5.2 \times 10^{-6}\ M_{sun}/yr$

HD 93129A: X-ray mass-loss rate measurement

Two independent X-ray absorption mass-loss rate diagnostics give consistent results:

$\dot{M} = 6.8 \times 10^{-6}\ M_{sun}/yr$:line profiles

$\dot{M} = 5.2 \times 10^{-6}\ M_{sun}/yr$:broadband

Factor of 3 or 4 reduction with respect to traditional (unclumped) Hα diagnostics

Lower mass-loss rate: consistent with Hα?

Lower mass-loss rate: consistent with Hα?

Yes! With clump volume filling factor of f_{cl} = 12

$\dot{M} = 7 \times 10^{-6}\ M_{sun}/yr$

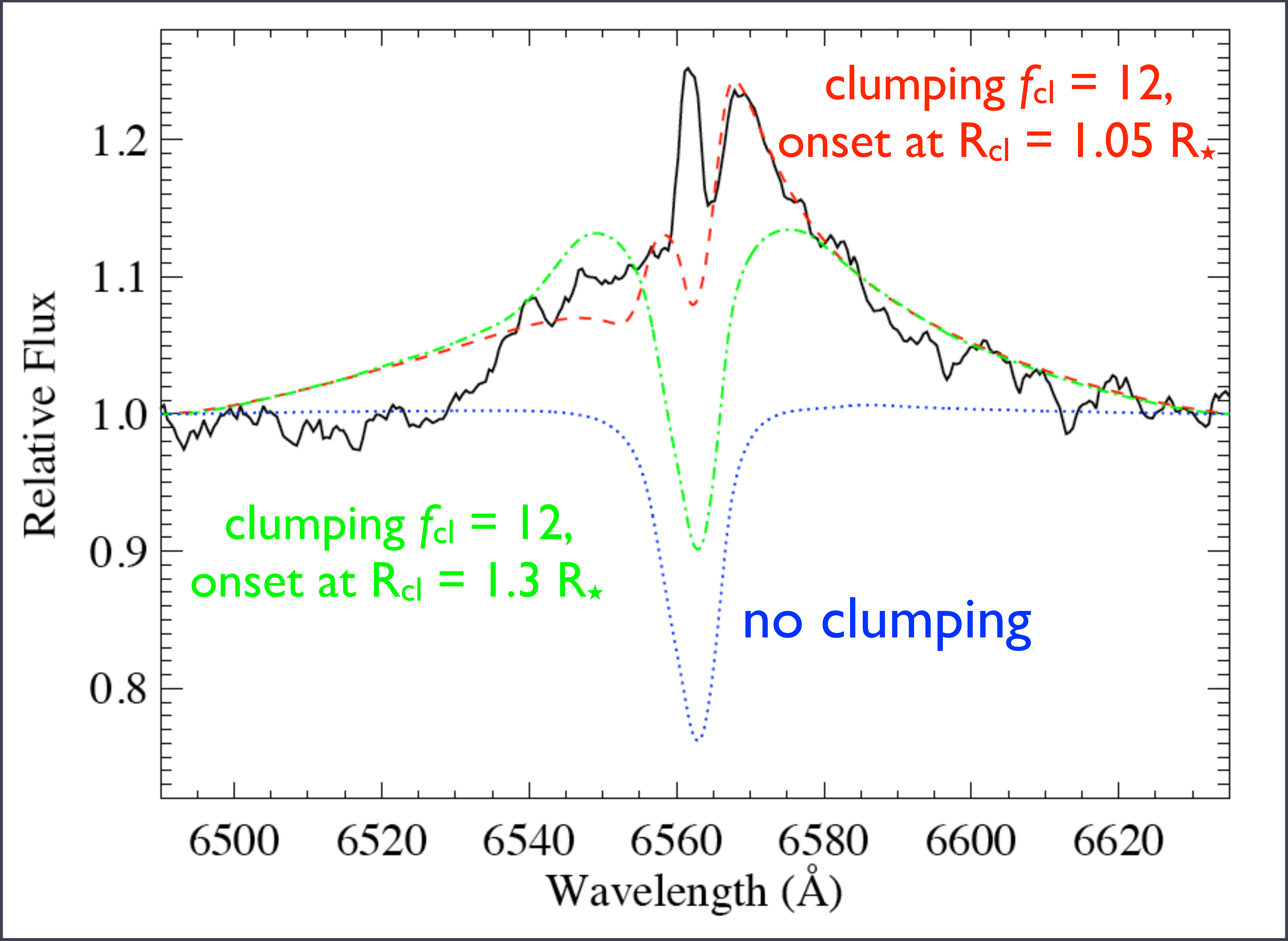

Conclusions

- Embedded Wind Shocks, consistent with LDI
- Wind attenuation is very important
- Mass-loss rate is reduced by factor of 3 to 4
- Shock onset radius is consistent with LDI simulations...but clumping onset is closer to the photosphere

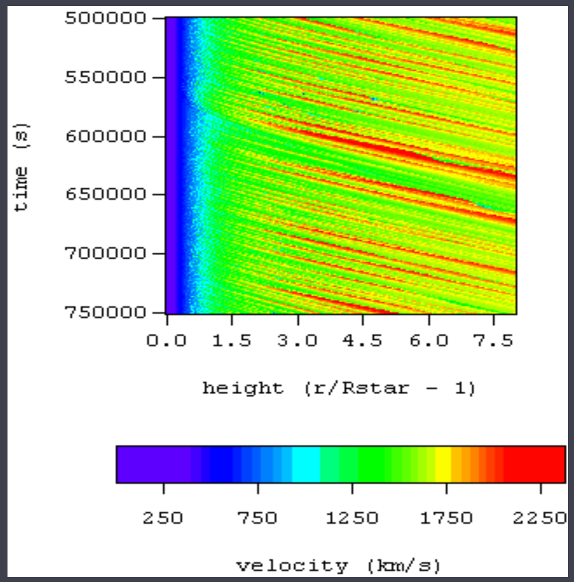

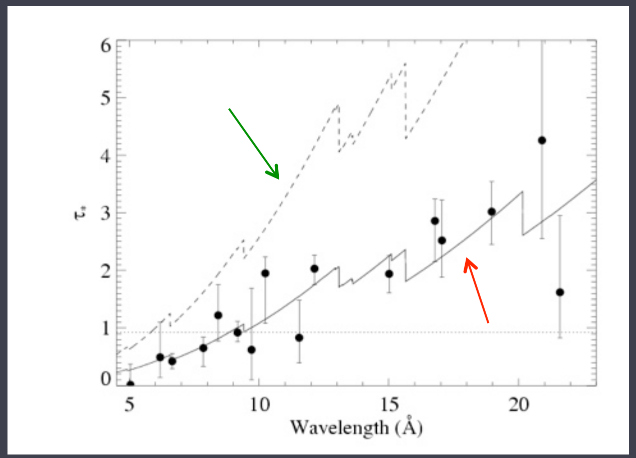

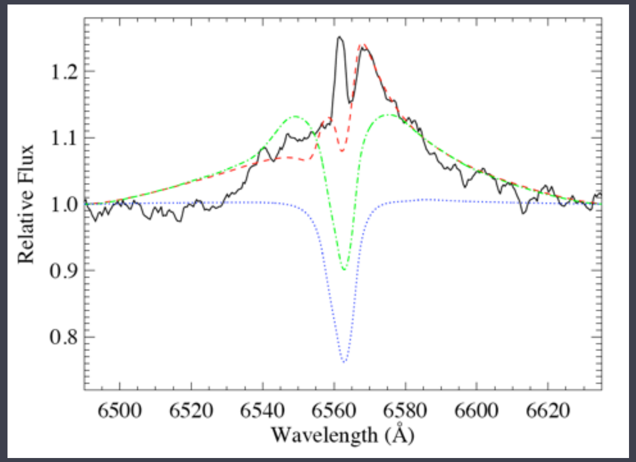

X-ray Emission from Single Massive Stars

Constraints on Wind-Shock Physics and Mass-Loss Rates

David Cohen
Swarthmore College

with Stan Owocki & Jon Sundqvist (U. Delaware), Maurice Leutenegger (GSFC),
Marc Gagné & Véronique Petit (West Chester University), Alex Fullerton (STScI),
Emma Wollman (Swarthmore ’09; Caltech), Erin Martell (Swarthmore ’09; U. Chicago),
James MacArthur (Swarthmore ’11; Sandia National Laboratory)

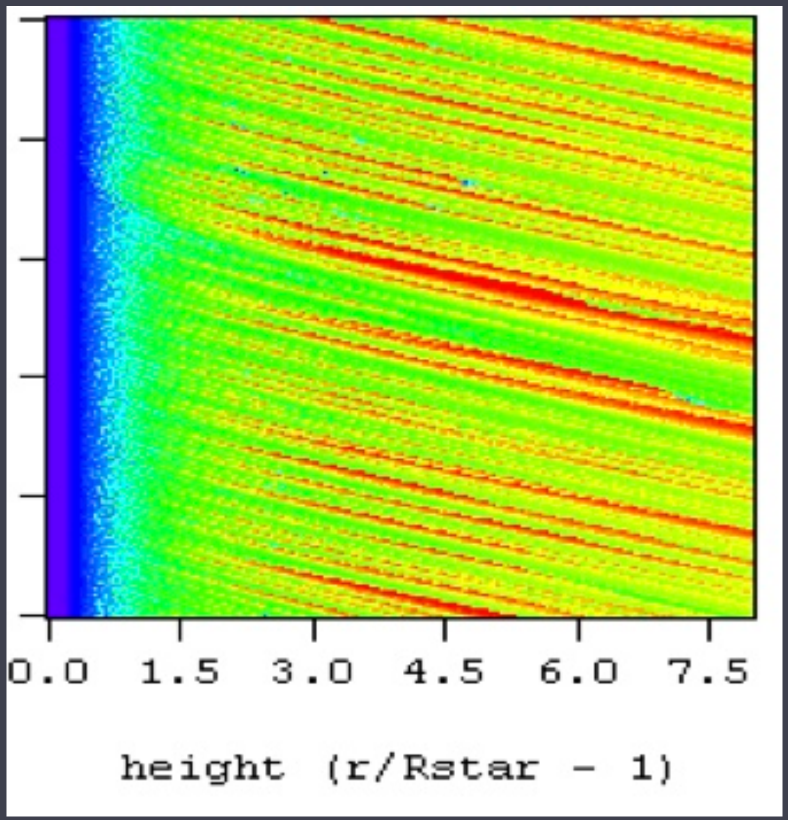

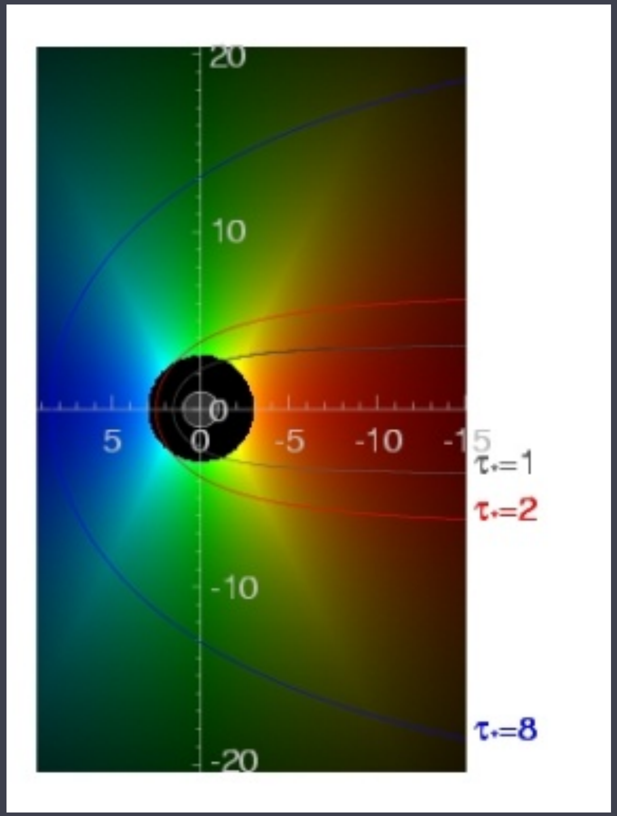

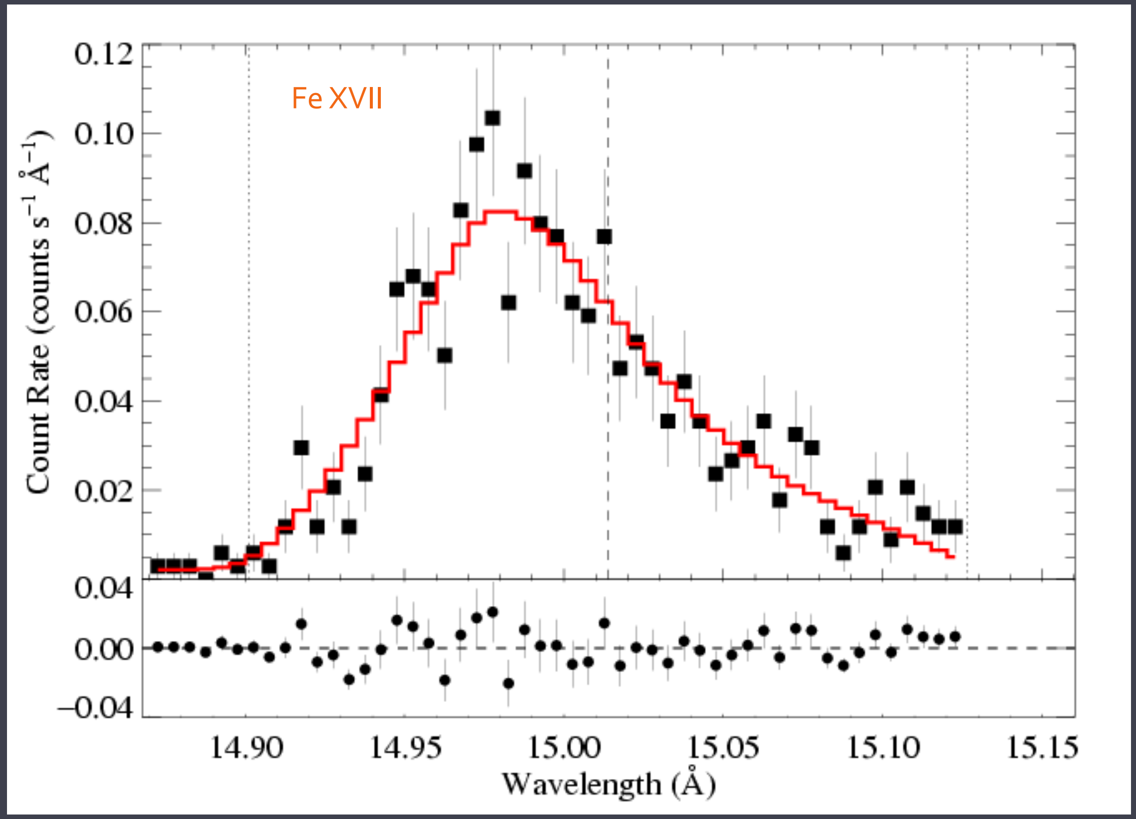

Extra Slides

windtabs wind absorption model

X-ray opacity

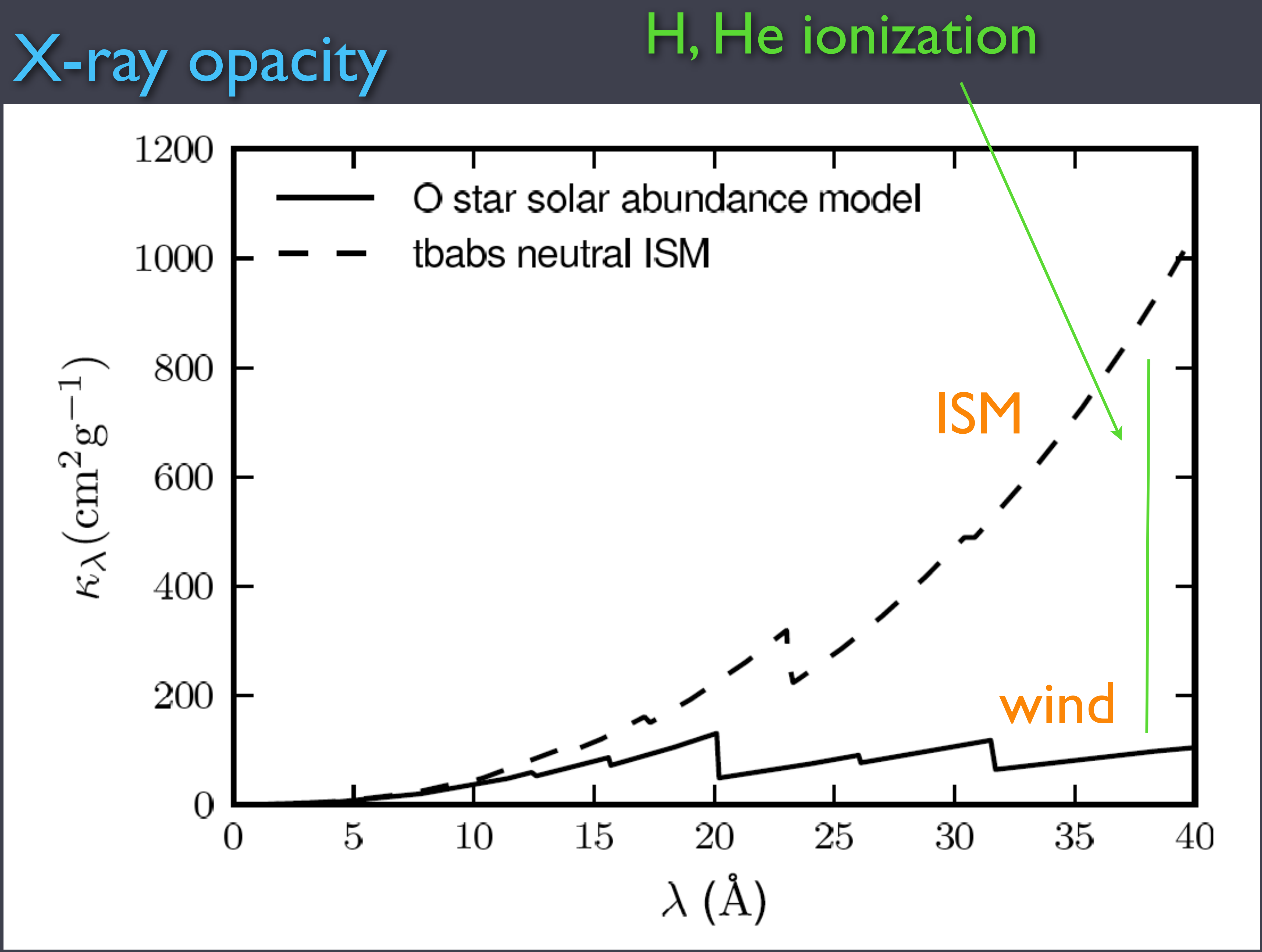

X-ray opacity

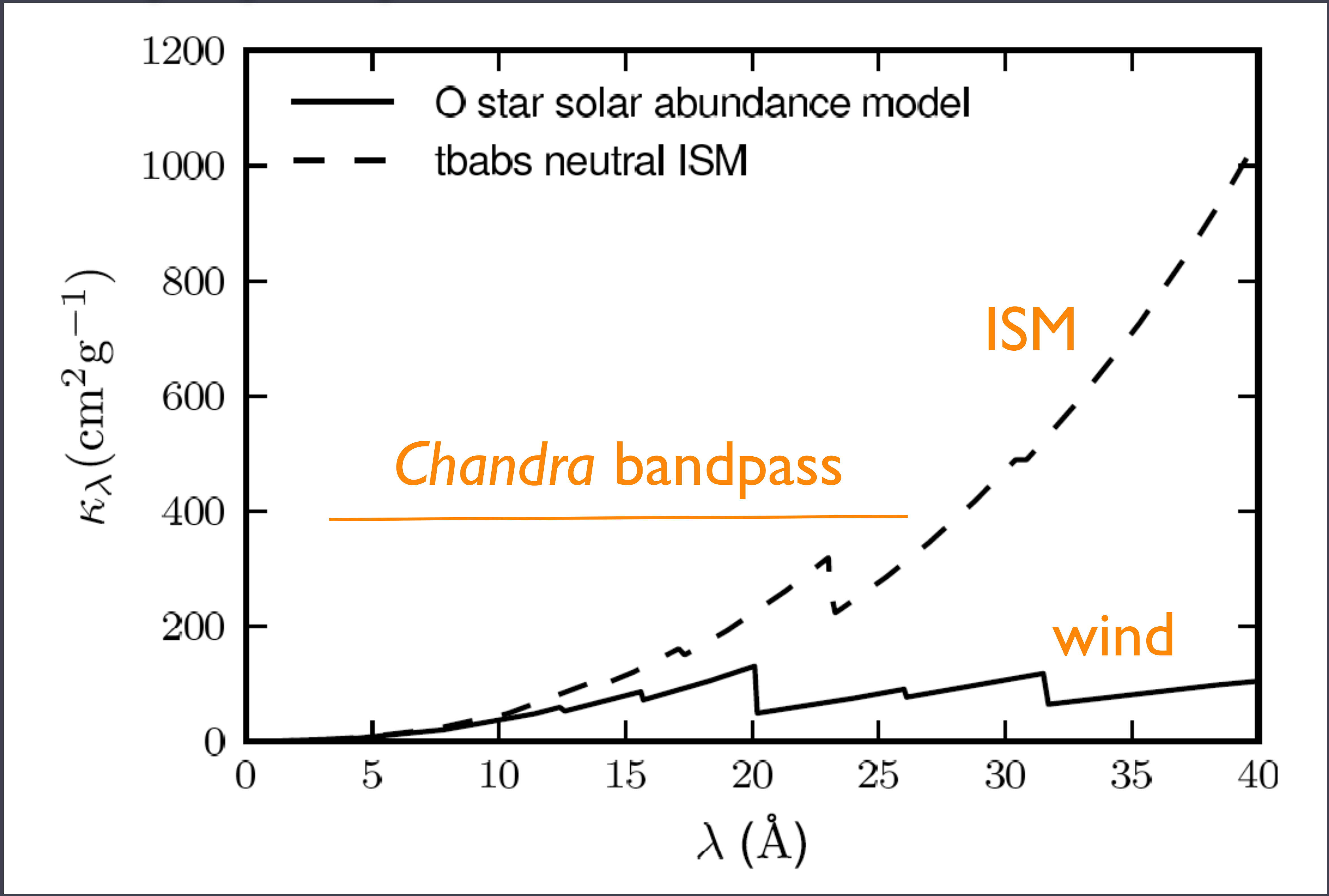

X-ray opacity: zoom in abundance effects

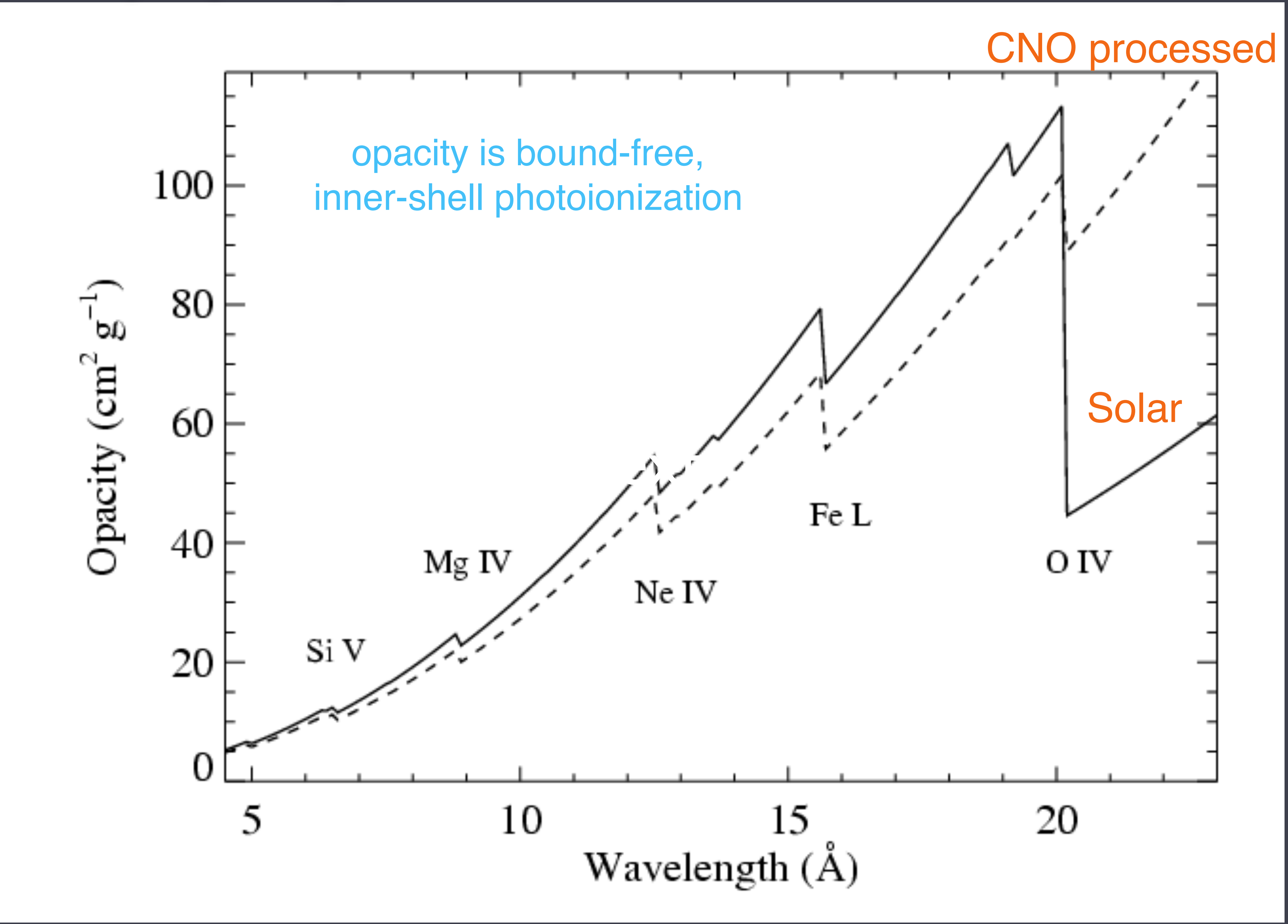

abundance effects

do *not* matter much in the *Chandra* bandpass

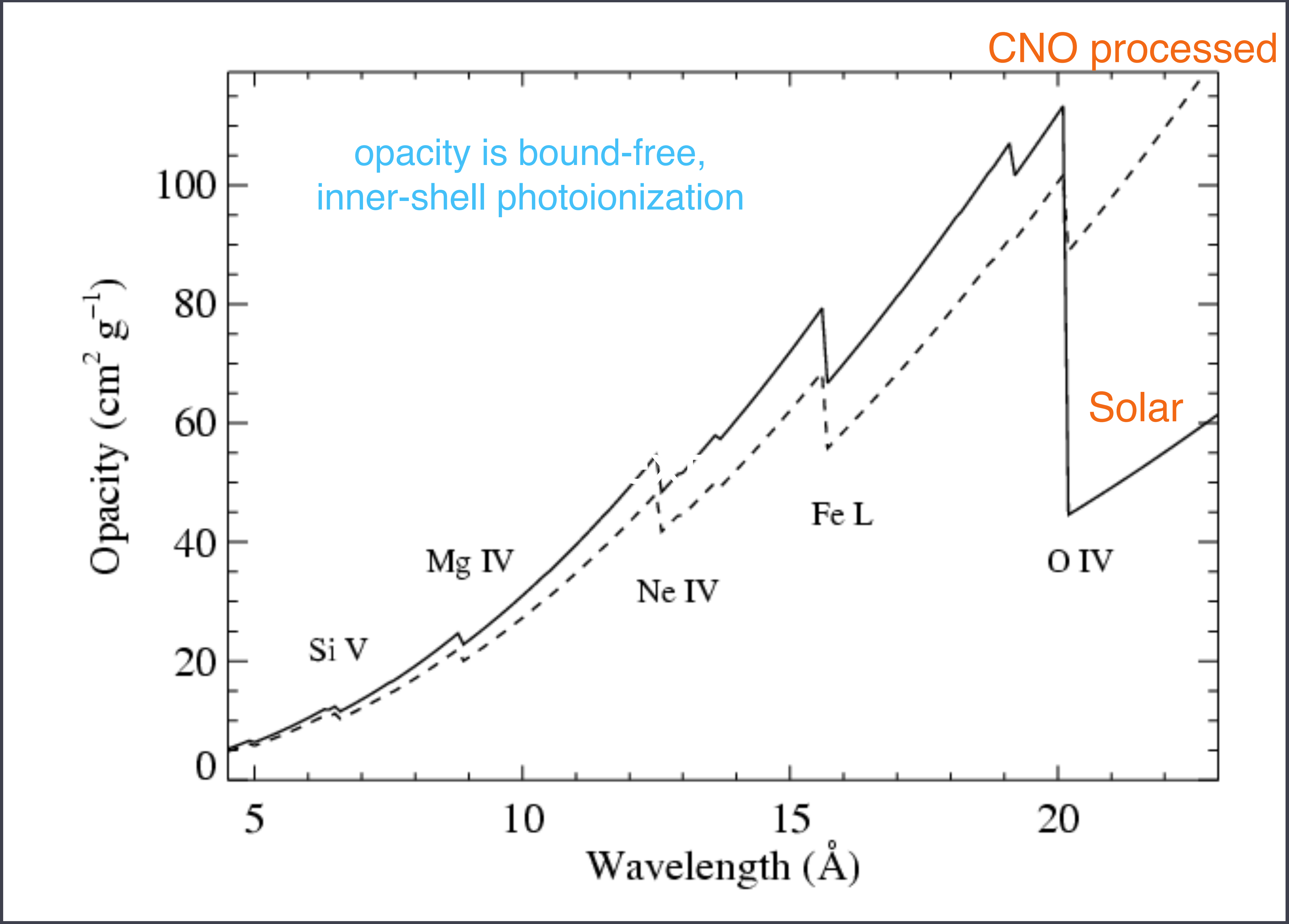

Radiation transport through the wind

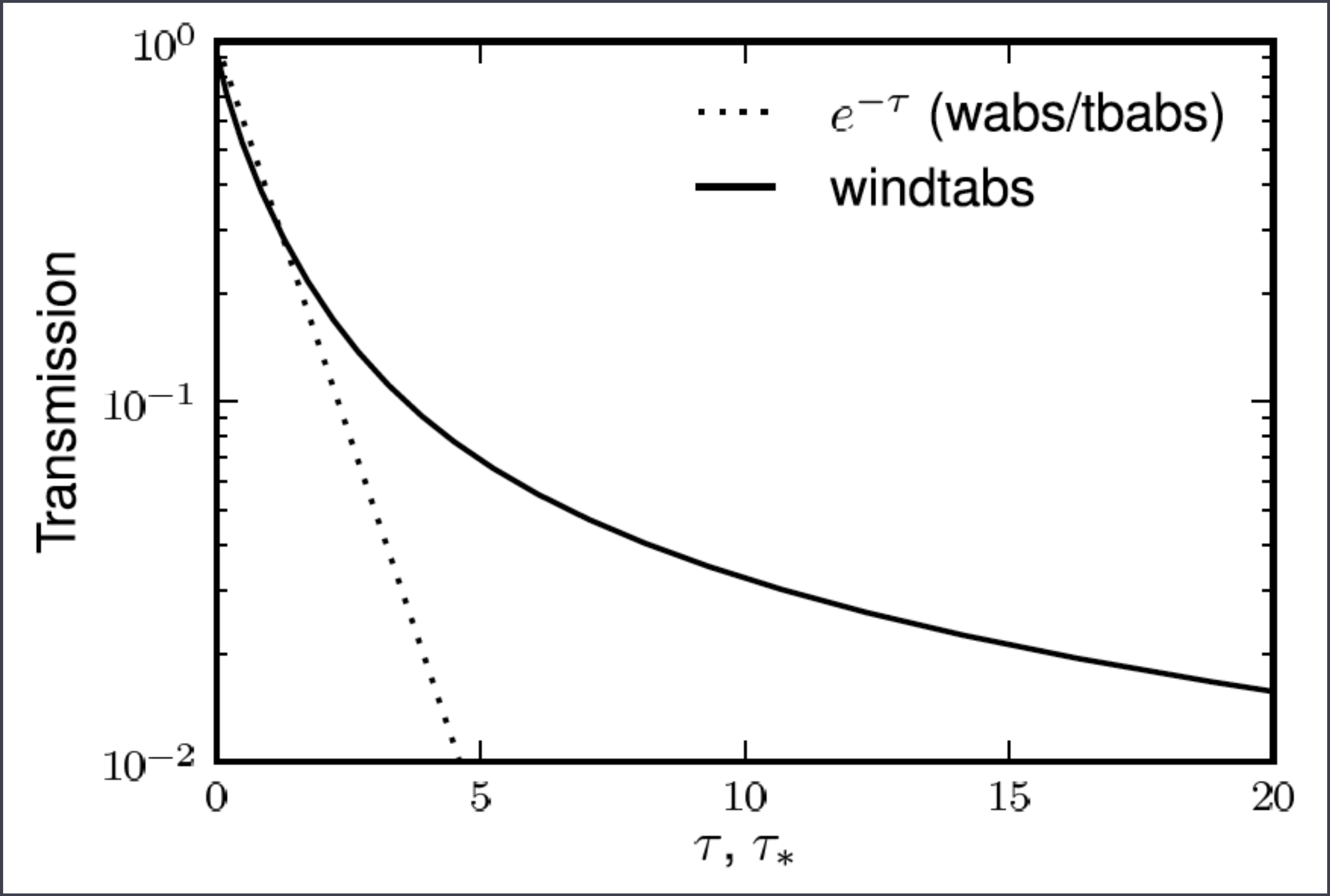

distributed emission escapes more easily

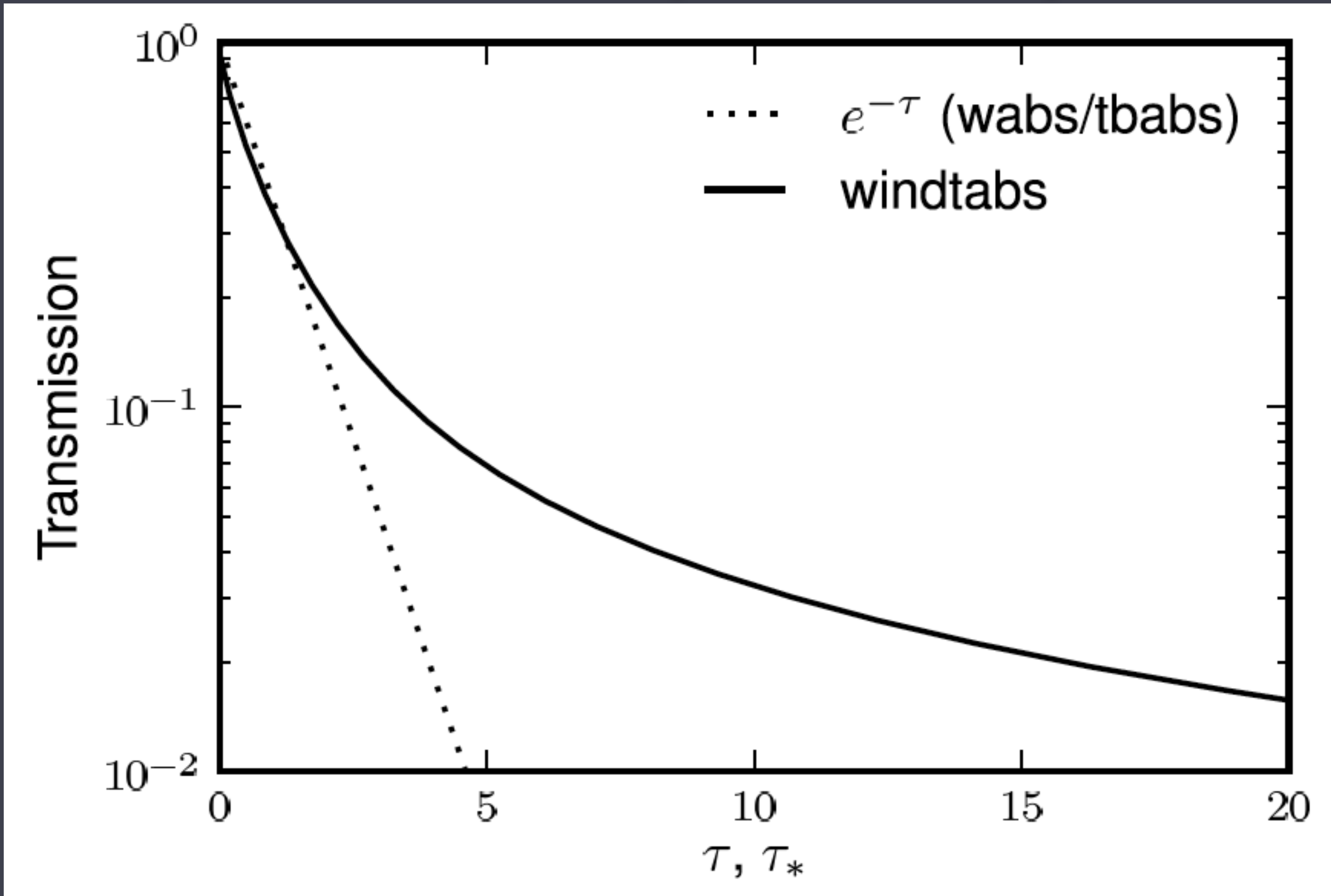

combine opacity and RT models: *windtabs* (Leutenegger et al. 2010)

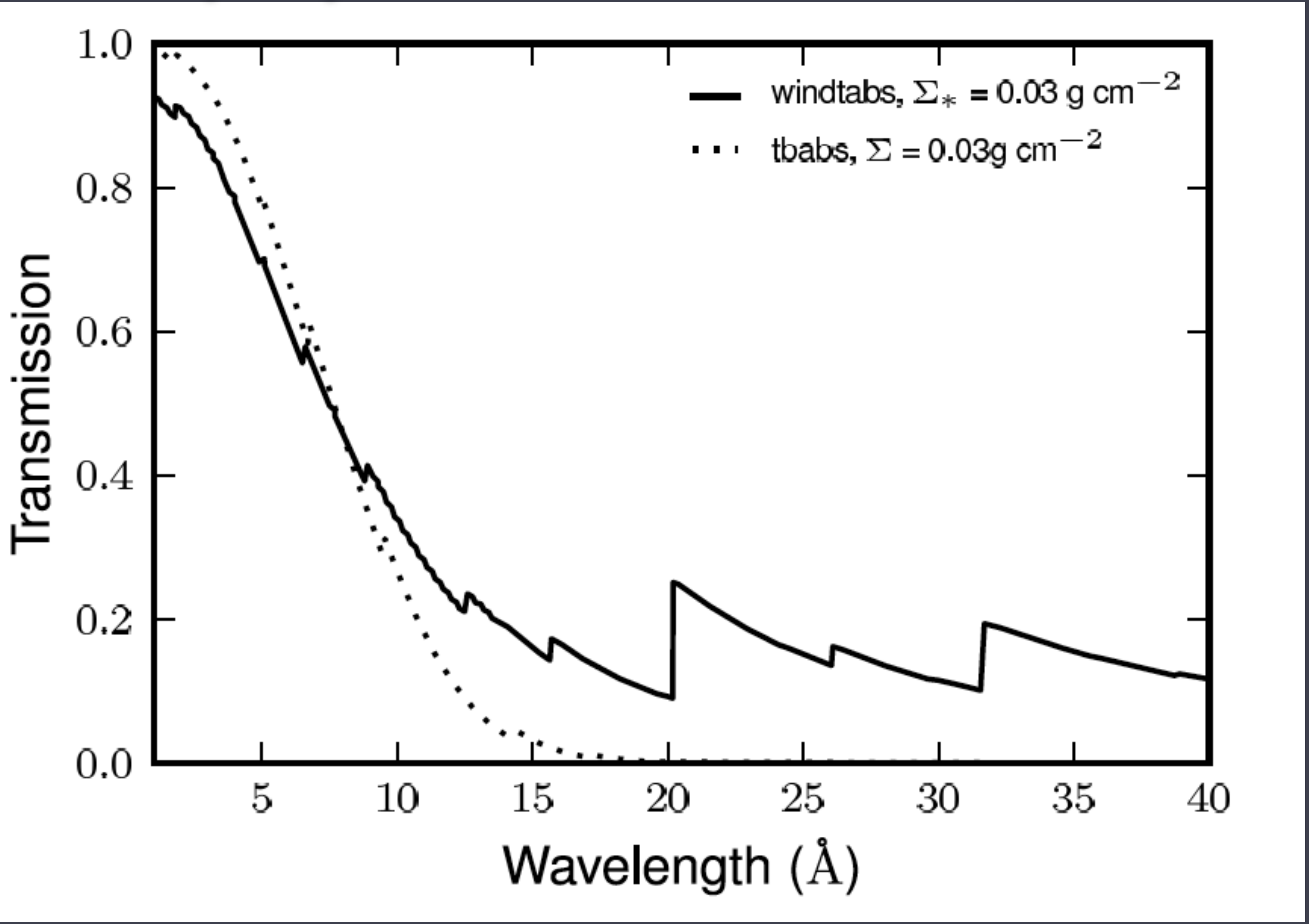

soft X-rays are attenuated by the wind

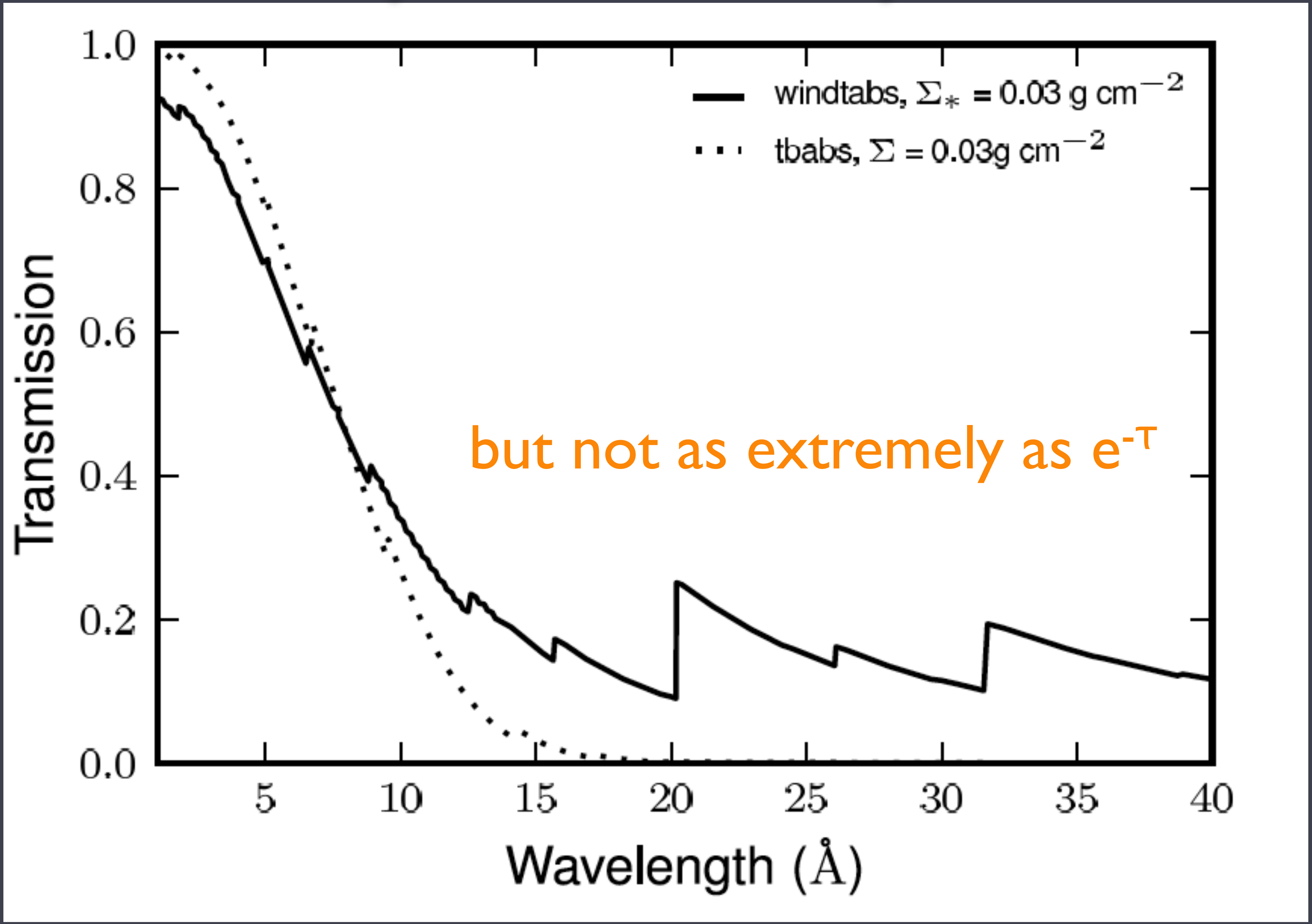

Extra Slides

Helium-like f/i line ratio: diagnostic of distance from photosphere

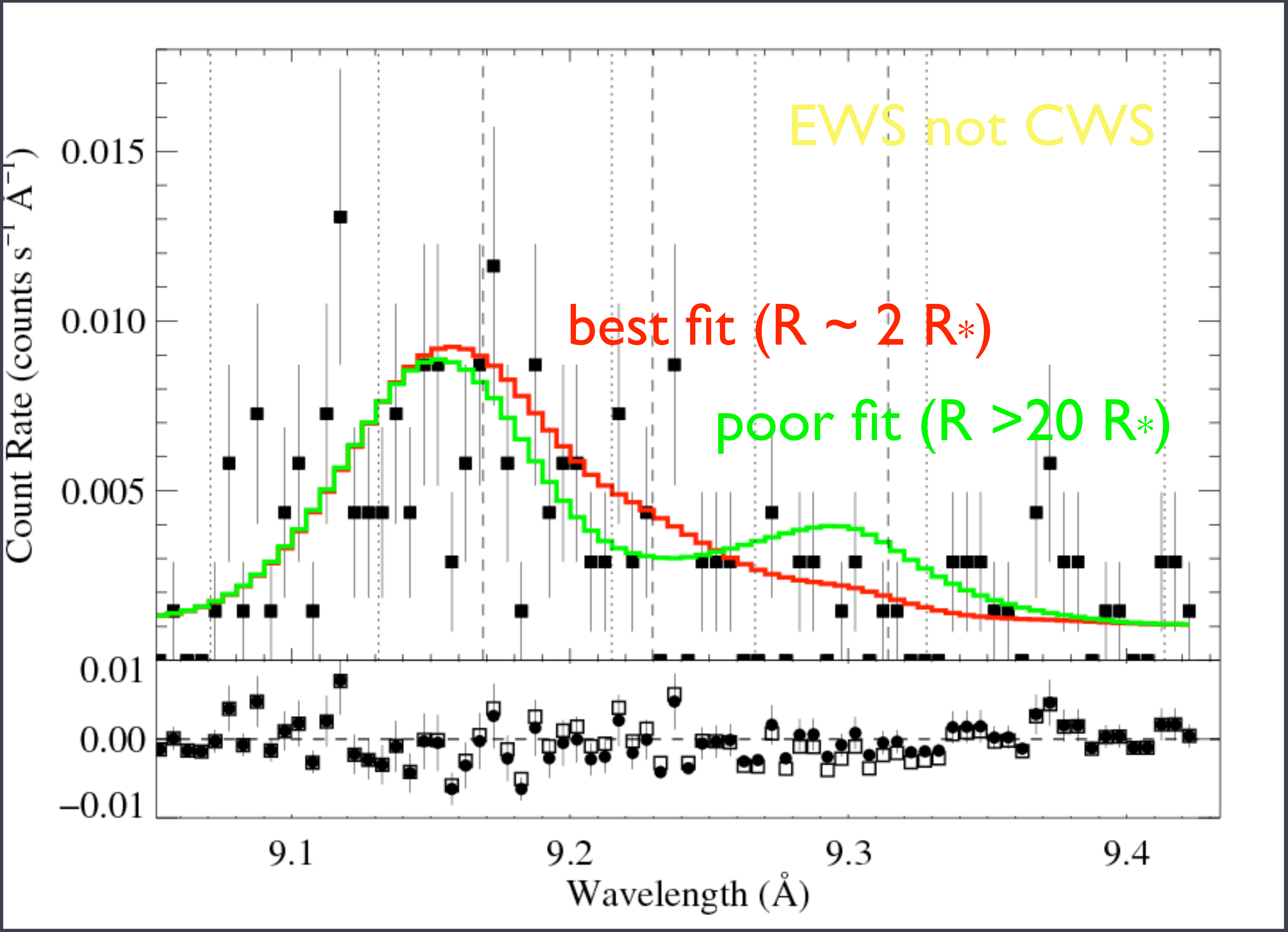

Incidentally, you **can** fit the *Chandra* line profiles with a porous model

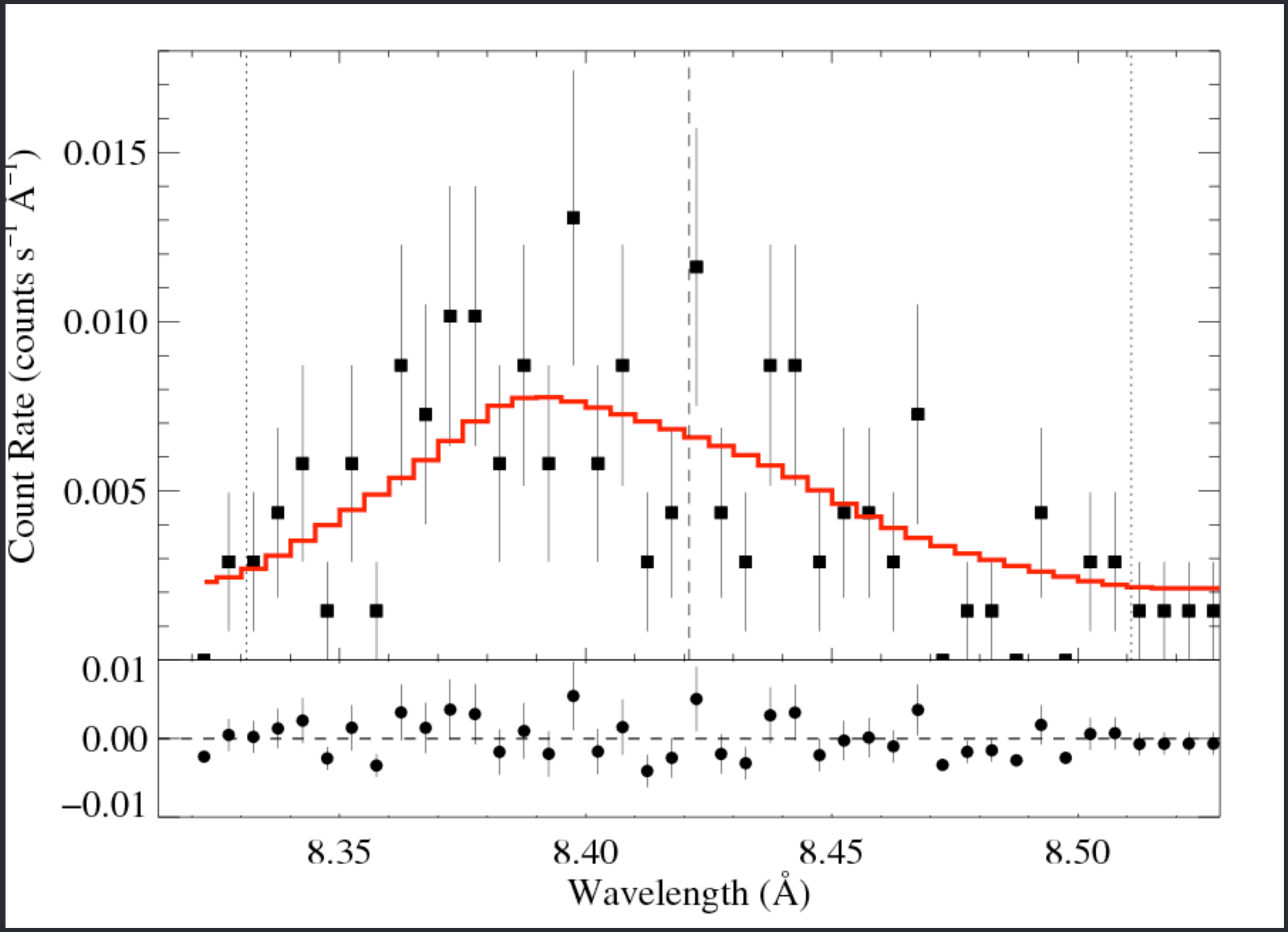

But, the fit requires a porosity length of 5 R_*!

Chandra ACIS image, redder = softer X-rays

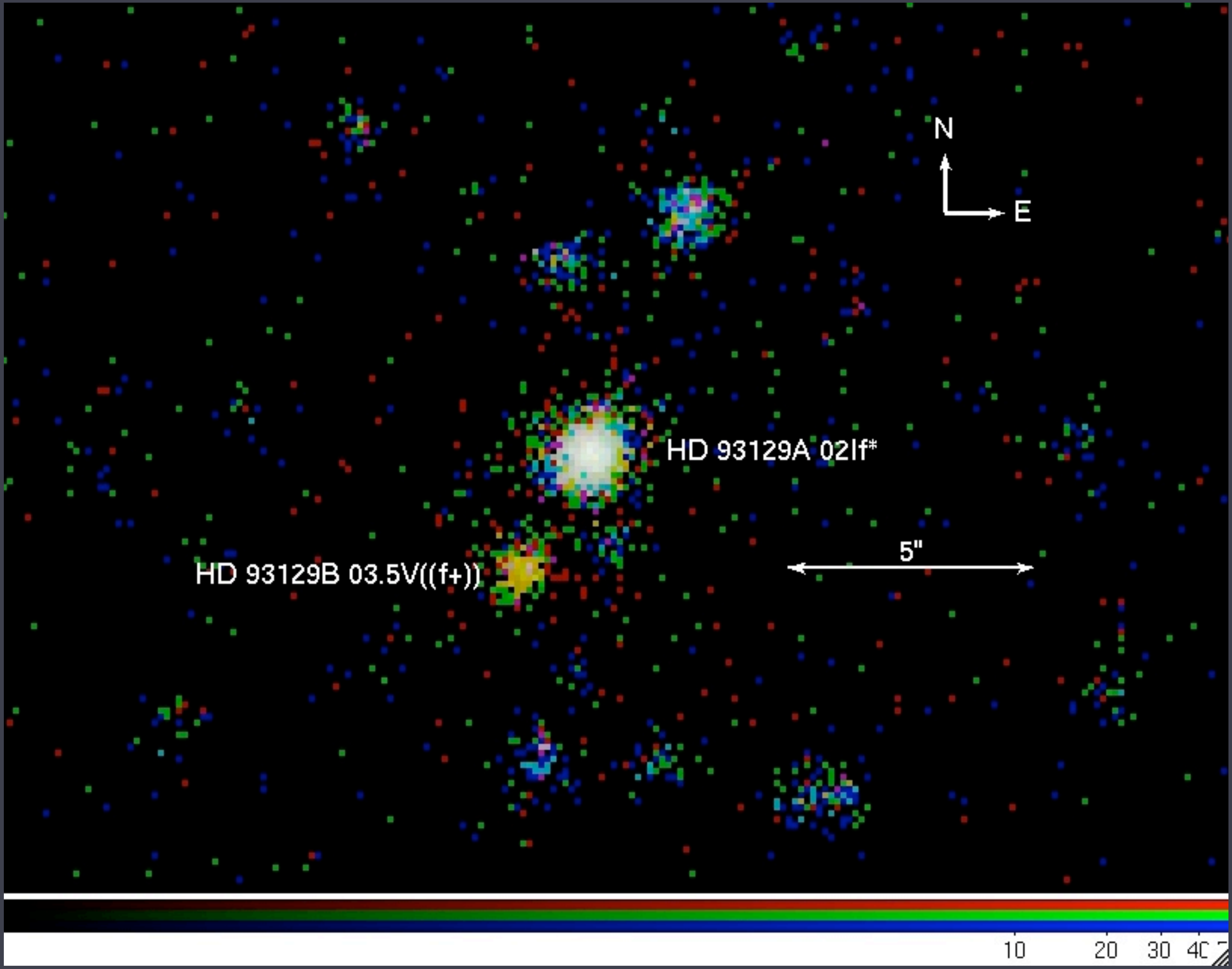

components A & B separated by 2.7″

Chandra ACIS spectra of A & B